Control of quantum phenomena: past, present and future

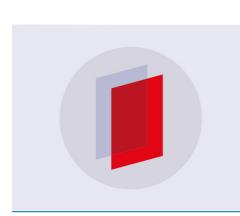To cite this article: Constantin Brif *et al* 2010 *New J. Phys.* **12** 075008

View the article online for updates and enhancements.

Related content

- Ultrafast molecules and clusters
  I V Hertel and W Radloff

- Femtosecond pulse shaping as analytic tool in mass spectrometry
  Tim Laarmann, Ihar Shchatsinin, Pushkar Singh et al.

- Controllability of open quantum systems with Kraus-map dynamics
  Rong Wu, Alexander Pechen, Constantin Brif et al.

Recent citations

- Information backflow as a resource for entanglement
  Nicolás Mirkin *et al*

- Optimal periodic control of spin systems: Application to the maximization of the signal-to-noise ratio per unit time
  N. Jbili *et al*

- Geometric formalism for constructing arbitrary single-qubit dynamically corrected gates
  Junkai Zeng *et al*

New Journal of Physics

Control of quantum phenomena: past, present and future

Constantin Brif, Raj Chakrabarti[1] and Herschel Rabitz[2]
Department of Chemistry, Princeton University, Princeton, NJ 08544, USA
E-mail: cbrif@princeton.edu, rchakra@purdue.edu and hrabitz@princeton.edu

Abstract. Quantum control is concerned with active manipulation of physical and chemical processes on the atomic and molecular scale. This work presents a perspective of progress in the field of control over quantum phenomena, tracing the evolution of theoretical concepts and experimental methods from early developments to the most recent advances. Among numerous theoretical insights and technological improvements that produced the present state-of-the-art in quantum control, there have been several breakthroughs of foremost importance. On the technology side, the current experimental successes would be impossible without the development of intense femtosecond laser sources and pulse shapers. On the theory side, the two most critical insights were (i) realizing that ultrafast atomic and molecular dynamics can be controlled via manipulation of quantum interferences and (ii) understanding that optimally shaped ultrafast laser pulses are the most effective means for producing the desired quantum interference patterns in the controlled system. Finally, these theoretical and experimental advances were brought together by the crucial concept of adaptive feedback control (AFC), which is a laboratory procedure employing measurement-driven, closed-loop optimization to identify the best shapes of femtosecond laser control pulses for steering quantum dynamics towards the desired objective. Optimization in AFC experiments is guided by a learning algorithm, with stochastic methods proving to be especially effective. AFC of quantum phenomena has found numerous applications in many areas of the physical and chemical sciences, and this paper reviews the extensive experiments. Other subjects discussed include quantum optimal control theory, quantum control landscapes, the role of theoretical control

---

[1] Present address: School of Chemical Engineering, Purdue University, Forney Hall of Chemical Engineering, 480 Stadium Mall Drive, West Lafayette, IN 47907, USA.

[2] Author to whom any correspondence should be addressed.

designs in experimental realizations and real-time quantum feedback control. The paper concludes with a perspective of open research directions that are likely to attract significant attention in the future.

Contents

1. Introduction

For many decades, physicists and chemists have employed various spectroscopic methods to carefully observe quantum systems on the atomic and molecular scale. The fascinating feature of quantum control is the ability to not just observe but actively manipulate the course of physical and chemical processes, thereby providing hitherto unattainable means to explore quantum dynamics. This remarkable capability along with a multitude of possible practical applications have attracted enormous attention to the field of control over quantum phenomena. This area of research has experienced extensive development during the last two decades and continues to grow rapidly. A notable feature of this development is the fruitful interplay between theoretical and experimental advances.

Various theoretical and experimental aspects of quantum control have been reviewed in a number of articles and books [1]–[45]. This paper starts with a short review of historical developments as a basis for evaluating the current status of the field and forecasting future directions of research. We try to identify important trends, follow their evolution from the past through the present and cautiously project them into the future. This paper is not intended to be a complete review of quantum control, but rather a perspective on the field.

In section 2, we discuss the historical evolution of relevant key ideas from the first attempts to use monochromatic laser fields for selective excitation of molecular bonds, through the inception of the crucial concept of control via manipulation of quantum interferences, and to the emergence of advanced contemporary methods that employ specially tailored ultrafast laser pulses to control the quantum dynamics of a wide variety of physical and chemical systems in a precise and effective manner. After this historical summary, we review in more detail the recent progress in the field, focusing on significant theoretical concepts, experimental methods

and practical advances that have shaped the development of quantum control during the last decade. Section 3 is devoted to quantum optimal control theory (QOCT), which is currently the leading theoretical approach for identifying the structure of controls (e.g. the shape of laser pulses) that enable attaining the quantum dynamical objective in the best possible way. We present the formalism of QOCT (i.e. the types of objective functionals used in various problems and methods employed to search for optimal controls), consider the issues of controllability and existence of optimal control solutions, survey applications and discuss the advantages and limitations of this approach. In section 4, we review the theory of quantum control landscapes, which provides a basis to analyze the complexity of finding optimal solutions. Topics discussed in that section include landscape topology (i.e. the characterization of critical points), optimality conditions for control solutions, Pareto optimality for multi-objective control, homotopy trajectory control methods and the practical implications of control landscape analysis. The important theoretical advances in the field of quantum control have laid the foundation for the fascinating discoveries occurring in laboratories where closed-loop optimizations guided by learning algorithms alter the quantum dynamics of real physical and chemical systems in dramatic and often unexpected ways. Section 5, which constitutes a very significant portion of this paper, is devoted to laboratory implementations of adaptive feedback control (AFC) of quantum phenomena. We review numerous AFC experiments that have been performed during the last decade in areas ranging from photochemistry to quantum information sciences. These experimental studies (most of which employ shaped femtosecond laser pulses) clearly demonstrate the capability of AFC to manipulate the dynamics of a broad variety of quantum systems and explore the underlying physical mechanisms. The role of theoretical control designs in experimental realizations is discussed in section 6. In particular, we emphasize the importance of theoretical studies for the feasibility analysis of quantum control experiments. Section 7 presents the concepts and potential applications of real-time feedback control (RTFC). Both measurement-based and coherent types of RTFC are described, along with current technological obstacles limiting more extensive use of these approaches in the laboratory. Future directions of quantum control are considered in section 8, including important unsolved problems and some emerging new trends and applications. Finally, concluding remarks are given in section 9.

2. Early developments of quantum control

The historical origins of quantum control lie in early attempts to use lasers for the manipulation of chemical reactions, in particular, selective breaking of bonds in molecules. Lasers, with their tight frequency control and high intensity, were considered ideal for the role of molecular-scale 'scissors' to precisely cut an identified bond, without damage to others. In the 1960s, when the remarkable characteristics of lasers were initially realized, it was thought that transforming this dream into reality would be relatively simple. These hopes were based on intuitive, appealing logic. The procedure involved tuning the monochromatic laser radiation to the characteristic frequency of a particular chemical bond in a molecule. It was suggested that the energy of the laser would naturally be absorbed in a selective way, causing excitation and, ultimately, breakage of the targeted bond. Numerous attempts were made in the 1970s to implement this idea [46]–[48]. However, it was soon realized that intramolecular vibrational redistribution of the deposited energy rapidly dissipates the initial local excitation and thus generally prevents selective bond breaking [49]–[51]. This process effectively increases the rovibrational temperature in the molecule in the same manner as incoherent heating does, often resulting in breakage of the weakest bond(s), which is usually not the target of interest.

2.1. Control via two-pathway quantum interference

Several important steps towards modern quantum control were made in the late 1980s. Brumer and Shapiro [52]–[55] identified the role of quantum interference in optical control of molecular systems. They proposed using two monochromatic laser beams with commensurate frequencies and tunable intensities and phases for creating quantum interference between two reaction pathways. The theoretical analysis showed that by tuning the phase difference between the two laser fields, it would be possible to control the branching ratios of molecular reactions [56]–[58]. The method of two-pathway quantum interference can also be used for controlling population transfer between bound states [59, 60] (in this case, the number of photons absorbed along two pathways often must be either all even or all odd to ensure that the wave functions excited by the two lasers have the same parity; most commonly, one- and three-photon excitations were considered).

The principle of coherent control via two-pathway quantum interference was demonstrated during the 1990s in a number of experiments, including control of population transfer in bound-to-bound transitions in atoms and molecules [59]–[64], control of energy and angular distributions of photoionized electrons [65]–[68] and photodissociation products [69] in bound-to-continuum transitions, control of cross-sections of photochemical reactions [70]–[72] and control of photocurrents in semiconductors [73, 74]. However, practical applications of this method are limited by a number of factors. In particular, it is quite difficult in practice to match excitation rates along the two pathways, either because one of the absorption cross-sections is very small or because other competing processes intervene. Another practical limitation, characteristic of experiments in optically dense media, is undesirable phase and amplitude locking of the two laser fields [75]. Due to these factors and other technical issues (e.g. imperfect focusing and alignment of the two laser beams), the modulation depths achieved in two-pathway interference experiments were modest: typically, about 25–50% for control of population transfer between bound states [60]–[62], [64] (the highest reported value was about 75% in one experiment [63]) and about 15–25% for control of dissociation and ionization branching ratios in molecules [70, 71]. Two-pathway interference control is a nascent form of full multi-pathway control offered by operating with broad-bandwidth optimally shaped pulses.

2.2. Pump–dump control

In the 1980s, Tannor and Rice [76] and Tannor *et al* [77] proposed a method for selectively controlling intramolecular reactions by using two successive femtosecond laser pulses with a tunable time delay between them. The first laser pulse (the 'pump') generates a vibrational wave packet on an electronically excited potential-energy surface of the molecule. After the initial excitation, the wave packet evolves freely until the second laser pulse (the 'dump') transfers some of the population back to the ground potential-energy surface into the desired reaction channel. Reaction selectivity is achieved by using the time delay between the two laser pulses to control the location at which the excited wave packet is dumped to the ground potential-energy surface [7, 11]. For example, it may be possible to use this method to move the ground-state wave function beyond a barrier obstructing the target reaction channel. In some cases, the second pulse transfers the population to an electronic state other than the ground state (e.g. to a higher excited state) in a pump–repump scheme.

The feasibility of the pump–dump control method was demonstrated in a number of experiments [78]–[82]. The pump–dump scheme can also be used as a time-resolved

spectroscopy technique to explore transient molecular states and thus obtain new information about the dynamics of the molecule at various stages of a reaction [83]–[90]. In pump–dump control experiments, the system dynamics can often be explained in the time domain in a simple and intuitive way to provide a satisfactory qualitative interpretation of the control mechanism. The pump–dump method gained considerable popularity [7, 11, 30] due to its capabilities to control and investigate molecular dynamics. However, the employment of transform-limited laser pulses significantly restricts the effectiveness of this technique as a practical control tool. More effective control of the wave-packet dynamics and, consequently, higher reaction selectivity can be achieved by optimally shaping one or both of the pulses. For example, even a chirp of the pump pulse may improve the effectiveness of control by producing more localized wave packets (the use of pulse chirping will be discussed in section 2.6 in more detail). Recent experimental applications of the pump–dump scheme with shaped laser pulses (optimized using adaptive methods) will be discussed in section 5.

2.3. Control via stimulated Raman adiabatic passage (STIRAP)

In the late 1980s, Bergmann and collaborators [91]–[94] demonstrated a very efficient adiabatic method for population transfer between discrete quantum states in atoms or molecules. In this approach known as STIRAP, two time-delayed laser pulses (typically, of nanosecond duration) are applied to a three-level Λ-type configuration to achieve complete population transfer between the two lower levels via the intermediate upper level. Interestingly, the pulse sequence employed in the STIRAP method is counter-intuitive, i.e. the Stokes laser pulse that couples the intermediate and final states precedes (but overlaps) the pump laser pulse that couples the initial and intermediate states. The laser electric fields should be sufficiently strong to generate many cycles of Rabi oscillations. The laser-induced coherence between the quantum states is controlled by tuning the time delay, so that the transient population in the intermediate state remains almost zero, thus avoiding losses by radiative decay. Detailed reviews of STIRAP and related adiabatic passage techniques can be found in [10, 16]. While the efficiency of the STIRAP method, under appropriate conditions, is very high, its applicability is restricted to control of population transfer between a few discrete states as arise in atoms and small (diatomic and triatomic) molecules. In larger polyatomic molecules, the very high density of levels generally prevents successful adiabatic passage [10, 16].

2.4. Control via wave-packet interferometry

Another two-pulse approach for control of population transfer between bound states employs Ramsey interference of optically excited wave packets [95, 96]. In this method, referred to as wave-packet interferometry (WPI) [42], two time-delayed laser pulses excite an atomic, molecular or quantum-dot transition, resulting in two wave packets on an excited state. Quantum interference between the two coherent wave packets can be controlled by tuning the time delay between the laser pulses. For control of population transfer, constructive or destructive interference between the excited wave packets gives rise to larger or smaller excited-state population, respectively. The same control mechanism is also applicable to other problems such as control of atomic radial wave functions and control of molecular alignment. WPI was demonstrated with Rydberg [97]–[99] and fine-structure [100, 101] wave packets in atoms, vibrational [102]–[106] and rotational [107] wave packets in molecules, and exciton fine-structure wave packets in semiconductor quantum dots [108, 109] (for a detailed review of

coherent control applications of WPI, see [42]; the use of WPI for molecular state reconstruction is reviewed in [110]). Once again, much more effective manipulation of quantum interferences is possible in this control scheme when shaped laser pulses are used instead of transform-limited ones (see section 5 for details).

2.5. Introduction of QOCT

Although the control approaches discussed in sections 2.1–2.4 were initially perceived as quite different, it is now clear that on a fundamental level all of them employ the mechanism of quantum interference induced by control laser fields. A common feature of these methods is that they generally attempt to manipulate the evolution of quantum systems by controlling just one parameter: the phase difference between two laser fields in control via two-pathway quantum interference; the time delay between two laser pulses in pump–dump control, STIRAP and WPI. While single-parameter control may be relatively effective in some simple systems, more complex systems and applications require more flexible and capable control resources. The single-parameter control schemes have been unified and generalized by the concept of control with specially tailored ultrashort laser pulses. Rabitz and co-workers [111]–[113] and others [114, 115] suggested that it would be possible to steer the quantum evolution to a desired product channel by specifically designing and tailoring the time-dependent electric field of the laser pulse to the characteristics of the system. Specifically, QOCT may be used to design laser pulse shapes that are best suited for achieving the desired goal [111]–[122]. An optimally shaped laser pulse typically has a complex form, both temporally and spectrally. The phases and amplitudes of different frequency components are optimized to excite an interference pattern among distinct quantum pathways, to best achieve the desired dynamics. The first optimal fields for quantum control were computed by Shi *et al* [111], who showed that the amplitudes of the interfering vibrational modes of a laser-driven molecule could add up constructively in a given bond. We will review QOCT and its applications in more detail in section 3 (for earlier reviews of QOCT, see [7, 11, 14, 38, 40]).

2.6. Control with linearly chirped pulses

Laser pulse-shaping technology rapidly developed during the early 1990s [4, 5, 12]. However, the capabilities of pulse shaping were not fully exploited in quantum control until the first experimental demonstrations of AFC in 1997–1998 [123, 124]. Initially, ultrashort laser pulses with time-varying photon frequencies were used to tune just the linear chirp, which represents an increase or decrease of the instantaneous frequency as a function of time under the pulse envelope[3]. Linearly chirped femtosecond laser pulses were successfully applied for control of various atomic and molecular processes, including control of vibrational wave packets [125]–[131], control of population transfer between atomic states [132]–[134] and between molecular vibrational levels [135]–[137] via 'ladder-climbing' processes, control of electronic excitations in molecules [138]–[142], selective excitation of vibrational modes in coherent anti-Stokes Raman scattering (CARS) [143], improvement of the resolution of CARS spectroscopy [144, 145], and control of photoelectron spectra [146] and transitions through multiple highly excited states [147] in strong-field ionization of atoms. In particular, when the

---

[3] The instantaneous frequency $\omega(t)$ of a linearly chirped pulse with a carrier frequency ω_0 is given at time t by $\omega(t) = \omega_0 + 2bt$, where b is the chirp parameter that can be negative or positive.

emission and absorption bands of a molecule strongly overlap, pulses with negative and positive chirp excite vibrational modes predominantly in the ground and excited electronic states, respectively [125], [129]–[131]. Chirped pulses can also be used to control the localization of vibrational wave packets in diatomic molecules, with the negative and positive chirp increasing and decreasing the localization, respectively [126]–[128]. Based on this effect, pump pulses with negative chirp were used to enhance selectivity in the pump–dump control of photodissociation reactions [128]. Recently, the localization effect of negatively chirped pulses was used to protect vibrational wave packets against rotationally induced decoherence [148]. Due to their effectiveness in various applications, chirped laser pulses are widely used in quantum control. However, by the end of the 1990s, many experimenters realized that more sophisticated pulse shapes, beyond just linear chirp, provide a much more powerful and flexible tool for control of quantum phenomena in complex physical and chemical systems. Femtosecond pulse-shaping technology is utilized to the fullest extent in AFC experiments where laser pulses are optimally tailored to meet the needs of complex quantum dynamics objectives [13, 15, 18, 19, 22], [25]–[29], [31, 37, 41]. The enormous growth of this field during the last decade is reviewed in section 5.

2.7. Control via non-resonant dynamic Stark effect (NRDSE)

Optimal control of quantum phenomena in atoms and molecules usually operates at laser intensities sufficient to be in the non-perturbative regime. Thus, controlled dynamics will naturally utilize the dynamic Stark shift among other available physical processes in order to reach the target. In a recent quantum control development, Stolow and co-workers proposed and experimentally demonstrated manipulation of molecular processes exclusively employing the NRDSE [149]–[152]. In this approach, a quantum system is controlled by an infrared laser pulse in the intermediate field-strength regime (non-perturbative but non-ionizing). Laser frequency and intensity are chosen to eliminate the complex competing processes (e.g. multiphoton resonances and strong-field ionization), so that only the NRDSE contributes to the control mechanism. By utilizing Raman coupling, control via NRDSE reversibly modifies the effective Hamiltonian during system evolution, thus making it possible to affect the course of intramolecular dynamic processes. For example, a suitably timed infrared laser pulse can act as a 'photonic catalyst' by reversibly modifying potential energy barriers during a chemical reaction without inducing any real electronic transitions [152]. Control via NRDSE was successfully applied to create field-free 'switched' wave packets (which can be employed e.g. for molecular axis alignment) [149, 150] and modify branching ratios in non-adiabatic molecular photodissociation [151, 152].

2.8. Control of nuclear spins with radiofrequency (RF) fields

One of the earliest examples of coherent control of quantum dynamics is manipulation of nuclear spin ensembles using RF fields [153]. The main application of nuclear magnetic resonance (NMR) control techniques is high-resolution spectroscopy of polyatomic molecules (e.g. protein structure determination) [154]–[157]. While control of an isolated spin by a time-dependent magnetic field is a simple quantum problem, in reality, NMR spectroscopy of molecules containing tens or even hundreds of nuclei involves many complex issues such as the effect of interactions between the spins, thermal relaxation, instrumental noise and influence

IOP Institute of Physics ◆ DEUTSCHE PHYSIKALISCHE GESELLSCHAFT

of the solvent. Therefore, modern NMR spectroscopy often employs thousands of precisely sequenced and phase-modulated pulses. Among the important NMR control techniques are composite pulses, refocusing and pulse shaping. In particular, the use of shaped RF pulses in NMR makes it possible to improve frequency selectivity, suppress solvent contribution, simplify high-resolution spectra and reduce the size and duration of experiments [158]. In recent years, NMR became an important testbed for developing control methods for applications in quantum information sciences [159]–[163]. In order to perform fault-tolerant quantum computations, the system dynamics must be controlled with an unprecedented level of precision, which requires even more sophisticated designs of control pulses than in high-resolution spectroscopy. In particular, QOCT was recently applied to identify optimal sequences of RF pulses for the operation of NMR quantum information processors [163, 164].

3. Quantum optimal control theory

The most comprehensive means for coherently controlling the evolution of a quantum system (e.g. a molecule) undergoing a complex dynamical process is through the coordinated interaction between the system and the electromagnetic field whose spectral content and temporal profile may be continuously altered throughout the process. For a specified control objective, and with restrictions imposed by many possible constraints, the time-dependent field required to manipulate the system in a desired way can be designed using QOCT [14, 38, 40]. This general formulation encompasses both the weak and strong field limits and incorporates as special cases the one-parameter methods such as control via two-pathway quantum interference and pump–dump control.

3.1. Description of controlled quantum dynamics

Optimal control theory has an extensive history in traditional engineering applications [165, 166], but control of quantum phenomena imposes special features. Consider the time evolution of a controlled quantum system,

$$\frac{\mathrm{d}}{\mathrm{d}t}U(t) = -\frac{\mathrm{i}}{\hbar}[H_0 - \varepsilon(t) \cdot \mu]U(t), \quad U(0) = I. \tag{1}$$

Here, $U(t)$ is the unitary evolution operator of the system at time t, I is the identity operator, H_0 is the free Hamiltonian, μ is the dipole operator and $\varepsilon(t)$ is the control function at time t. For the control function, we will use the notation $\varepsilon(\cdot) \in \mathbb{K}$ (where $\mathbb{K}$ is the space of locally bounded, sufficiently smooth, square integrable functions of time defined on some interval $[0, T]$, with T fixed). Equation (1) adequately describes the coherent quantum dynamics of a molecular system interacting with a laser electric field in the dipole approximation or a spin system interacting with a time-dependent magnetic field. We will consider finite-level quantum systems and denote the dimension of the system's Hilbert space as N[4].

For quantum systems undergoing environmentally induced decoherence, there are many dynamical models depending on the character of the system–environment coupling. If the system and environment are initially uncoupled, the evolution of the system's reduced density

---

[4] If one is not concerned with the physically irrelevant global phase of the evolution operator, the control problem can be restricted to the Hamiltonian represented by a traceless Hermitian matrix, and $U \in SU(N)$, where $SU(N)$ is the special unitary group.

matrix ρ from $t = 0$ to t is described by a completely positive, trace preserving map: $\rho(t) = \Phi(\rho_0)$ where $\rho_0 = \rho(0)$. This map (which is often called the Kraus map) can be expressed using the operator-sum representation (OSR) [167]:

$$\rho(t) = \Phi(\rho_0) = \sum_{j=1}^{n} K_j(t) \rho_0 K_j^{\dagger}(t), \tag{2}$$

where K_j are Kraus operators ($N \times N$ complex matrices), which satisfy the condition $\sum_{j=1}^{n} K_j^{\dagger} K_j = I_N$, and I_N denotes the identity operator on the Hilbert space of dimension N. There exist infinitely many OSRs (with different sets of Kraus operators) for the same Kraus map. Various types of quantum master equations can be derived from the Kraus OSR under additional assumptions [168, 169]. In particular, for the generic class of Markovian environments, the dynamics of an open quantum system can be described using the quantum master equation of Lindblad type [168]–[170]:

$$\frac{d}{dt}\rho(t) = -\frac{i}{\hbar}[H_0 - \varepsilon(t) \cdot \mu, \rho(t)] + \sum_{i=1}^{N^2-1} \gamma_i \left[L_i \rho(t) L_i^{\dagger} - \frac{1}{2} L_i^{\dagger} L_i \rho(t) - \frac{1}{2} \rho(t) L_i^{\dagger} L_i \right], \tag{3}$$

where γ_i are non-negative constants and L_i are Lindblad operators ($N \times N$ complex matrices) that represent the non-unitary effect of coupling to the environment. For a closed system, (3) reduces to the von Neumann equation, $\dot{\rho}(t) = -(i/\hbar)[H_0 - \varepsilon(t) \cdot \mu, \rho(t)]$. For simplicity, we will formulate QOCT below using the Schrödinger equation (1) for the unitary evolution operator; analogous formulations using the von Neumann equation or the Lindblad master equation for the density matrix are available in the literature [120], [171]–[174].

3.2. Control objective functionals

The general class of control objective functionals (cost functionals of Bolza type) can be written as

$$J[U(\cdot), \varepsilon(\cdot)] = F(U(T)) + \int_0^T G(U(t), \varepsilon(t)) \, dt, \tag{4}$$

where F is a continuously differentiable function on $U(N)$, and G is a continuously differentiable function on $U(N) \times \mathbb{R}$. The optimal control problem may be stated as the search for

$$J_{\text{opt}} = \max_{\varepsilon(\cdot)} J[U(\cdot), \varepsilon(\cdot)], \tag{5}$$

subject to the dynamical constraint (1). If only the term $\int_0^T G(U(t), \varepsilon(t)) \, dt$ is present, the cost functional is said to be of Lagrange type, whereas if only the term $F(U(T))$ is present, the functional is said to be of Mayer type [166]. Three classes of problems corresponding to different choices of $F(U(T))$ have received most attention in the quantum control community to date: (i) evolution-operator control, (ii) state control and (iii) observable control.

For evolution-operator control, the goal is to generate $U(T)$ such that it is as close as possible to the target unitary transformation W. The Mayer-type cost functional in this case can be generally expressed as

$$F_1(U(T)) = 1 - \|W - U(T)\|, \tag{6}$$

where $\| \cdot \|$ is an appropriate normalized matrix norm, i.e. $F_1(U(T))$ is maximized when the distance between $U(T)$ and W is minimized. This type of objective is common in quantum computing applications [175], where $F_1(U(T))$ is the fidelity of a quantum gate [176, 177]. One frequently used form of the objective functional $F_1(U(T))$ is obtained utilizing the squared Hilbert–Schmidt norm [178] in (6) with an appropriate normalization (i.e. $\|X\| = (2N)^{-1}\text{Tr}(X^\dagger X)$) [179]–[181]:

$$F_1(U(T)) = \frac{1}{N}\Re \,\text{Tr}[W^\dagger U(T)]. \tag{7}$$

Other forms of the objective functional, which employ different matrix norms in (6), are possible as well [181]–[184]. For example, a modification of (7), $F_1(U(T)) = N^{-1}|\text{Tr}[W^\dagger U(T)]|$, which is independent of the global phase of $U(T)$, can be used. Note that $F_1(U(T))$ is independent of the initial state, as the quantum gate must produce the same unitary transformation for any input state of the qubit system [175].

For state control, the goal is to transform the initial state ρ_0 into a final state $\rho(T) = U(T)\rho_0 U^\dagger(T)$ that is as close as possible to the target state ρ_f. The corresponding Mayer-type cost functional is

$$F_2(U(T)) = 1 - \|U(T)\rho_0 U^\dagger(T) - \rho_f\|, \tag{8}$$

where $\| \cdot \|$ is an appropriate normalized matrix norm (e.g. the Hilbert–Schmidt norm can be used) [185]–[188].

For observable control, the goal is typically to maximize the expectation value of a target quantum observable Θ (represented by a Hermitian operator). The corresponding Mayer-type cost functional is [116], [189]–[192]

$$F_3(U(T)) = \text{Tr}[U(T)\rho_0 U^\dagger(T)\Theta]. \tag{9}$$

An important special case is state-transition control (also known as population transfer control), for which $\rho_0 = |\psi_i\rangle\langle\psi_i|$ and $\Theta = |\psi_f\rangle\langle\psi_f|$, where $|\psi_i\rangle$ and $|\psi_f\rangle$ are eigenstates of the free Hamiltonian H_0; in this case, the objective functional (9) has the form $F_3(U(T)) = P_{i \to f} = |\langle\psi_f|U(T)|\psi_i\rangle|^2$, which is the probability of transition (i.e. the population transfer yield) between the energy levels of the quantum system [193, 194]. In many chemical and physical applications of quantum control, absolute yields are not known, and therefore maximizing the expectation value of an observable (e.g. the population transfer yield) is a more appropriate laboratory goal than minimizing the distance to a target expectation value.

Also, in quantum control experiments (see section 5), measuring the expectation value of an observable is much easier than estimating the quantum state or evolution operator. Existing methods of quantum-state and evolution-operator estimation rely on tomographic techniques [195]–[202], which are extremely expensive in terms of the number of required measurements (e.g. in quantum computing applications, standard methods of state and process tomography require numbers of measurements that scale exponentially in the number of qubits [175], [202]–[206]). Therefore, virtually all quantum control experiments so far have used observable control with objective functionals of the form (9). For example, in an AFC experiment [148], in which the goal was to maximize the degree of coherence, the expectation value of an observable representing the degree of quantum state localization was used as a coherence 'surrogate,' instead of state purity or von Neumann entropy which are nonlinear functions of the density matrix and hence would require state estimation. Nevertheless, future laboratory applications of quantum control, in particular in the field of quantum information

sciences, will require evolution-operator control and state control, with the use of objective functionals of the types (6) and (8), respectively, together with novel state and process estimation methods [205]–[214].

Recently, attention has turned to problems requiring simultaneous maximization of several control objectives [215]–[219]. In the framework of QOCT, these optimization problems are sometimes handled through the use of a weighted-sum objective functional, such as [216, 217]

$$F_4(U(T)) = \sum_{k=1}^{n} \alpha_k \text{Tr}[U(T)\rho_0 U^\dagger(T)\Theta_k], \tag{10}$$

which extends (9) to multiple quantum observables. Also, general methods of multi-objective optimization [220]–[222] have been recently applied to various quantum control problems [217]–[219].

Another common goal in quantum control is to maximize a Lagrange-type cost functional subject to a constraint on $U(T)$ [223, 224]. For example, this type of control problem can be formulated as follows:

$$\max_{\varepsilon(\cdot)} \int_0^T G(\varepsilon(t))\, \mathrm{d}t, \quad \text{subject to } F(U(T)) = \chi, \tag{11}$$

where $F(U(T))$ is the Mayer-type cost functional for evolution-operator, state, or observable control (as described above), and χ is a constant that corresponds to the target value of F. Often, the goal is to minimize the total field fluence, in which case $G(\varepsilon(t)) = -\frac{1}{2}\varepsilon^2(t)$ is used.

3.3. Controllability of quantum systems

One of the fundamental issues of quantum control is to assess the system's controllability. A quantum system is controllable in a set of configurations, $\mathcal{S} = \{\zeta\}$, if for any pair of configurations $\zeta_1, \zeta_2 \in \mathcal{S}$ there exists a time-dependent control $\varepsilon(\cdot)$ that can drive the system from the initial configuration ζ_1 to the final configuration ζ_2 in a finite time T. Here, the notion of configuration means the state of the system ρ, the expectation value of an observable $\text{Tr}(\rho\Theta)$, the evolution operator U or the Kraus map Φ, depending on the specific control problem. Controllability of closed quantum systems with unitary dynamics has been well studied [225]–[244]. Controllability analysis was also extended to open quantum systems [245]–[252].

Controllability is determined by the equation of motion as well as properties of the Hamiltonian. For a closed quantum system with unitary dynamics (1), evolution-operator controllability implies that for any unitary operator W there exists a finite time T and a control $\varepsilon(\cdot)$, such that $W = U(T)$, where $U(T)$ is the solution of (1). For an N-level closed system, a necessary and sufficient condition for evolution-operator controllability is that the dynamical Lie group $\mathfrak{G}$ of the system (i.e. the Lie group generated by the system's Hamiltonian) be $U(N)$ (or $SU(N)$ for a traceless Hamiltonian) [235]–[237].

Unitary evolution preserves the spectrum of the quantum state (i.e. the eigenvalues of the density matrix). All density matrices that have the same eigenvalues form a set of unitarily equivalent states (e.g. the set of all pure states). Therefore, under unitary evolution, a quantum system can be state controllable only within a set of unitarily equivalent states [235, 236]. Density-matrix controllability means that for any pair of unitarily equivalent density matrices ρ_1 and ρ_2 there exists a control $\varepsilon(\cdot)$ that drives ρ_1 into ρ_2 (in a finite time). It has

been shown [235]–[237] that density-matrix controllability is equivalent to evolution-operator controllability. For specific classes of density matrices, the requirements for controllability are weaker [229]–[231]. For example, pure-state controllability requires that the system's dynamical Lie group $\mathfrak{G}$ is transitive on the sphere $\mathbb{S}^{2N-1}$. For infinite-level quantum systems evolving on non-compact Lie groups, such as those arising in quantum optics, the conditions for controllability are more stringent [243, 244, 251, 253].

3.4. Searching for optimal controls

To solve for optimal controls that maximize an objective functional (of the types discussed in section 3.2), it is convenient to define a functional $\tilde{J}$ that explicitly incorporates the dynamical constraint (1):

$$\tilde{J}[U(\cdot), \phi(\cdot), \varepsilon(\cdot)] = F(U(T)) + \lambda \int_0^T G(U(t), \varepsilon(t))\, \mathrm{dt}$$

$$- 2\Re \int_0^T \mathrm{Tr}\left\{\phi^\dagger(t)\left[\frac{\mathrm{d}U(t)}{\mathrm{dt}} + \frac{\mathrm{i}}{\hbar}\left(H_0 - \varepsilon(t)\cdot\mu\right)U(t)\right]\right\}\mathrm{dt}. \qquad (12)$$

Here, λ is a scalar weight and an auxiliary operator $\phi(t)$ is a Lagrange multiplier employed to enforce satisfaction of equation (1).

Various modifications of the objective functional (12) are possible; for example, QOCT can be formulated for open systems with non-unitary dynamics [120], [171]–[174], [254]–[258]. Modified objective functionals can also comprise additional spectral and fluence constraints on the control field [259, 260], take into account nonlinear interactions with the control field [261, 262], deal with time-dependent and time-averaged targets [256], [263]–[265], and include the final time as a free control parameter [266, 267]. It is also possible to formulate QOCT with time minimization as a control goal (time optimal control) [268]–[271]. As mentioned earlier, QOCT can also be extended to incorporate optimization of multiple objectives [215]–[219].

A necessary condition for a solution of the optimization problem (5) subject to the dynamical constraint (1) is that the first-order functional derivatives of $\tilde{J}$ with respect to $U(\cdot)$, $\phi(\cdot)$ and $\varepsilon(\cdot)$ are equal to zero. Correspondingly, optimal controls can be obtained by solving the resulting Euler–Lagrange equations. Equivalently, optimal controls can be derived through application of the Pontryagin maximum principle (PMP) [165, 223, 224]. Satisfaction of the first-order conditions following from the PMP is a necessary but not sufficient condition for optimality of a control $\varepsilon(\cdot)$. So-called Legendre conditions on the Hessian, which depend on the type of cost, are also required for optimality [165, 166].

An important issue is the existence of optimal control fields (i.e. maxima of the objective functional) for realistic situations that involve practical constraints on the applied laser fields. It is important to distinguish between the existence of an optimal control field and controllability; in the former case, a field is designed, subject to particular constraints, that guides the evolution of the system towards a specified target until a maximum of the objective functional is reached, while in the latter case, the exact coincidence between the attained evolution operator (or state) and the target evolution operator (or state) is sought. The existence of optimal controls for quantum systems was analyzed in a number of works. Peirce *et al* [112] proved the existence of optimal solutions for state control in a spatially bounded quantum system that necessarily has spatially localized states and a discrete spectrum. Zhao and Rice [272] extended this analysis to

a system with both discrete and continuous states and proved the existence of optimal controls over the evolution in the subspace of discrete states. Demiralp and Rabitz [185] showed that, in general, there is a denumerable infinity of solutions to a particular class of well-posed quantum control problems; the solutions can be ordered in quality according to the achieved optimal value of the objective functional. The existence of multiple control solutions has important practical consequences, suggesting that there may be broad latitude in the laboratory, even under strict experimental restrictions, for finding successful controls for well-posed quantum objectives. The existence and properties of critical points (including global extrema) of objective functionals for various types of quantum control problems were further explored using the analysis of control landscapes [179]–[181], [189]–[194], [273] (see section 4).

A number of optimization algorithms were adapted or specially developed for use in QOCT, including the conjugate gradient search method [114], the Krotov method [177, 274, 275], monotonically convergent algorithms [276]–[282], non-iterative algorithms [283], the gradient ascent pulse engineering algorithm [164], a hybrid local/global algorithm [256] and homotopy-based methods [284]–[286]. Faster convergence of iterative QOCT algorithms was demonstrated using 'mixing' strategies [287]. Also, the employment of propagation toolkits [288]–[290] greatly increases the efficiency of numerical optimizations and allows for fast combinatorial optimization [291]. Detailed discussions of the QOCT formalism and algorithms are available in the literature [11, 14, 38, 40].

3.5. An example of QOCT applied to a molecular system

In order to illustrate optimal control of molecules, we consider an instructive example. In one of the pioneering QOCT studies, Kosloff *et al* [114] considered two electronic states (ground and excited) of a model molecular system, with the wave function (in the coordinate representation) of the form[5]

$$\psi(\mathbf{r}, t) = \langle \mathbf{r} | \psi(t) \rangle = \begin{pmatrix} \psi_e(\mathbf{r}, t) \\ \psi_g(\mathbf{r}, t) \end{pmatrix}, \tag{13}$$

where ψ_g and ψ_e are projections of the wave function on the ground and excited states, respectively. The time evolution of the wave function is determined by the Schrödinger equation:

$$i\hbar \frac{\partial}{\partial t} \begin{pmatrix} \psi_e(\mathbf{r}, t) \\ \psi_g(\mathbf{r}, t) \end{pmatrix} = \begin{pmatrix} H_e(\mathbf{r}) & H_{ge}(\mathbf{r}, t) \\ H_{ge}^\dagger(\mathbf{r}, t) & H_g(\mathbf{r}) \end{pmatrix} \begin{pmatrix} \psi_e(\mathbf{r}, t) \\ \psi_g(\mathbf{r}, t) \end{pmatrix}, \tag{14}$$

where $H_i(\mathbf{r}) = \mathbf{p}^2/(2m) + V_i(\mathbf{r})$ ($i = g, e$), $\mathbf{p}$ is the momentum operator, and $V_g(\mathbf{r})$ and $V_e(\mathbf{r})$ are the adiabatic potential energy surfaces for the ground and excited states, respectively. The off-diagonal term $H_{ge}(\mathbf{r}, t)$ represents the field-induced coupling between the molecular states:

$$H_{ge}(\mathbf{r}, t) = -\mu_{ge}(\mathbf{r})\varepsilon(t), \tag{15}$$

where $\mu_{ge}(\mathbf{r})$ is the electric dipole operator and $\varepsilon(t)$ is the time-dependent electric field of the control laser pulse applied to the molecule.

---

[5] For the sake of notation consistency, the control problem is presented here slightly differently than in the original work [114].

The goal is to control a dissociation reaction in the presence of two distinct exit channels on the ground potential-energy surface. The corresponding objective functional (including the dynamical constraint) is given by

$$\tilde{J} = \langle \psi(T)|P|\psi(T)\rangle - \lambda \int_0^T \varepsilon^2(t)\,\mathrm{d}t - 2\Re \int_0^T \langle \chi(t)| \left(\frac{\partial}{\partial t} + \frac{\mathrm{i}}{\hbar}H \right) |\psi(t)\rangle\,\mathrm{d}t. \tag{16}$$

The first term in (16) represents the main control goal, where P is the projection operator on the state corresponding to the target exit channel (i.e. the part of the wave function that is beyond the target saddle point on the ground-state surface and is characterized by the outgoing momentum); the second term is used to manage the fluence of the control field, with λ being a scalar weight factor; the third term includes an auxiliary state $|\chi(t)\rangle$ that is a Lagrange multiplier employed to enforce satisfaction of the Schrödinger equation (H is the 2×2 Hamiltonian matrix defined by (14)). In order to find the control field that maximizes the objective, the first-order functional derivatives of $\tilde{J}$ with respect to $\chi(\cdot)$, $\psi(\cdot)$ and $\varepsilon(\cdot)$ are set to zero, producing the following Euler–Lagrange equations:

$$\mathrm{i}\hbar\frac{\partial}{\partial t}|\psi(t)\rangle = H|\psi(t)\rangle, \quad |\psi(0)\rangle = |\psi_0\rangle, \tag{17}$$

$$\mathrm{i}\hbar\frac{\partial}{\partial t}|\chi(t)\rangle = H|\chi(t)\rangle, \quad |\chi(T)\rangle = P|\psi(T)\rangle, \tag{18}$$

$$\varepsilon(t) = -\frac{1}{\hbar\lambda}\Im\left\{ \langle \chi_\mathrm{g}(t)|\mu_\mathrm{ge}|\psi_\mathrm{e}(t)\rangle + \langle \chi_\mathrm{e}(t)|\mu_\mathrm{ge}|\psi_\mathrm{g}(t)\rangle \right\}. \tag{19}$$

An initial guess is selected for the control field (e.g. a pair of transform-limited pulses with a time delay between them, as in pump–dump control), and equations (17)–(19) are solved using an appropriate algorithm, as discussed in section 3.4 above. This optimization procedure identifies a shaped control field $\varepsilon_\mathrm{opt}(\cdot)$ that maximizes photoinduced molecular dissociation into the target channel. Successful application of QOCT to this model molecular system [114] demonstrated the benefits of optimally tailoring the time-dependent laser field to achieve the desired dynamic outcome.

3.6. Applications of QOCT

Originally, QOCT was developed to design optimal fields for manipulation of molecular systems [111]–[122] and has been applied to a myriad of problems (e.g. rotational, vibrational, electronic, reactive and other processes) [11, 14, 40]. Some recent applications include, for example, control of molecular isomerization [292]–[295], control of electron ring currents in chiral aromatic molecules [296], control of current flow patterns through molecular wires [297] and control of heterogeneous electron transfer from surface attached molecules into semiconductor band states [298]. Beyond molecules, QOCT has been applied to various physical objectives, including, for example, control of electron states in semiconductor quantum structures [299]–[301], control of atom transport in optical lattices [302], control of Bose–Einstein condensate transport in magnetic microtraps [303], control of a transition of ultracold atoms from the superfluid phase to a Mott insulator state [304], control of coherent population transfer in superconducting quantum interference devices [305] and control of the local electromagnetic response of nanostructured materials [306]. Recent interest has rapidly grown in applications of QOCT to the field of quantum information sciences, including optimal

protection of quantum systems against decoherence [188, 257], [307]–[317], optimal operation of quantum gates in closed systems [176, 177, 224, 253], [318]–[332] and in open systems (i.e. in the presence of decoherence) [184], [333]–[348], optimal generation of entanglement [266, 267, 347], [349]–[351] and optimal (i.e. maximum-rate) transfer of quantum information [352]. In a recent experiment with trapped ion qubits, shaped pulses designed using QOCT were applied to enact single-qubit gates with enhanced robustness to noise in the control field [353]. Optimal control methods were also applied to the problem of storage and retrieval of photonic states in atomic media, including both theoretical optimization [354]–[356] and experimental tests [357]–[359].

3.7. Advantages and limitations of QOCT

An advantage of QOCT relative to the laboratory method of AFC (to be discussed in detail in section 5) is that the former can be used to optimize a well-defined objective functional of virtually any form, while the latter relies on information obtained from measurements and thus is best suited to optimize expectation values of directly measurable observables. In numerical optimizations, there is practically no difference in effort between computing the expectation value of an observable, the density matrix or the evolution operator. In the laboratory, however, it is much more difficult to estimate a quantum state or, even more so, the evolution operator, than to measure the expectation value of an observable. Moreover, state estimation error increases rapidly with the Hilbert-space dimension [198, 360]. The very large number of measurements required for accurate quantum state/process tomography [202]–[205] renders (at least, presently) the use of adaptive laboratory methods for state/evolution-operator control rather impractical (although not impossible).

QOCT is often used to explore new quantum phenomena in relatively simple models to gain physical insights. The realization of quantum control is ultimately performed in the laboratory. In this context QOCT fits into what is called open-loop control. Generally, in open-loop control, a theoretical control design (e.g. obtained by using QOCT or another theoretical method) is implemented in the laboratory with the actual system. Unfortunately, there are not many problems for which theoretical control designs are directly applicable in the laboratory. QOCT is most useful when detailed knowledge of the system's Hamiltonian is available. Moreover, for open quantum systems, it is essential to know the details of the system–environment interaction. Therefore, the practical applicability of QOCT in the context of open-loop control is limited to very simple systems, i.e. mostly to cases when a small number of degrees of freedom can be controlled separately from the remainder of the system. This may be possible when the controlled subsystem has characteristic frequencies well separated from those of other transitions, and/or evolves on a time scale that is very different from that of the rest of the larger system. A well-known example of such a separately controllable subsystem is nuclear spins in a molecule, which can be very well controlled using RF fields without disturbing rotational, vibrational and electronic degrees of freedom. Another example is a subset of several discrete levels in an atom or diatomic molecule, the transitions between which can be controlled in a very precise way without any significant leakage of population to other states. However, for a majority of interesting physical and chemical phenomena, controlled systems are too complex and/or too strongly coupled to other degrees of freedom. For such complex systems, the accuracy of control designs obtained using model-based QOCT is usually inadequate, and hence laboratory AFC is generally the preferred strategy. In these situations, QOCT may be

more useful for feasibility analysis and exploration of control mechanisms, as basic features of the controlled dynamics can be identified in many cases even using relatively rough models.

4. Quantum control landscapes

An important practical goal of quantum control is the discovery of optimal solutions for manipulating quantum phenomena. Early studies [112, 185, 272] described conditions under which optimal solutions exist, but did not explore the complexity of finding them. Underlying the search for optimal controls is the landscape that specifies the physical objective as a function of the control variables. Analysis of quantum control landscapes [39] can not only establish the existence of optimal control solutions and determine their types (e.g. global versus local maxima and true maxima versus saddle points), but also deal with establishing necessary conditions for convergence of optimization algorithms to global maxima along with bounds on the scaling of convergence effort. Surprisingly, these properties are independent of details of a particular Hamiltonian (provided that the system is controllable), which makes the results of landscape analysis applicable across a wide range of controlled quantum phenomena.

4.1. Control landscape definition and critical points

Properties of the search space associated with Mayer-type cost functionals play a fundamental role in the ability to identify optimal controls. To characterize these properties, it is convenient to express the cost functional in a form where the dynamical constraints are implicitly satisfied. Consider a control problem with a fixed target time T for a closed quantum system with unitary evolution. Denote by $V_T : \varepsilon(\cdot) \mapsto U(T)$ the endpoint map from the space of control functions to the space of unitary evolution operators, induced by the Schrödinger equation (1), so that $U(T) = V_T(\varepsilon(\cdot))$. A Mayer-type cost functional $F(U(T))$ itself describes a map F from the space of evolution operators to the space of real-valued costs. Thus the composition of these maps, $J = F \circ V_T : \mathbb{K} \to \mathbb{R}$, is a map from the space of control functions to the space of real-valued costs. This map generates the functional $J[\varepsilon(\cdot)] = F(V_T(\varepsilon(\cdot)))$. We will refer to the functional $J[\varepsilon(\cdot)]$ as the *control landscape*. The optimal control problem may then be expressed as the unconstrained search for

$$J_{\text{opt}} = \max_{\varepsilon(\cdot)} J[\varepsilon(\cdot)]. \tag{20}$$

The topology of the control landscape (i.e. the character of its critical points, including local and global extrema) determines whether local search algorithms will converge to globally optimal solutions to the control problem [361]. Studies of quantum control landscape topology are presently an active research area [39], [179]–[181], [189], [191]–[194], [233, 362].

The critical points (extrema) of the landscape are controls, at which the first-order functional derivative of $J[\varepsilon(\cdot)]$ with respect to the control field is zero for all time, i.e.

$$\frac{\delta J[\varepsilon(\cdot)]}{\delta \varepsilon(t)} = 0, \quad \forall t \in [0, T]. \tag{21}$$

The critical manifold $\mathcal{M}$ of the control landscape is the collection of all critical points:

$$\mathcal{M} = \{\varepsilon(\cdot) \mid \delta J/\delta \varepsilon(t) = 0, \ \forall t \in [0, T]\}. \tag{22}$$

A central concept in landscape topology is the classification of a critical point as regular or singular [363, 364]. Most generally, a critical point of $J[\varepsilon(\cdot)]$ is regular if the map V_T is locally

surjective in its vicinity, i.e. if for any local increment $\delta U(T)$ in the evolution operator there exists an increment $\delta \varepsilon(\cdot)$ in the control function such that $V_T(\varepsilon(\cdot) + \delta \varepsilon(\cdot)) = V_T(\varepsilon(\cdot)) + \delta U(T)$. This condition is equivalent to requiring that the elements $\mu_{ij}(t)$ of the time-dependent dipole-operator matrix (in the Heisenberg picture) form a set of N^2 linearly independent functions of time [181]. In turn, this condition is satisfied for all non-constant admissible controls if and only if the quantum system is evolution-operator controllable [181, 226]. Note that for landscapes of some particular physical objectives the conditions for regularity of the critical points can be less stringent. For example, in the important special case of state-transition control, a critical point is regular if the matrix elements $\mu_{ij}(t)$ contain a set of just $2N - 1$ linearly independent functions of time. This condition is satisfied for all non-constant admissible controls if and only if the quantum system is pure-state controllable (which is a weaker condition than evolution-operator controllability, as discussed in section 3.3).

A critical point of $J[\varepsilon(\cdot)]$ is singular if the map V_T is not locally surjective in the point's vicinity. Using the chain rule, one obtains

$$\frac{\delta J}{\delta \varepsilon(t)} = \left\langle \nabla F(U(T)), \frac{\delta U(T)}{\delta \varepsilon(t)} \right\rangle, \tag{23}$$

where $\nabla F(U(T))$ is the gradient of F at $U(T)$, $\delta U(T)/\delta \varepsilon(t)$ is the first-order functional derivative of $U(T)$ with respect to the control field and $\langle A, B \rangle = \text{Tr}(A^\dagger B)$ is the Hilbert–Schmidt inner product. From (23), if a critical point of J is regular, $\nabla F(U(T))$ must be zero. A critical point is called kinematic if $\nabla F(U(T)) = 0$ and non-kinematic if $\nabla F(U(T)) \neq 0$. Thus, all regular critical points are kinematic. A singular critical point may be either kinematic or non-kinematic; in the latter case, $\delta J/\delta \varepsilon(t) = 0$ whereas $\nabla F(U(T)) \neq 0$ [364]. On quantum control landscapes, the measure of regular critical points appears to be much greater than that of singular ones [364]. Therefore attention has been focused on the characterization of regular critical points, and several important results have been obtained [39]. Nevertheless, singular critical points on quantum control landscapes have been recently studied theoretically [364] and demonstrated experimentally [365].

The condition for kinematic critical points, $\nabla F(U(T)) = 0$, can be cast in an explicit form for various types of quantum control problems. For evolution-operator control with the objective functional $J = F_1(U(T))$ of (7), this condition becomes [179, 180]

$$W^\dagger U(T) = U^\dagger(T) W, \tag{24}$$

i.e. $W^\dagger U(T)$ is required to be a Hermitian operator. It was shown [179, 180] that this condition implies $W^\dagger U(T) = Y^\dagger(-I_m \oplus I_{N-m})Y$, where Y is an arbitrary unitary transformation and $m = 0, 1, \ldots, N$. There are $N + 1$ distinct critical submanifolds labeled by m, with corresponding critical values of J given by $J_m = 1 - (2m/N)$. The global optima corresponding to $m = 0$ and N (with $J_0 = 1$ and $J_N = -1$, respectively) are isolated points, while local extrema corresponding to $m = 1, 2, \ldots, N - 1$ are smooth, compact, Grassmannian submanifolds embedded in $U(N)$. It can be shown that all regular local extrema are saddle-point regions [180].

For observable control with the objective functional $J = F_3(U(T))$ of (9), the condition for a kinematic critical point becomes [189, 193, 233]

$$[U(T)\rho_0 U^\dagger(T), \Theta] = 0, \tag{25}$$

i.e. the density matrix at the final time is required to commute with the target observable operator. This condition was studied in the context of optimization of Lagrange-type cost functionals with an endpoint constraint [362, 366, 367] as well as in the context of regular

critical points for Mayer-type cost functionals [189, 233]. Let R and S denote unitary matrices that diagonalize ρ_0 and Θ, respectively, and define $\tilde{U}(T) = S^\dagger U(T) R$. Condition (25) that $\rho(T)$ and Θ commute is equivalent to the condition that the matrix $\tilde{U}(T)$ is in the double coset $\mathcal{M}_\pi$ of some permutation matrix P_π [191]:

$$\tilde{U}(T) \in \mathcal{M}_\pi = \mathrm{U}(\mathbf{n}) P_\pi \mathrm{U}(\mathbf{m}). \tag{26}$$

Here, $\mathrm{U}(\mathbf{n})$ is the product group $\mathrm{U}(n_1) \times \cdots \times \mathrm{U}(n_r)$, where $\mathrm{U}(n_l)$ corresponds to the lth eigenvalue of ρ_0 with n_l-fold degeneracy, and $\mathrm{U}(\mathbf{m})$ is the product group $\mathrm{U}(m_1) \times \cdots \times \mathrm{U}(m_s)$, where $\mathrm{U}(m_l)$ corresponds to the lth eigenvalue of Θ with m_l-fold degeneracy. Thus, each critical submanifold $\mathcal{M}_\pi$ corresponds to a particular choice of the permutation π. All permutations on N indices form the symmetric group $\mathfrak{S}_N$, and the entire critical manifold $\mathcal{M}$ is given by $\mathcal{M} = \bigcup_{\pi \in \mathfrak{S}_N} \mathcal{M}_\pi$. The structure of $\mathcal{M}$ depends on any degeneracies in the spectra of ρ_0 and Θ. When both ρ_0 and Θ are fully nondegenerate, then $\mathrm{U}(\mathbf{n}) = \mathrm{U}(\mathbf{m}) = [\mathrm{U}(1)]^N$, and $\mathcal{M}$ consists of $N!$ disjoint N-dimensional tori, labeled by the permutation matrices. The occurrence of degeneracies in the spectra of ρ_0 and Θ will merge two or more tori together, thereby reducing the number of disjoint critical submanifolds and increasing their dimensions [191].

4.2. Optimality of control solutions

Satisfaction of condition (21) for a critical point is a necessary but not sufficient condition for optimality of a control [166, 223]. For Mayer-type cost functionals, a sufficient condition for optimality is negative semidefiniteness of the Hessian of J, which is defined as

$$\mathcal{H}(t, t') := \frac{\delta^2 J}{\delta \varepsilon(t') \delta \varepsilon(t)}. \tag{27}$$

The characteristics of critical points (in particular, the presence or absence of local optima) are important for the convergence properties of search algorithms [39]. To classify critical points as global maxima and minima, local maxima and minima, and saddle points, one examines the second-order variation in J for an arbitrary control variation $\delta \varepsilon(\cdot)$, which for Mayer-type functionals can be written as

$$\delta^2 J = \mathcal{Q}_F(\delta U(T), \delta U(T)) + \langle \nabla F(U(T)), \delta^2 U(T) \rangle, \tag{28}$$

where $\delta U(T)$ and $\delta^2 U(T)$ are the first- and second-order variations, respectively, of $U(T)$ caused by a control variation $\delta \varepsilon(\cdot)$, and $\mathcal{Q}_F$ is the Hessian quadratic form of $F(U)$. Assuming that the critical point $\varepsilon(\cdot)$ is regular, one obtains

$$\delta^2 J = \mathcal{Q}_F(\delta U(T), \delta U(T)). \tag{29}$$

Explicit expressions for the Hessian and/or Hessian quadratic form were obtained for evolution-operator control [179]–[181] and observable control [190, 361].

    The optimality of regular critical points can be determined by inspecting the number of positive, negative and null eigenvalues of the Hessian (or, equivalently, the coefficients of the Hessian quadratic form when written in a diagonal basis). An issue of special interest is to determine whether any of the regular critical points are local maxima (frequently referred to as local traps due to their ability to halt searches guided by gradient algorithms before reaching the global maximum). Detailed analyses for evolution-operator control and observable control reveal [39], [179]–[181], [190, 361] that all regular optima are global and the remainder of regular critical points (i.e. except for the global maximum and global minimum) are saddles.

This discovery means that no local traps exist in the control landscapes of controllable closed quantum systems. The same result was also obtained for observable-control landscapes of controllable open quantum systems with Kraus-map dynamics [273]. Due attention still needs to be given to consideration of singular critical points, although numerical evidence suggests that their effect on optimization is likely insignificant [364].

4.3. Pareto optimality for multi-objective control

Many practical quantum control problems seek to optimize multiple, often competing, objectives. In such situations the usual notion of optimality is replaced by that of Pareto optimality. The *Pareto front* of a multi-objective control problem is the set of all controls such that all other controls have a lower value for at least one of the objectives [220]–[222]. The analysis of the Pareto front reveals the nature of conflicts and tradeoffs between different control objectives. The structure of the landscape for multi-observable control is of interest and follows directly from that of single-observable control [217]. Of particular relevance to many chemical and physical applications is the problem of simultaneous maximization of the expectation values of multiple observables. Such simultaneous maximization is possible if the intersection $\bigcap_k \mathcal{M}_k^{(\max)}$ (where $\mathcal{M}_k^{(\max)}$ is the maximum submanifold for the kth observable) is nonempty and a point in the intersection can be reached under some control $\varepsilon(\cdot)$; in this regard, the dimension of the intersection manifold $\bigcap_k \mathcal{M}_k^{(\max)}$ has been analyzed [218]. It has been shown that the common QOCT technique of running many independent maximizations of a cost functional like (10) (using different weight coefficients $\{\alpha_k\}$) is incapable of sampling many regions of the Pareto front [218]. Alternative methods for Pareto front sampling are discussed further below.

4.4. Landscape exploration via homotopy trajectory control

The absence of local traps in landscapes for observable control and evolution-operator control with Mayer-type cost functionals has important implications for the design of optimization algorithms. Many practical applications require algorithms capable of searching quantum control landscapes for optimal solutions that satisfy additional criteria, such as minimization of the field fluence or maximization of the robustness to laser noise. So-called *homotopy trajectory control* algorithms (in particular, diffeomorphic modulation under observable-response-preserving homotopy, or D-MORPH) [284]–[286] can follow paths to the global maximum of a Mayer-type cost functional, exploiting the trap-free nature of the control landscape, while locally optimizing auxiliary costs. The essential prerequisite for successful use of these algorithms is the existence of a connected path between the initial and target controls. Homotopy trajectory control is closely related to the notion of a level set that is defined as the collection of controls that all produce the same value of the cost functional J. Theoretical analysis [39, 285, 286] predicts that for controllable quantum systems each level set is a continuous manifold. A homotopy trajectory algorithm is able to move on such a manifold exploring different control solutions that result in the same value of the cost functional, but may differ in other properties (e.g. field fluence or robustness). A version of the D-MORPH algorithm was also developed for evolution-operator control of closed quantum systems; it was able to identify optimal controls generating a target unitary transformation up to machine precision [324].

Homotopy trajectory algorithms are also very useful for exploring quantum control landscapes for multiple objectives. For example, in order to track paths in the space of expectation values of multiple observables while locally minimizing a Lagrange-type cost, multi-observable trajectory control algorithms were developed [217]. Such algorithms are generally applicable to the treatment of multi-objective quantum control problems (Pareto quantum optimal control) [218]. They can traverse the Pareto front to identify admissible tradeoffs in optimization of multiple control objectives (e.g. maximization of multiple observable expectation values). This method can continuously sample the Pareto front during the course of one optimization run [218] and thus can be more efficient than the use of standard QOCT with cost functionals of the form (10). Also, the D-MORPH algorithm was recently extended to handle optimal control problems involving multiple quantum systems and multiple objectives [219].

4.5. Practical importance of control landscape analysis

The absence of local traps in control landscapes of controllable quantum systems has very important implications for the feasibility of AFC experiments (see section 5). The relationship between the quantum control landscape structure and optimization complexity of algorithms used in AFC has been the subject of recent theoretical analyses [39], [368]–[370]. Results of these studies support the vast empirical evidence [361] indicating that the favorable landscape topology strongly correlates with fast mean convergence times to the global optimum. The trap-free control landscape topology also ensures convergence of gradient-based optimization algorithms to the global maximum. These algorithms can be used to search for optimal solutions to a variety of quantum control problems. In addition to theoretical studies (mostly using QOCT), gradient algorithms are also applicable in quantum control experiments [371], provided that measurement of the gradient is sufficiently robust to laser and detection noise. The use of deterministic algorithms in AFC experiments is discussed in more detail in section 5.19.

4.6. Experimental observation of quantum control landscapes

Significant efforts have been recently devoted to experimental observation of quantum control landscapes, aiming both at testing the predictions of the theoretical analysis and at obtaining a better understanding of control mechanisms. Roslund *et al* [372] observed quantum control level sets for maximization of non-resonant two-photon absorption in a molecule and second harmonic generation (SHG) in a nonlinear crystal and found them to be continuous manifolds (closed surfaces) in the control landscape. A diverse family of control mechanisms was encountered, as each of the multiple control fields forming a level set preserves the observable value by exciting a distinct pattern of constructive and destructive quantum interferences.

Wollenhaupt, Baumert and co-workers [373, 374] used parameterized pulse shapes to reduce the dimensionality of the optimization problem (maximization of the Autler–Townes contrast in strong-field ionization of potassium atoms) and observed the corresponding two-dimensional quantum control landscape. In order to better understand the performance of AFC, the evolution of different optimization procedures was visualized by means of trajectories on the surface of the measured control landscape. Marquetand *et al* [375] observed a two-dimensional quantum control landscape (for maximization of the retinal photoisomerization yield in bacteriorhodopsin) and used it to elucidate the properties of molecular wave-packet evolution on an excited potential energy surface.

The theoretical analysis of control landscape topology has been carried out with no constraints placed on the controls (see section 4.1). A main conclusion from these studies is the inherent lack of local traps on quantum control landscapes under normal circumstances. Recently, Roslund and Rabitz [376] experimentally demonstrated the trap-free monotonic character of control landscapes for optimization of frequency unfiltered and filtered SHG. For unfiltered SHG, the landscape was randomly sampled and interpolation of the data was found to be devoid of traps up to the level of data noise. In the case of narrow-band-filtered SHG, trajectories taken on the landscape revealed the absence of traps, although a rich local structure was observed on the landscape in this case. Despite the inherent trap-free nature of the landscapes, significant constraints on the controls can distort and/or isolate portions of the erstwhile trap-free landscape to produce apparent (i.e. false) traps [376]. Such artificial structure arising from the forced sampling of the landscape has been seen in some experimental studies [373]–[375], in which the number of control variables was purposely reduced.

5. AFC in the laboratory

There are important differences between quantum control theory and its experimental implementation. Control solutions obtained in theoretical studies strongly depend on the employed model Hamiltonian. However, for real systems controlled in the laboratory, the Hamiltonians usually are not known well (except for the simplest cases), and the Hamiltonians for the system–environment coupling are known to an even lesser degree. An additional difficulty is the computational complexity of accurately solving the optimal control equations for realistic polyatomic molecules. Another important difference between control theory and experiment arises from the difficulty of reliably implementing theoretical control designs in the laboratory, due to instrumental noise and other limitations. As a result, optimal theoretical control designs generally will not be optimal in the laboratory. Notwithstanding these comments, control simulations continue to be very valuable, and they even set forth the logic leading to practical laboratory control as explained below.

A crucial step towards selective laser control of physical and chemical phenomena on the quantum scale was the introduction of AFC (also referred to as closed-loop laboratory control or learning control). AFC was proposed and theoretically grounded by Judson and Rabitz in their paper 'Teaching lasers to control molecules' in 1992 [377]. In AFC, a loop is closed in the laboratory, with results of measurements on the quantum system used to evaluate the success of the applied control and to refine it, until the control objective is reached as best as possible. At each cycle of the loop, the external control (e.g. a shaped laser pulse) is applied to the system (e.g. an ensemble of molecules). The signal (e.g. the yield of a particular reaction product or population in a target state) is detected and fed back to the learning algorithm (e.g. a genetic algorithm). The algorithm evaluates each control based on its measured outcome with respect to a predefined control goal, and searches through the space of available controls to move towards an optimal solution.

While AFC can be simulated on the computer [377]–[390], the important advantage of this approach lies in its ability to be directly implemented in the laboratory. Most importantly, the optimization is performed in the laboratory with the actual system, and thus is independent of any model. As a result, the AFC method works remarkably well for systems even of high complexity, including, for example, large polyatomic molecules in the liquid phase, for which only very rough models are available. Secondly, there is no need to measure the laser field

in AFC, because any systematic characterization of the control 'knobs' (such as pulse shaper parameters) is sufficient. This set of control 'knobs' determined by the experimental apparatus defines the parameter space searched by the learning algorithm for an optimal laser shape. This procedure naturally incorporates any laboratory constraints on the control laser fields. Thirdly, optimal controls identified in AFC are characterized by a natural degree of robustness to instrumental noise, since non-robust solutions will be rejected by the algorithm. Fourthly, in AFC, it is possible to operate at a high-duty cycle of hundreds or even thousands of experiments per second, by exploiting (i) the conceptual advantage of the evolving quantum system solving its own Schrödinger equation in the fastest possible fashion and (ii) the technological advantage of high-repetition-rate pulsed laser systems under full automation. Fifthly, in AFC, a new quantum ensemble (e.g. a new molecular sample) is used in each cycle of the loop, which completely avoids the issue of back action exerted by the measurement process on a quantum system. Thus AFC is technologically distinct from measurement-based RTFC [391]–[396], in which the same quantum system is manipulated until the final target objective is reached and for which measurement back action is an important effect that needs to be taken into account (see section 7).

5.1. Femtosecond pulse-shaping technology

The majority of current AFC experiments employ shaped ultrafast laser pulses. In such experiments, one usually starts with a random or nearly random selection of trial shaped pulses of length $\sim 10^{-13}$ s or less. The pulses are shaped by modulating the phases and/or amplitudes of the spatially resolved spectral components, for example, by means of a liquid crystal modulator (LCM), an acousto-optic modulator (AOM) or a micromechanical mirror array. The experiments employ fully automated computer control of the pulse shapes guided by a learning algorithm. The shaped laser pulses produced by this method can be viewed as 'photonic reagents,' which interact with matter at the atomic or molecular scale to facilitate desired controlled outcomes of various physical and chemical phenomena.

Significant femtosecond pulse-shaping capabilities were already available in the early 1990s, with the development of a programmable multi-element liquid-crystal phase modulator that operated on a millisecond time scale [397]. Devices with two LCMs made possible simultaneous and independent phase and amplitude modulation of spectral components [398, 399]. Similar capabilities are also available with AOM-based pulse shapers [400]. These and other developments have been reviewed [4, 5, 12, 27]. During the last decade, physical and chemical applications of AFC motivated further advances in femtosecond pulse-shaping technology, including arbitrary amplitude and phase modulation in an acousto-optic programmable dispersive filter [401], enhanced resolution of LCMs [402, 403], compact and robust pulse shaping [404], pulse-shape modulation at nanosecond time scales using an electro-optical gallium arsenide array with controlled waveguides [405] and spectral line-by-line pulse shaping [406, 407]. The development of polarization pulse shaping [408, 409] brought an additional dimension to control of quantum phenomena, which is particularly important in some applications (e.g. for increasing the yield of multiphoton ionization in molecules); recent improvements in this area also include full control of the spectral polarization of ultrashort laser pulses [410], simultaneous phase, amplitude and polarization shaping [411]–[415], and a simplified ultrafast polarization shaper using a birefringent prism [416]. Most recently, the shaping of ultraviolet (UV) femtosecond pulses has been demonstrated, including phase

modulation [417], simultaneous phase and amplitude modulation [418], and polarization shaping [419, 420].

5.2. Optical applications of AFC

The AFC approach can be used to produce optical fields with prescribed properties, which, in turn, can be applied to control physical and chemical phenomena (e.g. in atoms, molecules and semiconductor structures). In particular, some of the earliest AFC experiments aimed at the maximal compression of femtosecond laser pulses [421]–[426]. In these experiments, the light produced through SHG of the shaped pulse in a thin nonlinear crystal served as the feedback signal. The SHG yield is directly proportional to the intensity of the incident light pulse, and, for pulses with a fixed energy, the most intense pulse is the shortest one. AFC-optimized compression of broadband laser pulses was also demonstrated using a feedback signal derived from two-photon absorption in semiconductors [427]. Application of AFC makes it possible to generate maximally compressed laser pulses in a simple and effective way, without requiring knowledge of the input pulse's shape. Such adaptive pulse compressors (with AOM-based pulse shapers and SHG-based feedback signal) are now employed as built-in components in some commercially available femtosecond amplification systems. However, since the amplification process is nearly linear, the full-scale application of AFC is usually not necessary, as pulses can be compressed in a single feedback step using spectral interferometry. The resulting transform-limited pulses can be used as a starting point for the study and control of various photophysical and photochemical processes (e.g. they can be used to excite and track localized fine structure and Rydberg wave packets in atoms and vibrational wave packets in molecules). In many AFC experiments, transform-limited pulses are used as a reference to separate the intensity dependence which is ubiquitous in nonlinear processes.

Another optical application of AFC is optimal amplification of chirped femtosecond laser pulses [428, 429]. The AFC method is used to minimize the higher-order phase dispersion that is inherent in the amplification process. Furthermore, AFC was applied to generate almost arbitrary target temporal shapes starting with uncharacterized input pulses [430, 431]. These experiments used a cross-correlation measurement [430] and electric field characterization via frequency-resolved optical gating [431] of the output pulses as the feedback signal. As polarization-shaping technology for femtosecond laser pulses developed [408, 409], AFC was used to generate pulses with target polarization profiles [432, 433]. One experiment [432] used the SHG feedback signal to compensate for material dispersion and time-dependent modulation of the polarization state. Another experiment [433] employed a sophisticated feedback signal based on dual-channel spectral interferometry to generate shaped femtosecond pulses whose ellipticity increased at a constant rate. In a further development, a recent experiment [434] used polarization-shaped laser pulses and AFC to manipulate the optical near field on a nanometer scale.

5.3. AFC of high-harmonic generation

Among important physical applications of AFC is coherent manipulation of soft x-rays produced via high-harmonic generation. In a pioneering experiment, Murnane, Kapteyn and co-workers [435] used shaped ultrashort, intense laser pulses (with 6–8 optical cycles) for AFC of high-harmonic generation in atomic gases. Their results demonstrate that optimally shaped

laser pulses identified by the learning algorithm can improve the efficiency of x-ray generation by an order of magnitude, manipulate the spectral characteristics of the emitted radiation and 'channel' the interaction between nonlinear processes of different orders. All these effects result from complex interferences between the quantum amplitudes of the atomic states, created by the external laser field. The learning algorithm guides the pulse shaper to tailor the laser field to produce the optimal interference pattern. Several consequent AFC experiments [436]–[438] explored various aspects of optimal high-harmonic generation in atomic gases, including the analysis of the control mechanism via a comparison of experimental data with predictions of theoretical models. Further experimental studies used AFC for optimal spatial control of high-harmonic generation in hollow fibers [439, 440], optimal control of the brilliance of high-harmonic generation in gas jet and capillary setups [441], and optimal control of the spectral shape of coherent soft x-rays [442]. The latter work [442] was a precursor to a more recent development, in which spectrally shaped femtosecond x-ray fields were themselves used to adaptively control photofragmentation yields of SF_6 [443]. Advances in the optimal control of high-harmonic generation (including related AFC experiments) have been recently reviewed [35, 41].

Beyond the physical interest in achieving control over high-harmonic generation, these experiments also demonstrated a dramatic degree of inherent robustness to laser-field noise in strongly nonlinear control. This behavior can be understood in terms of an extensive null space of the Hessian at the top of the control landscape, implying a very gentle slope near the global maximum [190, 194]. This characteristic of the quantum control landscape makes it possible to tolerate much of the laser noise while maintaining a high control yield. Such robustness is expected to be a key attractive feature of observable control across virtually all quantum phenomena.

5.4. AFC of multiphoton transitions in atoms

Control of bound-to-bound multiphoton transitions in atoms with optimally shaped femtosecond laser pulses provides a vivid illustration of the control mechanism based on multi-pathway quantum interference. Non-resonant multiphoton transitions involve many routes through a continuum of virtual levels. The interference pattern excited by the multiple frequency components of the control pulse can enhance or diminish the total transition probability. The interference effect depends on the spectral phase distribution of the laser pulse. A number of experiments [444]–[446] used AFC to identify pulse shapes that are optimal for enhancing or canceling the probability of making a transition. In particular, it was possible to tailor *dark pulses* that do not excite the atom at all due to destructive quantum interference. On the other hand, AFC was able to find shaped pulses that induce transitions as effectively as transform-limited pulses, even though their peak intensities are much lower. Due to the relative simplicity of the atomic systems studied, it was possible to compare the results of the AFC experiments with theoretical predictions and verify the control mechanism based on quantum interference of multiple laser-driven transition amplitudes. In a related experiment [447], AFC was helpful for demonstrating that transform-limited pulses are not optimal for inducing resonant multiphoton transitions. It was shown that optimally shaped pulses enhance resonant multiphoton transitions significantly beyond the level achieved by maximizing the pulse's peak intensity. A recent experiment [448] considered non-resonant multiphoton absorption in atomic sodium in the strong-field limit. It was demonstrated that in this regime the stimulated emission induced by the

dynamic Stark shift becomes important, which makes transform-limited pulses not optimal for strong-field non-resonant multiphoton transitions. AFC was used to discover strong-field shaped laser pulses that optimally counteract the dynamic Stark shift-induced stimulated emission and thus maximize the absorption probability.

A more complex problem in atomic physics is control of multiphoton ionization. In one experiment [449], AFC was applied to optimize multiphoton ionization of atomic calcium by shaped femtosecond laser pulses. The feedback signals were measured using ion and electron spectroscopy, and the optimization results were used to elucidate the intermediate resonances involved in the photoionization process. Another experiment [450] studied photoionization of potassium atoms controlled by phase-locked pairs of intense femtosecond laser pulses. Measurements of the Autler–Townes doublet in the photoelectron spectra enabled analysis of the induced transient processes. The AFC experimental results were helpful for exploring the control mechanism based on the selective population of dressed states.

5.5. AFC of Rydberg wave packets in atoms

In one of the first applications of AFC, in 1999, Bucksbaum and co-workers [451] manipulated the shape of an atomic radial wave function (a so-called Rydberg wave packet). Non-stationary Rydberg wave packets were created by irradiating cesium atoms with shaped ultrafast laser pulses. A variation of the quantum holography method [452] was used to measure the atomic radial wave function generated by the laser pulse. In order to reconstruct the wave function, the amplitude of each energy eigenstate in the total wave packet was measured independently via state selective field ionization. The distance between the measured and target wave packet provided the feedback signal. In the weak-field limit, a simple linear relationship exists between the amplitudes of the energy eigenstates in the wave-packet decomposition and the amplitudes of the corresponding spectral components of the control laser field. Based on this relationship, a simple gradient-type algorithm was employed to adjust the spectral phase distribution of the control field. AFC equipped with this algorithm was able to change the shape of the Rydberg wave packet to match the target within two iterations of the feedback control loop. If the wave packet is created in the strong-field regime, then a more sophisticated learning algorithm is generally required to implement AFC.

5.6. AFC of electronic excitations in molecules

The first AFC experiment was reported in 1997 by Wilson and co-workers [123]. Femtosecond laser pulses shaped by a computer-controlled AOM were used to excite an electronic transition in molecules (laser dye IR125 in methanol solution). The measured fluorescence served as the feedback signal in AFC to optimize the population transfer from the ground to the first excited molecular electronic state. Both excitation efficiency (the ratio of the excited-state population to the laser energy) and effectiveness (the total excited-state population) were optimized. Similar AFC experiments were later performed with different molecules in the liquid phase: laser dyes LDS750 in acetonitrile and ethanol solutions [453], DCM in methanol solution [454], rhodamine 101 in methanol solution [455], coumarin 515 in ethanol solution [456], coumarin 6 in a range of non-polar solvents (linear and cyclic alkanes) [457], the charge-transfer coordination complex $[Ru(dpb)_3](PF_6)_2$ (where dpb is 4,4′-diphenyl-2,2′-bipyridine) in methanol solution [458] and acetonitrile solution [459]–[461], a donor–acceptor

macromolecule (a phenylene ethynylene dendrimer tethered to perylene) in dichloromethane solution [462] and perylene in chloroform solution [463]. Two-photon electronic excitations in flavin mononucleotide (FMN) in aqueous solution were controlled using multi-objective optimization (a genetic algorithm was employed to simultaneously maximize the fluorescence intensity and the ratio of fluorescence and SHG intensities) [464]. Molecular electronic excitations were also optimized in AFC experiments in the solid state, with a crystal of α-perylene [463, 465].

Since these AFC experiments are performed in the condensed phase, an important issue is the degree of coherence of the controlled dynamics. This issue has been recently explored in a series of AFC experiments [457], in which the level of attained control was investigated by systematically varying properties of the environment. Specifically, AFC was applied to optimize the stimulated emission from coumarin 6 (a laser dye molecule) dissolved in cyclohexane, and the recorded optimal pulse shape (characterized by a significantly nonlinear negative chirp) was used with several other solvents (linear and cyclic alkanes). In these experiments, the molecule was excited in the linear absorption regime in order to exclude the trivial intensity dependence characteristic of multiphoton processes. The results revealed an inverse correlation between the obtained degree of control (as measured by the enhancement of stimulated emission relative to that achieved by excitation with the transform-limited pulse) and the viscosity of the solvent. This study indicates that the control mechanism involves a coherent process (i.e. based on quantum interference of coherent pathways) and that environmentally induced decoherence limits the leverage of control on the particular molecular system. Also, in a recent AFC experiment [462], the photoemission yield of a donor–acceptor macromolecule was maximized, and a coherent control mechanism was identified by analyzing the pulse optimization process and optimal pulse features. Another AFC experiment [466] controlled FMN and riboflavin (RBF) dissolved in water, through a vibronic transition driven by a shaped 400 nm control pulse followed by a delayed 800 nm pulse that produced irreversible further excitation. Fluorescence depletion served as a feedback signal. The experiment only functioned when the delay between the two pulses was less than ~ 1 ps, indicating that the underlying control mechanism employs coherent dynamics (see further discussion of this experiment in section 5.12).

5.7. AFC of photodissociation reactions in molecules

A long-standing goal of photochemistry is selective control of molecular fragmentation. During the last decade, AFC employing shaped femtosecond laser pulses has been applied to achieve significant successes towards meeting this goal [18, 26, 37]. Selective quantum control of photodissociation reactions in molecules using AFC was first demonstrated by Gerber and co-workers in 1998 [124]. They studied photodissociation of the organometallic complex $CpFe(CO)_2Cl$ (where $Cp = C_5H_5$) that contains particular types of iron–ligand bonds and exhibits different fragmentation channels upon excitation with shaped femtosecond laser pulses. The branching ratio $[CpFe(CO)Cl]^+/[FeCl]^+$ was maximized and minimized in AFC experiments employing an evolutionary algorithm. The experiment was performed in a molecular beam, and the feedback signal was obtained from measurements of the ionized photofragments in a time-of-flight mass spectrometer. Using AFC, it was possible to change the branching ratio between $5:1$ and $1:1$.

The success of the AFC experiment described above triggered an ongoing wave of research activity in this area. In particular, Gerber's group explored various aspects of AFC

of photodissociation and photoionization reactions in molecules. In one AFC experiment [467], the relative yields of photodissociation and photoionization of iron pentacarbonyl, $Fe(CO)_5$, were controlled in the gas phase, using femtosecond laser pulses with carrier wavelengths at 800 and 400 nm (the latter produced via SHG of the former). The AFC-based optimization (both maximization and minimization) of the branching ratio $[Fe(CO)_5]^+/Fe^+$ demonstrated that the control mechanism is not simply intensity dependent, but rather employs the spectral phase distribution of the shaped laser pulse to steer the dynamics of the excited molecular vibrational wave packet towards the target reaction channel. Another gas-phase AFC experiment [468] also analyzed the relative importance of intensity-dependent and coherent effects in the control of photochemical reactions that involve nonlinear (multiphoton) optical excitations. The control goals were the direct photoionization of $CpFe(CO)_2Cl$ (i.e. maximization of the $[CpFe(CO)_2Cl]^+$ yield) and selective photofragmentation (i.e. maximization of the branching ratio $[CpFe(CO)Cl]^+/[FeCl]^+$). For each pulse shape during the AFC-based optimization, target reaction yield and SHG efficiency (which is directly proportional to pulse intensity) were recorded. In the case of direct ionization control, a clear correlation between $[CpFe(CO)_2Cl]^+$ yield and SHG efficiency was observed, which implies that the photoionization control mechanism is mainly intensity dependent. However, for fragmentation control, no correlation between $[CpFe(CO)Cl]^+/[FeCl]^+$ ratio and SHG efficiency was found. Moreover, for different pulses with the same SHG intensity, a large range of different $[CpFe(CO)Cl]^+/[FeCl]^+$ values was obtained, depending on the specific pulse shape. These results indicate that while photofragmentation involves multiphoton excitation, it is not regulated by the pulse intensity alone. Rather, the control mechanism for a particular photofragmentation reaction requires a specially tailored laser pulse to guide the complex wave-packet dynamics towards the desired outcome. Results of a similar AFC experiment [469] that analyzed photofragmentation of CH_2ClBr in the gas phase (including maximization and minimization of the $[CH_2Br]^+/[CH_2Cl]^+$ ratio) also indicate that the control mechanism involves manipulation of the wave-packet dynamics on neutral dissociative surfaces rather than purely intensity-dependent effects. Experiments that demonstrated AFC of photofragmentation in the molecules $CpFe(CO)_2Cl$ and $CpFe(CO)_2Br$ [470] will be discussed later in the context of optimal dynamic discrimination (ODD) of similar quantum systems.

In 2001, Levis and co-workers [471] used AFC with shaped, strong-field laser pulses to demonstrate selective cleavage and rearrangement of chemical bonds in polyatomic organic molecules (in the gas phase), including $(CH_3)_2CO$ (acetone), CH_3COCF_3 (trifluoroacetone) and $C_6H_5COCH_3$ (acetophenone). Control over the formation of CH_3CO from $(CH_3)_2CO$, CF_3 or CH_3 from CH_3COCF_3, and $C_6H_5CH_3$ (toluene) from $C_6H_5COCH_3$ was achieved with high selectivity. The use of strong laser fields (with intensities of about $10^{13}\,W\,cm^{-2}$) helps to effectively increase the available bandwidth, as transitions to excited molecular states are facilitated by the dynamic Stark shift. This effect opens up many reaction pathways that are inaccessible in the weak-field (perturbative) regime due to resonant spectral restrictions [18]. While theoretical treatment of the complex strong-field molecular dynamics is extremely difficult, this complexity in no way affects employment of AFC in the laboratory, where the molecule solves its own Schrödinger equation on a femtosecond time scale. By operating at a high-duty control cycle, a learning algorithm is typically able to identify optimal laser pulses in a matter of minutes.

Significant attention has been devoted to the analysis of quantum dynamical processes involved in molecular photofragmentation control achieved in gas-phase AFC

experiments with shaped femtosecond laser pulses. Wöste and co-workers [472]–[474] studied mechanisms of photofragmentation control for $CpMn(CO)_3$ optimizing the branching ratios $[CpMn(CO)]^+/[CpMn(CO)_3]^+$ and $[CpMn(CO)_2]^+/[CpMn(CO)_3]^+$. Weinacht and co-workers [475]–[478] analyzed mechanisms underlying control of photofragmentation in a series of AFC experiments with similar molecules: CH_3COCF_3 (trifluoroacetone), CH_3COCCl_3 (trichloroacetone) and CH_3COCD_3 (tri-deuterated acetone). The yield of the $[CX_3]^+$ fragment and the $[CX_3]^+/[CH_3]^+$ ratio (where X is F, Cl and D for trifluoroacetone, trichloroacetone and tri-deuterated acetone, respectively) were optimized in these AFC experiments using intense shaped laser pulses. AFC was also used to optimize the branching ratios $Br^+/[CH_2Br]^+$ and $[CH_2I]^+/[CH_2Br]^+$ in photofragmentation of CH_2BrI (bromoiodomethane) [478, 479]. In a number of works [472], [474]–[476], AFC experiments were supplemented by theoretical *ab initio* quantum calculations to help clarify photofragmentation control mechanisms. In several other studies [477]–[479], a change in the basis of the control variables made it possible to reduce the dimension of the search space and thus elucidate control mechanisms of selective molecular photofragmentation. In another work [480], pump–probe spectroscopy was utilized to explore the control mechanism of photofragmentation of $CHBr_2COCF_3$ (1,1-3,3,3 dibromo-trifluoroacetone) in AFC experiments with intense shaped laser pulses. In particular, optimization of the $[CF_3]^+/[CHBr_2]^+$ ratio revealed a charge-transfer-based control mechanism.

Selective control of molecular fragmentation in the gas phase was demonstrated in several other AFC experiments with shaped femtosecond laser pulses. Wöste and co-workers [481]–[484] controlled the photoionization and photofragmentation dynamics of alkali clusters. Jones and co-workers [485] optimized the S_N^+/S_M^+ ratios for various N and M values in the strong-field photofragmentation of S_8 molecules. It was found that optimally shaped pulses dramatically outperform the transform-limited pulses. Wells *et al* [486] controlled the vibrational population distribution in transient CO^{2+} to manipulate the branching ratio of the CO^{2+} and $C^+ + O^+$ products. Hill and co-workers [487] controlled the amplitude of the bending vibrational mode in highly ionized CO_2 (during strong-field Coulomb explosion) to enhance the symmetric six-electron fragmentation channel, $CO_2^{6+} \rightarrow O^{2+} + C^{2+} + O^{2+}$. They constrained the search space by expressing the spectral phase of the laser pulse as a Taylor series, in order to elucidate the controlled photodissociation dynamics. Laarmann *et al* [488, 489] achieved selective cleavage of strong backbone bonds in amino acid complexes (in particular, a peptide bond in Ac-Phe-NHMe and Ac-Ala-NHMe), while keeping weaker bonds intact. Based on these results, they suggested the possibility of employing AFC with optimally tailored laser pulses as an analytical tool in the mass spectrometry of complex polyatomic systems (with potential applicability e.g. to protein sequencing of large biopolymers). In a recent AFC experiment, Levis and co-workers [490] used intense laser pulses to manipulate the branching ratios of various photofragmentation products of dimethyl methylphosphonate, a simulant for the nerve agent sarin. The optimization in this experiment was performed in the presence of a high background of a hydrocarbon and water in the extraction region of a time-of-flight mass spectrometer. The ability to achieve highly selective control under these conditions demonstrates that AFC may provide the means to identify complex airborne molecules. As mentioned in section 5.3, photofragmentation of SF_6 was controlled (including optimization of the ratio $[SF_5]^+/[SF_3]^+$) in an AFC experiment [443] that used spectrally shaped femtosecond x-ray fields produced from intense shaped laser pulses via high-harmonic generation.

Recently, Dantus and co-workers [491, 492] reported a study of molecular fragmentation using intense femtosecond pulses, in which they did not use algorithm-guided AFC, but

rather evaluated a large set of predetermined pulse shapes. They concluded that the yields of photofragmentation products are mainly controlled by the pulse intensity, while the details of the pulse shape (e.g. the spectral phase distribution) are not important. The contradiction between this conclusion and the results of numerous AFC experiments discussed above appears to be explained by the fact that Dantus and co-workers often performed their measurements [491] at laser intensities above the saturation threshold for ionization. As pointed out by Levis [493], the experimental conditions employed by the Dantus group can obscure connections to coherent processes that occur below the saturation threshold. Since these coherent processes play the main role in control mechanisms underlying reaction selectivity achieved by optimally shaped laser pulses, the proper experimental conditions must be satisfied for coherent control of photoinduced molecular fragmentation. Analogous proper laboratory conditions must be satisfied in any quantum control experiment, dictated by the nature of the dynamics involved. Moreover, the search over a set of predetermined pulse shapes [491] cannot guarantee discovery of optimal controls, even if the employed set is very large. In a parameter space of the size characteristically available from a typical pulse shaper, only a dedicated optimization algorithm is capable of consistently identifying optimal control fields that commonly lie in a null space of the full search space. This situation is fully consistent with classical engineering control practice where optimization is the design tool employed almost without exception to meet complex operational objectives.

5.8. AFC of multiphoton ionization in molecules

The use of polarization-shaped femtosecond laser pulses can significantly enhance the level of control over multiphoton ionization in molecules. In 2004, Brixner *et al* [494] demonstrated that a suitably polarization-shaped laser pulse increased the photoionization yield in K_2 beyond that obtained with an optimally shaped linearly polarized laser pulse. This effect is explained by the existence of different multiphoton ionization pathways in the molecule involving dipole transitions that are preferably excited by different polarization directions of the laser field. Suzuki *et al* [495] applied AFC with polarization-shaped laser pulses to multiphoton ionization of I_2 molecules and optimized the production of oddly charged (I_2^+ and I_2^{3+}) and evenly charged (I_2^{2+}) molecular ions. Weber *et al* [496] performed AFC experiments with polarization-shaped laser pulses to optimize the photoionization yield in NaK molecules. Free optimization of the pulse phase, amplitude and polarization resulted in a higher ionization yield than parameterized optimization with a train of two pulses.

Wöste and co-workers [497]–[502] investigated AFC of multiphoton ionization in K_2 and NaK using femtosecond laser pulses with phase and amplitude modulation, but without polarization shaping. In particular, good agreement between the optimal shapes of laser pulses obtained theoretically (via QOCT) and experimentally (via AFC) was reported [499]. Significant attention was also devoted to studying the properties of controlled ionization dynamics and revealing underlying control mechanisms. In one series of AFC experiments [500], the photoionization dynamics was explored using control pulse cleaning (CPC), which is a process of removing extraneous control field features by applying pressure in the optimization algorithm with an appropriate cost function on the spectral components of the pulse [378]. Weak pressure applied in the case of isotope-selective ionization of K_2 was sufficient to remove unnecessary pulse components and thus expose the participating vibronic transitions. For ionization of NaK, strong pressure was applied and multi-objective optimization was performed. The resultant Pareto-optimal curve revealed the correlation of

the two conflicting objectives of maximizing the ionization yield versus cleaning the control pulse. The optimal ionization pathway depends on CPC strength, which helps identify the important electronic transitions to particular vibrational states. These results demonstrate that the spectra of optimal pulses obtained with CPC contain important information about the control mechanism. In another series of AFC experiments [501], the control mechanism of multiphoton ionization in NaK was analyzed by systematically reducing the complexity of the search space. The spectral phase function of the control pulse was expressed as a truncated Fourier series, whose parameters were examined with respect to the ionization yield and the obtained optimal field. By progressively reducing the number of phase modulation parameters, it was possible to generate optimized pulses that allowed for a simple mechanistic interpretation of the controlled dynamics. In an earlier study, Leone and co-workers [503] applied AFC to optimize the weak-field pump–probe photoionization signal in Li_2 and used first-order time-dependent perturbation theory to investigate the dynamics of a rotational wave packet excited by the pump pulse and explain the corresponding control mechanism.

Wöste and co-workers [498], [504]–[506] also demonstrated that AFC is capable of achieving isotope-selective ionization of diatomic molecules such as K_2 and NaK. They showed that optimally tailored control pulses can increase the divergence between the dynamics of excited vibrational wave packets in distinct isotopomers (these studies will be discussed in more detail in section 5.12 below).

5.9. AFC of molecular alignment

The controlled alignment of molecules has attracted considerable attention as it can provide a well-defined sample for subsequent additional control experiments. At high laser intensities ($\sim 10^{13}$–$10^{14}\,W\,cm^{-2}$), dynamical variations of molecular polarization can have a significant effect on alignment. By shaping the temporal profile of such an intense femtosecond laser pulse, it is possible to achieve control over molecular alignment. Quantum dynamics of laser-induced molecular alignment is amenable to theoretical treatment and optimization [216], [507]–[511] and can be successfully controlled using simple ultrafast laser pulses [512]–[516]. AFC provides a very effective general laboratory tool for alignment manipulation, making the best use of laser resources. AFC of molecular alignment with intense shaped laser pulses was successfully demonstrated at room temperature for N_2 [517, 518] and CO [519].

5.10. Applications of AFC in nonlinear molecular spectroscopy

Shaped femtosecond laser pulses were successfully used to enhance resolution and improve detection in several areas of nonlinear spectroscopy and microscopy [44]. Of particular interest are experiments that employ AFC to identify optimal pulse shapes. One area of nonlinear molecular spectroscopy is control of vibrational modes via stimulated Raman scattering (SRS). In the gas phase, a number of AFC experiments [520]–[522] manipulated molecular vibrations excited via SRS by intense ultrafast laser pulses in the impulsive regime (i.e. when the duration of the control laser pulse is shorter than the vibrational period). In one of these experiments [520], control of the vibrational dynamics of K_2 was achieved via impulsive SRS in a degenerate four-wave-mixing optical setup. Different parameterizations of shaped femtosecond laser pulses in the frequency and time domains were employed to decipher the physical mechanism responsible for the achieved control. In other gas-phase experiments, mode suppression and enhancement in sulfur hexafluoride [521], mode-selective excitation in

carbon dioxide [521] and creation of shaped multimode vibrational wave packets with overtone and combination mode excitation in CCl_4 [522] were demonstrated using impulsive SRS at room temperature and high pressures. In the liquid phase, AFC was applied to control the relative intensities of the peaks in the Raman spectrum, corresponding to the symmetric and antisymmetric C–H stretch modes of methanol [523]–[526]. The modes were excited via SRS in the non-impulsive regime (i.e. the duration of the control laser pulse exceeded the vibrational period). The control pulse was shaped and the forward scattered Raman spectrum was measured to obtain the feedback signal, with the goal of achieving selective control of the vibrational modes. However, it was argued [527, 528] that in non-impulsive SRS the relative peak heights in the Raman spectrum do not reflect the relative populations of the vibrational modes and that control of the spectral features demonstrated in the experiments [523]–[526] does not involve quantum interference of vibrational excitations, but rather is based on classical nonlinear optical effects.

Another important area of nonlinear molecular spectroscopy is control of molecular vibrational modes via CARS. Materny and co-workers [529]–[534], Zhang *et al* [535] and von Vacano *et al* [536] used AFC in a CARS setup to optimally control vibrational dynamics in complex molecules. The Stokes pulse was shaped and the feedback signal was derived from the intensities observed in the CARS spectrum. In an AFC experiment with polymers (fluorobenzene sulfonate diacetylenes), selective excitation of one vibrational ground-state mode and suppression of all other modes was achieved, and the decay times of different modes were modified [529]. In liquid-phase AFC experiments, selective enhancement or suppression of one or more vibrational modes was demonstrated for toluene [530, 531], benzene [535] and β-carotene in hexane solution [532]. In a related experiment [533], AFC was used to obtain molecule-specific CARS spectra from a mixture of benzene and chloroform. Molecule-specific enhancement or suppression of the CARS spectral lines achieved in this AFC experiment is an example of ODD that will be discussed in more detail in section 5.12 below. Another related study [534] compared the selective excitation of molecular vibrational modes (achieved in AFC experiments with shaped femtosecond pulses) in the gas phase with carbon disulfide and in the liquid phase with toluene. Interestingly, it was found that the relative intensities of the CARS spectral lines could be changed more effectively in the liquid phase than in the gas phase. An experiment reported by von Vacano *et al* [536] employed the method of single-beam CARS spectroscopy with shaping of broadband pulses from a photonic crystal fiber. Each broadband pulse provides numerous pairs of pump and Stokes frequencies, and the spectral phase of the pulse was optimized with AFC to produce the desired interference pattern of the molecular vibrational modes. The optimally compressed and shaped pulses enabled the unambiguous assignment of the participating vibrational modes of toluene between 500 and 1000 cm^{-1} in a blue-shifted CARS signal.

Control of molecular vibrational dynamics is possible not only through Raman-type processes, but also directly in the infrared (IR) regime. Zanni and co-workers [537] demonstrated selective control of vibrational excitations on the ground electronic state of $W(CO)_6$, using shaped femtosecond mid-IR (5.2 μm, 1923 cm^{-1}) pulses. The spectral phase distribution of the pulse was optimized using AFC to achieve selective population of the excited vibrational levels of the T_{1u} CO-stretching mode. Systematic truncation of optimal pulses was employed to analyze the control mechanism. In a related AFC experiment [538], polarization-shaped mid-IR pulses were used to selectively control vibrational excitations of the two carbonyl stretching modes in $Mn(CO)_5Br$.

5.11. Applications of AFC in multiphoton microscopy

An important application of AFC with shaped femtosecond laser pulses is in multiphoton excited fluorescence (MPEF) microscopy. For a given pulse energy, the transform-limited pulse has maximum peak intensity, which helps to increase the fluorescence signal intensity, but unfortunately also increases the rate of photobleaching of the molecules (which is especially undesirable with samples of live cells). The use of optimally shaped pulses instead of a transform-limited pulse can reduce bleaching rate, enhance spatial resolution and increase contrast in biological fluorescence imaging. In a series of AFC experiments with shaped laser pulses, Midorikawa and co-workers [539]–[542] optimally controlled MPEF microscopy in different fluorescent biomolecules. Attenuation of photobleaching by a factor of four (without decreasing the fluorescence signal intensity) was demonstrated in two-photon excitation fluorescence (TPEF) from a green fluorescent protein [539]. Another AFC experiment [540] achieved selective control of two-photon and three-photon fluorescence in a mixture of two biosamples. The use of optimally tailored pulses helped to minimize the harmful three-photon fluorescence from the amino acid L-tryptophan, without a significant loss of useful two-photon fluorescence from a green fluorescence protein. Optimally shaped super-continuum pulses from a microstructure fiber were used in TPEF microscopy in another experimental study [541]. The pulse was shaped prior to propagation through the fiber, and AFC maximized the fluorescence signal contrast between two fluorescent proteins. A novel phase modulation technique for ultra-broadband laser pulses was developed for selective excitation of multiple fluorophores in TPEF microscopy [542]. This technique was applied to dual-color imaging of cells containing two types of fluorescent proteins, and AFC was employed to find the phase modulation that maximizes or minimizes the individual TPEF intensity from one of the fluorophores.

5.12. Applications of AFC for ODD

Discrimination of similar systems is important for many practical problems in science and engineering. In particular, selective identification of target molecules in a mixture of structurally and spectroscopically similar compounds is a challenge in such areas as selective excitation of multiple fluorescent proteins in microscopy of live samples, targeted component excitation in solid-state arrays and selective transformation of chemically similar molecules. Theoretical studies [219], [543]–[546] indicate that quantum systems differing even very slightly in structure may be distinguished by means of their dynamics when acted upon by a suitably tailored ultrafast control field. Such ODD can in principle achieve dramatic levels of control, and hence also provides a valuable test of the fundamental selectivity limits of quantum control despite noise and constrained laser resources. AFC provides a very effective laboratory means for practical implementation of ODD.

In 2001, Gerber and co-workers [547] experimentally demonstrated selective multiphoton excitation of two complex molecules, a laser dye DCM and $[Ru(dpb)_3](PF_6)_2$, in methanol solution. The goal was to electronically excite DCM while simultaneously suppressing electronic excitation of $[Ru(dpb)_3]^{2+}$. While these two molecules are electronically and structurally distinct, the DCM/$[Ru(dpb)_3]^{2+}$ emission ratio is practically unaffected by variations in single control parameters such as wavelength, intensity and linear chirp. Nevertheless, selective excitation was successfully achieved using AFC with shaped femtosecond laser pulses. The DCM/$[Ru(dpb)_3]^{2+}$ emission ratio was used as the feedback signal, and the evolutionary algorithm identified optimally shaped control pulses that improved the signal by approximately 50%.

These results obtained in the presence of complex solvent/solute interactions aroused significant interest in ODD. As mentioned in section 5.7, Gerber and co-workers [470] demonstrated AFC of photoproduct branching ratios in $CpFe(CO)_2Cl$ and $CpFe(CO)_2Br$. Despite the chemical similarity of these two molecules, AFC was sensitive enough to detect differences due to the electronic metal–halogen bonding properties. This finding suggests the possibility of performing ODD of individual compounds in mixtures of chemically similar molecules. Other examples of ODD include molecule-specific manipulation of CARS spectra from a mixture of benzene and chloroform [533], selective excitation of multiple fluorophores in TPEF microscopy [541, 542] and quantitative differentiation of dyes with overlapping one-photon spectra [548].

A recent experimental demonstration of ODD by Roth *et al* [466] achieved distinguishing excitations of two nearly identical flavin molecules in aqueous phase. The absorption spectra for FMN and RBF are practically indistinguishable throughout the entire visible and far UV. This implementation of ODD used a shaped UV pulse centered at 400 nm and a time-delayed unshaped IR pulse centered at 800 nm. The first pulse creates a coherent vibrational wave packet on an excited electronic state, and the second pulse disrupts the wave-packet motion and results in additional excitation to a higher state and consequential depletion of the recorded fluorescence signal. The effect of slight differences in the vibronic structure of the two molecules on the dynamics of the excited wave packets is amplified by tailoring the spectral phase of the UV pulse. Since further excitation produced by the second pulse depends on the precise structure, position and coherence of the tailored wave packet, it is possible to dynamically interrogate the two statically nearly identical systems and thereby produce a discriminating difference in their respective depleted fluorescence signals. In contrast, if the UV pulse is transform limited, then the fluorescence depletion signals from the flavins are indistinguishable. UV pulse shapes that optimally discriminate between FMN and RBF were discovered using AFC. The optimized depletion ratio D_{FMN}/D_{RBF} could be changed by $\sim \pm 28\%$, despite the initially indistinguishable linear and nonlinear optical spectra. Although the laser resources consisted of a modest ~ 3.5 nm of UV bandwidth and ~ 10 nm of IR bandwidth, significant selectivity was achieved with optimal UV pulses working in concert with the time-delayed unshaped IR pulse. Although the static spectra appear nearly identical, subtle differences in the molecular structure are nonetheless made profound during the tailored evolution of wave packets generated by optimal controls. System complexity (e.g. high vibrational state density, thermal population, solvent-induced line broadening) effectively enhances the ODD capabilities of the control field and compensates for the limited bandwidth constraint, thus making dramatic levels of control possible even in the weak-field limit.

Another example of ODD is isotope-selective ionization of molecules demonstrated in a number of AFC experiments by Wöste and co-workers [498], [504]–[506]. In particular, in an illustrative study [505, 506], they applied shaped femtosecond laser pulses to the $^{39,39}K_2$ and $^{39,41}K_2$ isotopomers and used AFC to maximize and minimize the isotope ion ratio $R = I(^{39,39}K_2)/I(^{39,41}K_2)$. K_2 molecules can be ionized in a three-photon process at relatively low pulse energies within the available wavelength range (810–833 nm). Differences between the evolutions of vibrational wave packets on an excited electronic state in the two isotopomers can be amplified by optimized control fields. Operation in this fashion made it possible to achieve significant selectivity of isotope ionization, with a variation by a factor of $R_{max}/R_{min} \sim 140$ between the maximal and minimal values of the isotope ion ratio. Information about the dynamics of the controlled vibrational wave packets was extracted from the optimal pulse shapes to help reveal ionization pathways [500, 505, 506].

5.13. AFC of energy flow in biomolecular complexes

Applications of quantum control to increasingly complex molecular systems have been considered. In particular, Motzkus and co-workers used AFC with shaped femtosecond laser pulses to control and analyze energy flow pathways in the light-harvesting antenna complex LH2 of *Rhodopseudomonas acidophila* (a photosynthetic purple bacterium) [549, 550] and *β*-carotene [551]. They demonstrated that by shaping the spectral phase distribution of the control pulse, it is possible to manipulate the branching ratio of energy transfer between intra- and inter-molecular channels in the donor–acceptor system of the LH2 complex [549]. Analysis of the transient absorption data was used to decipher the control mechanism and identify the molecular states participating in energy transfer within LH2 [550] and *β*-carotene [551]. These results indicate that coherent quantum control is possible even in very complex molecular systems in a condensed-phase environment.

5.14. AFC of photoinduced electron transfer

AFC has been applied to quantum control of inter-molecular photoinduced electron transfer. Yartsev and co-workers [552] reported an AFC experiment that maximized the yield of ultrafast electron injection from the sensitizer to TiO_2 nanocrystals in the core part of a dye-sensitized solar cell. The electron transfer process was monitored using the transient absorption signal. The impulsive structure of the optimal laser pulse was observed to correlate with the coherent nuclear motion of the photoexcited dye. The pulse shape and the transient absorption kinetics were explained by an impulsive stimulated (anti-Stokes) Raman scattering process, followed by electronic excitation.

5.15. AFC of photoisomerization in complex molecules

The control of molecular structure transformations is a coveted goal in chemistry. In particular, control of *cis–trans* isomerization has attracted much attention due to the importance of this process in chemistry and biology (e.g. it is a primary step of vision). AFC of *cis–trans* photoisomerization in cyanines (in the liquid phase) with shaped femtosecond laser pulses was first reported by Gerber and co-workers [553]. This experiment demonstrated that by using optimally shaped laser pulses it is possible to enhance or reduce isomerization efficiencies. The mechanism underlying isomerization control in this experiment was discussed in a number of theoretical works [554]–[556]. In particular, Hoki and Brumer [554] suggested that isomerization control involves an incoherent pump–dump process and that the role of quantum coherence effects in the evolution of the excited vibrational wave packet is negligible due to strong environmentally induced decoherence. On the other hand, Hunt and Robb [555] and Improta and Santoro [556] used a more sophisticated model and argued that control of isomerization does rely on quantum coherence of the photoexcited vibrational wave packet that moves on the multidimensional potential-energy surface of an excited electronic state. Moreover, Hunt and Robb [555] showed that the generation of the *trans* versus *cis* product is affected by the presence of an extended conical intersection seam on the potential-energy surface and that photoisomerization can therefore be coherently controlled by tuning the distribution of momentum components in the photoexcited vibrational wave packet. The validity of this coherent control mechanism was corroborated in a further AFC experiment by Yartsev and co-workers [557]. They demonstrated that optimally shaped laser pulses can be used to modify the momentum composition of the photoexcited wave packet

and thus achieve significant control of the absolute yield of isomerization (i.e. photoisomer concentration versus laser pulse energy). The coherent character of liquid-phase control of *cis–trans* photoisomerization in cyanines was further studied in another AFC experiment by Yartsev and co-workers [558]. They used a control scheme with an unshaped pump pulse and a time-delayed shaped dump pulse (an unshaped probe pulse was also applied to measure the effect of control). By using the optimally shaped dump pulse, they achieved control of photoisomerization closer to the decisive points of the reaction. This approach made it possible to explore the effect of the wave-packet's momentum composition at different time scales and assign the dynamics to distinct parts of the excited-state potential.

AFC of the retinal molecule in bacteriorhodopsin (from the all-*trans* to the 13-*cis* state) was demonstrated by Miller and co-workers [559]. This experiment employed both phase and amplitude modulation of femtosecond laser pulses and operated in the weak-field regime (with pulse energies of 16–17 nJ). By using optimally shaped pulses, it was possible to enhance or suppress the quantity of molecules in the 13-*cis* state by about 20%, relative to the yield observed using a transform-limited pulse with the same energy. They further explored the mechanism of coherent control of retinal photoisomerization in bacteriorhodopsin using time- and frequency-resolved pump–probe measurements [560]. Experimental data together with a theoretical analysis suggest that the isomerization yield depends on the coherent evolution of the photoexcited vibrational wave packet on an excited-state potential-energy surface in the presence of a conical intersection. According to this analysis, control of retinal photoisomerization is dominated by amplitude modulation of the spectral components of the excitation pulse. Gerber and co-workers [561] also demonstrated AFC of retinal isomerization in bacteriorhodopsin. In this experiment, they pioneered the control scheme with unshaped-pump and time-delayed shaped-dump femtosecond laser pulses. As mentioned above, the use of the optimally shaped dump pulse makes it possible to control the molecule in a region of the potential-energy surface where the decisive reaction step occurs. Moreover, by changing the time delay between the pulses, it is possible to obtain information on the wave-packet evolution.

The role of quantum coherence effects in control of retinal isomerization in bacterio-rhodopsin is still not fully clear, as a recent experiment by Bucksbaum and co-workers [562] found no dependence of the isomerization yield on the control pulse shape at pulse energies below 30 nJ. In the high-intensity regime (at pulse energies above 30 nJ), they found that the yield of the 13-*cis* isomer is maximized by a transform-limited pulse, which could indicate that the yield depends only on the pulse intensity, with quantum coherence not playing a significant role. These findings (especially for lower intensities) apparently contradict the optimization results obtained by Miller and co-workers [559]. It is possible that these discrepancies could be explained by differences in experimental setups. In particular, Bucksbaum and co-workers [562] used only phase modulation of the control pulse, whereas Miller and co-workers [559, 560] argued that control is mainly achieved by amplitude modulation. Additional experimental and theoretical work will be needed to fully explore the mechanisms underlying condensed-phase control of photoisomerization in complex molecular systems and to clarify the role of quantum coherence in the controlled dynamics. For example, recent theoretical studies [563, 564] suggest that coherent control of photoisomerization and other branching reactions in an excited state may be affected by and, moreover, take advantage of environmentally induced relaxation effects. Such cooperation between coherent control and environmentally induced decoherence may be important in various quantum phenomena [565] and hence its optimal exploitation deserves further investigation.

Other examples of structural transformations in complex molecules include ring opening in cyclohexadiene along with isomerization as well as cyclization reactions in *cis*-stilbene. Carroll *et al* [566, 567] demonstrated AFC of the photoinduced ring-opening reaction of 1,3-cyclohexadiene (CHD) to form 1,3,5-*cis*-hexatriene (Z-HT). The feedback signal was obtained from measurements of the UV absorption spectrum. The learning algorithm was able to identify optimal pulse shapes that increased the formation of Z-HT by a factor of two. For a different control objective, the AFC optimization produced pulse shapes that decreased solvent fragmentation while leaving the formation of Z-HT essentially unaffected. Kotur *et al* [568] used AFC with shaped ultrafast laser pulses in the deep UV to control the ring opening reaction of CHD to form 1,3,5-hexatriene (HT). The feedback signal was obtained from measurements of fragmentation products following strong-field ionization with a time-delayed IR laser pulse. The learning algorithm discovered shaped UV pulses that increased the HT yield by $\sim 37\%$ relative to an unshaped (nearly transform-limited) pulse of the same energy. Greenfield *et al* [569] demonstrated AFC of the photoisomerization and cyclization reactions in *cis*-stilbene dissolved in *n*-hexane. This experiment employed phase-modulated 266 nm femtosecond pulses to maximize or minimize the yields of *cis*- to *trans*-stilbene isomerization as well as *cis*-stilbene to 4*a*,4*b*-dihydrophenanthrene cyclization. The yields of both isomerization and cyclization were minimized by transform-limited pulses that enhanced competing multiphoton processes, while the yields were maximized by complex pulse shapes that helped to avoid multiphoton effects.

5.16. AFC of nuclear motion in fullerenes

Fullerenes are a class of molecules of considerable interest in many areas of science. Laarmann *et al* [570] employed AFC-optimized femtosecond laser pulses to coherently excite large-amplitude oscillations in C_{60} fullerene. The structure of the optimal pulses in combination with complementary two-color pump–probe data and time-dependent density functional theory calculations provided information on the underlying control mechanism. It was found that the strong laser field excites many electrons in C_{60}, and the nuclear motion is excited, in turn, due to coupling of the electron cloud to a radially symmetric breathing mode. Despite the complexity of this multi-particle system with various electronic and nuclear degrees of freedom, the optimal control fields generated essentially one-dimensional oscillatory motion for up to six cycles with an amplitude of $\sim 130\%$ of the molecular diameter.

5.17. Applications of AFC in semiconductors

Quantum control has found applications beyond atomic and molecular phenomena. In particular, it is possible to use optimal control methods to manipulate various processes in semiconductors. Kunde *et al* [571, 572] demonstrated AFC of semiconductor nonlinearities using phase-modulated femtosecond laser pulses, with the purpose of creating an ultrafast all-optical switch. The feedback signal was obtained by measuring the differential transmission (DT) in a control-probe setup. Optimizations were performed on the spectrally integrated DT as well as DT in narrow spectral windows. The learning algorithm was able to identify optimal pulse shapes that enhanced ultrafast semiconductor nonlinearities by almost a factor of four. Chung and Weiner [573] used AFC with phase-modulated femtosecond laser pulses to coherently control two-photon-induced photocurrents in two different semiconductor diodes. Because of their

spectrally distinct two-photon absorption responses, the diodes generated noticeably different photocurrent yields depending on the pulse shape. An evolutionary algorithm guided the AFC experiment to discover pulse shapes that maximize or minimize the photocurrent yield ratio for the two diodes.

5.18. AFC of decoherence

Manipulation of quantum interference requires that the system under control remains coherent, avoiding (or at least postponing) the randomization induced by coupling to an uncontrolled environment. Therefore, the ability to manage environmentally induced decoherence would bring substantial advantages to the control of many physical and chemical phenomena. In particular, decoherence is a fundamental obstacle to quantum information processing [175], and therefore the ability to protect quantum information systems against decoherence is indispensable.

The possibility of using AFC for optimal suppression of decoherence was first proposed by Brif *et al* [574], and numerical simulations in a model system were performed by Zhu and Rabitz [387]. Walmsley and co-workers [148] have recently used AFC to achieve coherent control of decoherence of molecular vibrational wave packets in the laboratory. The concept underlying this experiment is the use of coherent preparation of the quantum system to alter non-unitary decoherent dynamics induced by an uncontrolled environment. In this experiment, a gas-phase ensemble of K_2 at $400\,^{\circ}C$ was irradiated by a shaped femtosecond laser pulse, inducing a vibrational wave packet in the lowest excited electronic state $A^1\Sigma_u^+$ of the molecules. This wave packet undergoes dephasing (a form of decoherence that does not involve dissipation of energy). Dephasing is caused by coupling of the vibrational mode to the thermalized rotational quasi-bath. The amplitude of quantum beats in the fluorescence signal (measured at a chosen delay time after the excitation pulse) served as the feedback signal. This amplitude provides an estimate of the degree of wave-packet localization in the phase space and therefore can be used as a coherence surrogate. The optimal pulse identified by AFC increased the quantum-beat visibility from zero to more than four times the noise level and prolonged the coherence lifetime by a factor of ~ 2 relative to the beats produced by the transform-limited pulse. The main characteristic of the optimal pulse is a high degree of linear negative chirp. This indicates that the mechanism of decoherence control is based on exciting a wave packet that is initially amplitude squeezed in the phase-space representation. A theoretical analysis confirmed that the coherence lifetime is extended if the initial state is amplitude squeezed (corresponding to the initial orientation in the phase space along the classical trajectory).

A well-known strategy for suppressing decoherence in quantum systems is through application of pulse sequences designed to dynamically decouple the system from the environment [575]–[587]. Experiments [588]–[593] have employed theoretically designed pulse sequences based on particular environment models (i.e. an example of open-loop control). However, the actual noise power spectra for realistic environments can significantly differ from the models. To overcome this difficulty, Bollinger and co-workers [594] recently used AFC to tailor the dynamical decoupling pulse sequence to an actual experimental noise environment. In this experiment, the system was a quantum memory realized in an array of ~ 1000 $^9Be^+$ ions (cooled to a temperature of $\sim 1\,mK$) in a Penning ion trap, with qubit states realized using a ground-state electron–spin-flip transition. These qubit states are highly susceptible to magnetic field fluctuations, making such noise a significant source of decoherence. The qubits were

coherently controlled by directly driving the $\sim 124\,$GHz transition in a microwave setup similar to optical ones. A sequence of microwave π pulses used for qubit control in this laboratory configuration is technologically quite different from shaped femtosecond optical laser pulses typically employed in molecular control experiments; however, the fundamental concept of AFC is still fully applicable. The feedback signal was obtained from fluorescence detection on a cycling transition (with decoherence-induced errors manifested as nonzero fluorescence). The Nelder–Mead simplex method was utilized to search for optimal pulse positions in a fixed-length sequence of n pulses. Optimal pulse sequences discovered in the AFC experiment, without *a priori* knowledge of the noise environment, suppressed the qubit error rate by a factor of five to ten relative to benchmark model-based sequences.

5.19. Algorithmic advances for laboratory AFC

The learning algorithm is an important component of laboratory AFC. The majority of AFC experiments employ stochastic algorithms such as evolutionary strategies [595] and genetic algorithms [596]. Historically, genetic algorithms were characterized by the use of recombination, while evolutionary strategies primarily relied on mutation; however, modern algorithms guiding AFC experiments and simulations typically incorporate both types of genetic operations and are variably called genetic algorithms or evolutionary algorithms. These algorithms are very well suited to laboratory optimizations as they naturally match the discrete structure of control 'knobs' (e.g. the pixels of a pulse shaper) and are robust to noise. Moreover, robustness to noise in AFC experiments can be enhanced by incorporating the signal-to-noise ratio into the control objective functional [378, 597]. Various aspects of evolutionary algorithms and their application to AFC of quantum phenomena were assessed [598, 599]. Evolutionary algorithms can also be used in multi-objective optimization [600, 601], and the application of this approach to quantum control problems was studied theoretically [216]–[218], [602] and demonstrated in AFC experiments [464, 500].

Other types of stochastic algorithms include, for example, simulated annealing [603] and ant colony optimization [604, 605]. Simulated annealing was utilized in some AFC experiments [430, 542], and it seems best suited to situations where just a few experimental parameters are optimized [606, 607]. Ant colony optimization has recently been used in an AFC simulation [390], but it is yet to be tested in the laboratory.

As mentioned in section 4, the absence of local traps in control landscapes for controllable quantum systems has important practical consequences for the optimization complexity of AFC experiments. In particular, deterministic search algorithms can be used to reach a globally optimal solution. Deterministic algorithms (in particular, the downhill simplex method) were successfully implemented in several AFC experiments [431, 569, 594]. Recently, Roslund and Rabitz [371] demonstrated the efficiency of a gradient algorithm in laboratory AFC of quantum phenomena. They implemented a robust statistical method for obtaining the gradient on a general quantum control landscape in the presence of noise. The experimentally measured gradient was utilized to climb along steepest-ascent trajectories on the landscapes of three quantum control problems: spectrally filtered SHG, integrated SHG and excitation of atomic rubidium. The optimization with the gradient algorithm was very efficient, as it required approximately three times fewer experiments than needed by a standard genetic algorithm in these cases. High algorithmic efficiency is especially important for AFC of laser-driven processes in live biological samples, as damage (e.g. due to photobleaching) can be reduced

by decreasing the number of trial laser pulses. Still, evolutionary or other stochastic algorithms may be preferable over deterministic algorithms in many AFC experiments due to their inherent robustness to noise. Hybrid stochastic–deterministic algorithms (e.g. derandomized evolution strategies) seem to offer the most flexibility and efficiency [608].

6. Role of theoretical quantum control designs in the laboratory

A very significant portion of theoretical research in the area of quantum control is devoted to model-based computations which employ QOCT (or other similar methods) to design optimal control fields for various physical and chemical problems. Such computations are widespread in theoretical studies of molecular applications of quantum control and are becoming increasingly popular in considering the control of quantum information systems, including optimal operation of quantum gates and optimal generation of entanglement (see section 3.6). Notwithstanding these extensive QOCT-based control field designs, experiments seeking optimal control of molecular processes overwhelmingly employ AFC methods as described in section 5. Such experiments in most cases work remarkably well with random initial trials, and thus exhibit no evident need to operate or possibly start with theoretical control designs. This raises important questions about the practical usefulness of open-loop control and the role of theoretical methods such as QOCT in control experiments [23]. In considering this matter it is important to keep in mind that the AFC procedure grew out of observations from QOCT simulations and associated analyses.

6.1. Effect of system complexity

As discussed in section 3.7, the practical laboratory relevance of theoretical designs depends on the complexity of the system of interest, with simpler cases yielding theoretical models closer to reality. For example, in numerous NMR experiments employing RF fields to manipulate nuclear spins [153]–[157], including NMR realizations of quantum gates [159]–[162], theoretically designed sequences of pulses (some of which were developed using QOCT [163, 164]) can function quite well. The model of a collection of spins (with empirical coupling and decay constants) interacting with classical fields is often sufficiently accurate for NMR-based applications, allowing for successful employment of open-loop control. A QOCT-based design was also successfully applied experimentally to enhance the robustness of single-qubit gate operations in a system of trapped ions [353].

At the other extreme of system complexity are electronic and vibrational processes in polyatomic molecules whose dynamics cannot be accurately modelled at the present time. An objective assessment is that models used for polyatomic molecules in control computations are currently too simplified and computational techniques are inadequate for the true levels of complexity, resulting in theoretical designs that are not directly applicable to control experiments that work with *real* systems. There are several aspects of laser control of molecules, which make the difference between theoretical models and actual systems very important. First, optimal control is generally based on creating interference of multiple quantum pathways, which can be very sensitive to the detailed properties of the system (e.g. evolution of a laser-induced vibrational wave packet can be strongly influenced by small variations of a molecular potential energy surface, as is evident from experimental ODD results [466]). Therefore, even small inaccuracies of theoretical models or associated numerical procedures may result in control

designs that are not optimal for the actual systems. Second, the wavelength of the laser field is typically much larger than the molecule, which makes it impossible to focus the field on a particular group of atoms. In many applications, the goal is to attain control (e.g. generate an excitation or break a bond) in a localized part of a molecule. However, the external control field interacts with the molecule as a whole, possibly exciting a multitude of accessible transitions within the bandwidth of the laser (including multiphoton processes). The 'global' effect of photonic reagents becomes ever more important with stronger fields for which resonance-based 'localization' is not valid. An *ab initio* quantitative theoretical account of laser-driven molecular dynamics is presently not feasible, unless the studies are limited to cases of very simple molecules and weak fields. Third, it is difficult to calibrate the laser and pulse-shaping apparatus to reliably reproduce theoretical control designs in the laboratory. In many cases, directly using AFC optimization is much easier and much more effective than calibrating the laser and pulse shaper for the generation of theoretically computed control fields with the required accuracy.

These considerations lead to the conclusion that open-loop control experiments employing theoretical designs may be useful for some systems and impractical for others, depending on how well the system is known and which computational capabilities are available, consequently determining how accurately the controlled dynamics can be modeled. Thus, the boundary between systems for which modeling is sufficiently reliable and systems for which it is not depends on available Hamiltonian data, numerical algorithms and computational power. Of course, with time, better modeling will become available for more complex systems, although the exponential increase of the Hilbert-space dimension with system complexity is a fundamental feature of quantum mechanics, which significantly hinders the effectiveness of numerical control designs for practical laboratory implementation.

Consider, for example, quantum information processing systems that are typically modeled as collections of two-level particles (qubits) with controlled interactions between them [175]. *Prima facie*, such a system appears to be quite simple, so that controls for all desired transformations can be theoretically designed (e.g. using QOCT). However, the difficulty of accurately modeling the actual environmental noise is significant even for simple few-qubit systems. As was recently demonstrated with trapped-ion qubits, dynamical decoupling pulse sequences obtained via AFC significantly outperformed the best available theoretical designs [594]. Moreover, as the Hilbert-space dimension increases exponentially with the number of qubits, the unwanted effects of uncontrolled couplings between the qubits in multi-particle systems will be very difficult to model and, consequently, to manage via open-loop control. Therefore, the effectiveness of theoretical control designs for realistic quantum computers will depend on the ability to engineer systems in which couplings between small blocks of qubits can be made arbitrarily small. Hopefully, further technological advances will make such systems available, which in turn will make open-loop control with QOCT-based designs useful for practical quantum computing.

6.2. Importance of theoretical control designs for feasibility analysis

In molecules, the interactions between atoms are inherently strong in order to hold the atoms together. Therefore, in the foreseeable future, for optimal manipulation of electronic and vibrational processes in molecules with four and more atoms, AFC will continue to be much more effective than employing theoretical control designs. Notwithstanding this assessment,

theoretical control studies should continue to have high significance; however, for complex systems the value of theoretical studies is not in generating specific control designs for immediate laboratory use. Control solutions obtained via theoretical model-based computations (in particular, those employing QOCT) should play an important role by advancing the general understanding of the character of controlled dynamics and control mechanisms. One practically important issue is that while each cycle of a typical AFC experiment is very fast (from microseconds to milliseconds) and cheap, the initial setup of the experiment is usually quite difficult and expensive, since advanced methods of pulse shaping and control-yield measurement need to be incorporated together as well as adjusted to the particular nature of a physical or chemical system. Therefore, theory can be especially important in exploring the feasibility of various control outcomes for the quantum dynamics of a system of interest; even semiquantitative modeling may be successful for such purposes in many applications. Theoretical control simulations can provide important guidance for the selection of the experimental configuration, thereby helping to make AFC a more effective practical tool. Additional such high value utilizations of theory and simulations can be expected in the future.

6.3. Open-loop quantum control experiments with non-optimal designs

The open-loop control procedure is not limited to the use of optimal theoretical designs generated via QOCT and similar methods. Moreover, optimality is not always required in quantum control. In the conceptually allied field of synthetic chemistry, progress has often been achieved via intuition-guided trials leading to a gradual increase of reaction yields. Following this venerable tradition, some recent open-loop control experiments seek improvement by employing ultrafast shaped laser pulses with so-called 'rational' or 'judicious' control designs obtained using a combination of intuition and arguments based on some knowledge of system properties (e.g. spectral information or symmetry). This approach is popular in nonlinear spectroscopy and microscopy [44], [609]–[622] as well as in some other atomic [623]–[631], molecular [512]–[516], [632, 633] and solid-state [634]–[637] applications. While in many situations such 'rationally' designed control pulses enhance the spectroscopic resolution or increase the control yield as compared to results obtained with transform-limited pulses, in general they are not optimal. Experience gained from numerous quantum control experiments indicates that intuition generally fails to discover the most effective controls (except for the simplest systems), and therefore, in most cases, the degree of control can be increased via closed-loop optimization employing a suitable learning algorithm. In some situations, intuition-driven control may be effective for providing a guide to initial fields for subsequent optimization under AFC.

7. Concepts and applications of RTFC

Feedback is very important in classical engineering where it is routinely used for the control of complex systems in the presence of uncertainties. In quantum control, two important approaches based on the concept of feedback have been introduced for similar reasons. One is AFC, which was extensively discussed in section 5. A fundamental characteristic of AFC is that in each control cycle a fresh quantum ensemble is used (either a new sample is prepared or the system is reset to its initial state before each run), which makes measurement back action irrelevant. The other approach is RTFC [391]–[396], [638], in which the same quantum system is followed

in real time around the feedback loop, and the measurement (or interaction with a quantum 'controller') has a significant effect on the system's evolution.

There are two distinct types of RTFC, which differ in the nature of the controller. In one approach to RTFC, measurements are employed to probe the quantum system, and the gathered information is processed classically off-line in real time to assess the best, next control action [391]–[396]. The evolution of the controlled quantum system is governed by two effects: coherent (unitary) action exerted by the classical controller[6] and incoherent (non-unitary) back action exerted by the measurements. A generalized description of measurement-based RTFC employs quantum filtering theory [639]–[641]. Recently, another type of RTFC—referred to as coherent feedback control[7]—has drawn much attention [638], [642]–[648]. In this approach, no measurements with a classical output signal are performed; instead, an ancillary quantum system serves as the controller. The controller influences the evolution of the system of interest via a direct interaction between them. Additionally, external classical forces can also be used to act upon the system, the controller or both. The system of interest together with the controller are characterized by the entirely quantum nature of the information flow—coherence is not destroyed by measurements, which is the source of the name given to this type of control [638, 642]. Coherent feedback control can be viewed as a quantum analog of Watt's flyball governor—an automatic self-regulating quantum machine [649].

It was recently shown [650] that the evolution of a quantum system undergoing any type of RTFC (or a combination thereof), including effects of measurements, feedback actions and interactions with auxiliary quantum systems, can be generally represented by a Kraus map. This result has an important consequence for the optimization complexity of RTFC, since observable-control landscapes of open quantum systems with Kraus-map dynamics are free from local traps (under the controllability assumption) [273]. Remarkably, this trap-free landscape topology unifies virtually all types of control, including measurement-based RTFC, coherent RTFC, AFC and open-loop control (the Kraus-map description of open-system dynamics is also generally valid for the latter two types when the controlled system is coupled to an environment). The possibility of employing this general unifying feature of controlled quantum dynamics for the development of hybrid control schemes is discussed in section 8.4.

Although the history of AFC in the quantum realm is short (it was proposed in 1992 and first experimentally implemented in 1997), it has become a well-established and popular laboratory tool successfully employed in growing numbers of experimental studies (see section 5). In contrast, while RTFC of quantum systems was first proposed in 1983 [391], its laboratory implementation [642, 648], [651]–[653] thus far has been much less extensive. Implementing RTFC on the atomic or molecular scale encounters significant technical difficulties. One especially important obstacle is that many interesting quantum phenomena occur on a time scale that is too short to allow for processing of the measurement data in classical controllers based on conventional electronics (i.e. the issue of loop latency). Coherent RTFC can overcome the latency issue, but in this case the controller itself may require precise engineering to ensure quality control performance of the quantum system. Nevertheless, interest in potential applications of RTFC for manipulation of quantum systems is high and the theoretical activity in this field is growing [654]–[665]. Of particular importance (especially for applications in quantum information sciences) is the ability of RTFC to stabilize the dynamics of quantum

---

[6] The free evolution of the system can be included while the off-line modeling is performed.

[7] We will also use the term coherent RTFC. The choice of terminology is standard in the field and should not be confused with the notion of coherent control employed in AFC and QOCT.

systems in the presence of noise [646, 648], [666]–[669] and achieve robust control performance in the presence of uncertainties in the system Hamiltonian [670]. Other interesting possibilities include the use of RTFC for quantum error correction [671]–[676], generation and protection of entanglement [668], [677]–[682], cooling of quantum systems [651], [683]–[686] and quantum state purification [687]–[693]. In the related field of quantum metrology, real-time feedback was employed to approach fundamental quantum limits of measurement accuracy [694, 695]. Both theoretical and experimental aspects of RTFC should continue to draw significant attention in the future.

8. Future directions of quantum control

Common sense dictates that the future is notoriously difficult to predict, but it is also the nature of science to try and anticipate new directions that will expand current knowledge. The evident paths followed in the development of the quantum control field during the last two decades provide a basis for projection, with due caution, on how current trends may evolve upon going forward. Below we try to identify some critical theoretical and technological issues, where breakthroughs are required to significantly increase the capability of controlling quantum phenomena.

8.1. Input–output maps for quantum control simulations

Except for the special situation of measurement-based RTFC (where measurement back action is a distinctively non-classical feature), one may naively conclude that there are no fundamental differences between designing controls for quantum and classical systems. The distinctions seem to lie in solving classical equations of motion in one case and the Schrödinger equation in the other, but otherwise the method of finding the optimal control solution is basically the same. However, from a practical perspective, the difference between solving classical and quantum equations of motion is fundamental due to the exponential increase of the Hilbert-space dimension characteristic of quantum systems. This is the reason why simulating controlled quantum dynamics of multi-particle systems is so difficult.

A qualitative breakthrough in open-loop control of complex quantum systems would be possible, if a way could be found to replace the laborious calculations of quantum dynamics with 'black-box' models that essentially capture the main features of the processes leading to a particular control objective (e.g. breaking of a specific molecular bond). The goal is to perform a modest number of simulations and use the information to generate an input–output map from the applied control field to the resultant change in the control objective. In this fashion, the input–output map aims to capture the relationship between the control and the system's reaction to it. This approach is commonly used in classical control problems in many areas of engineering; however, at the present time, we do not know how to effectively determine these input–output maps for complex quantum systems, such as molecules.

An example of a method proposed for identifying nonlinear input–output maps for quantum control studies is the high-dimensional model representation (HDMR) technique [696]–[700]. The total number of points in the search space for a quantum control optimization problem (and for many other problems in science and technology) grows exponentially with the number of input variables (this situation is sometimes called the 'curse of dimensionality'). In HDMR, the input–output map is characterized by a hierarchy of contributions from the input variables acting independently, in pairs, triples etc. For many important problems, with

an appropriate choice of the variables, only low-order input variable cooperativity is significant. This property can be used to dramatically reduce the effort required to explore the map. Approaches such as HDMR are designed for systems with a large number of input variables with the aim of learning the input–output map using a number of simulations that grow relatively slowly (e.g. polynomially) with the number of input variables [700]. Specifically, the use of nonlinear functional HDMR-type maps for quantum control problems was discussed by Geremia *et al* [701]. Such input–output maps would be of value as well when generated from experimental data, as they would constitute the control landscape. Although much is now understood about the topology of quantum control landscapes, there is little information about non-critical point structural features.

Another approach popular for constructing nonlinear input–output maps employs neural networks [702, 703]. Recently, neural networks were used to model ultrafast laser control of SHG, molecular fluorescence yield and photoelectron spectra from resonant strong-field ionization of potassium atoms [704, 705]. However, it was found that the amount of data required for the training of a neural network significantly increases with the complexity of the correlations that are to be modeled. While reproduction of the training data worked very well, extrapolation to regions of the parameter space that were not covered by the training data was a challenge.

Development of efficient and accurate input–output maps for control of complex quantum phenomena remains an important objective. Ideally, after a modest effort at learning a map, it could then be used in a highly efficient manner to seek out new controls and dynamical regimes with favorable characteristics.

8.2. Analysis of quantum control landscapes

The introduction of quantum control landscapes in the last few years is an important theoretical advance in the field. The nature of the control landscape topology has direct implications for the ease of finding effective controls in the laboratory. The analysis of the control landscape topology and other structural features can provide the basis for investigating the complexity of optimizing different types of control objectives. In turn, this understanding can help identify the most suitable optimization algorithms for various theoretical and experimental applications of quantum control (see sections 4.4, 4.5 and 5.19). In addition, the landscape analysis may be extended to the study of quantum control problems involving simultaneous optimization of multiple objectives (see sections 4.3 and 4.4). This research area is still rapidly developing with much remaining for investigation. In particular, an open issue that deserves significant attention is the effect of field constraints (e.g. due to limited laboratory resources) upon the accessible regions of quantum control landscapes.

There are several additional research directions for which the analysis of the control landscape features may provide important insights. One ubiquitous problem with wide-ranging implications is evaluation of the robustness of control solutions to noise and imperfections, which depends on the degree of flatness of the control landscape around an optimal solution. Another interesting issue is related to a phenomenon discovered for observable control of an open quantum system prepared in a mixed state and coupled to a thermal environment [273]. Specifically, the range of the control landscape (i.e. the difference between the maximum and minimum expectation values of the target observable) decreases when the temperature of the environment rises. Therefore, an important application of control landscape analysis would be

determination of the fundamental thermodynamic limits on the control yield for open quantum systems.

8.3. Future applications of AFC

As discussed in section 5, AFC has proved to have broad practical success as a means for achieving optimal control of quantum phenomena in the laboratory. Particularly impressive is the breadth of applications, ranging from optical systems, to atoms, to semiconductor structures, to biologically relevant photochemical processes in complex molecules, etc. One clear trend is the extension of AFC applications towards the manipulation of increasingly more complex systems and phenomena. Along this avenue, implementation of AFC could bring significant benefits to such areas as near and even remote detection of chemical compounds (first steps in this direction have been recently made [490, 706]), optimal control of molecular electronics devices and optimal control of photochemical phenomena in live biological samples (including nonlinear microscopy and ODD, as indicated by several recent experiments [539]–[542]).

We can also envision increasing use of AFC for optimal quantum control of photophysical phenomena. One important area is coherent manipulation of quantum processes in solid-state systems, especially in semiconductor quantum structures [707, 708]. Another potential application is optimal storage and retrieval of photonic states in atomic-vapor and solid-state quantum memories [358, 359], [709]–[714]. The AFC methodology may also be applicable to physical problems where, instead of laser pulses, other means (e.g. voltages applied to an array of electrodes) are used to implement the control. Examples could include optimal control of coherent electron transport in semiconductors by means of adaptively shaped electrostatic potentials [715], coherent control of charge qubits in superconducting quantum devices by gate voltages [716, 717] and coherent control of photonic qubits in integrated optical circuits via the thermo-optic effect [718]. Several types of quantum systems (e.g. flux qubits in superconducting quantum devices, hyperfine-level qubits in trapped neutral atoms and ions, electron spins of donor atoms in silicon, etc) can be controlled by pulses of microwave radiation (e.g. the AFC-optimized dynamical decoupling [594] of trapped-ion qubits by a sequence of microwave π pulses was discussed in section 5.18). Many possible applications of AFC could have significant implications for progress in the field of quantum information sciences. A new domain of quantum control involves manipulation of relativistic quantum dynamics with extremely intense laser fields [719] for accelerating particles and even intervening in nuclear processes in analogy with what is happening in atomic-scale control. It is reasonable to forecast that AFC methods could become useful for optimal control of such laser-driven high-energy phenomena.

Despite significant advances achieved in the field of quantum control during the last decade, the experimental capabilities are limited by currently available laser resources. It is likely that existing practical limitations, in particular, the relatively narrow bandwidth of femtosecond lasers, restrict the achievable yields in some AFC experiments. One might expect that many new applications would open up if reliable sources of coherent laser radiation with a much wider bandwidth became available. Such resources could make possible the simultaneous manipulation of rotational, vibrational and electronic processes in molecules in a more effective fashion, thereby achieving hitherto unattainable levels of control. Moreover, if pulse-shaping technology can be extended to coherent radiation in the attosecond regime as well as in the range of MeV photon energies, a multitude of new applications in x-ray spectroscopy, medical physics and control of nuclear dynamics could arise.

8.4. Hybrid methods of quantum feedback control

Despite the significant technological difficulties on the path to routine practical application of RTFC, the potential benefits are alluring (see section 7). An interesting question is whether AFC, whose practical utility has already been well established, can be used to aid in the implementation of RTFC (measurement-based, coherent or both). Due to the apparent technological differences between AFC and RTFC, thus far they have been considered as separate branches of quantum control. However, it has been recently shown [650] that AFC and RTFC share a common fundamental landscape topology characterized by the absence of local traps (i.e. all sub-optimal extrema are saddles provided that the controllability condition is satisfied). Since the control landscape topology strongly influences the optimization complexity, this finding may have immediate practical importance. Moreover, the unification of the seemingly different AFC and RTFC approaches at a fundamental level suggests the possibility of developing new laboratory realizations that combine these currently distinct techniques of quantum feedback control in a synergistic way. For example, some form of AFC might be used to optimize the design or construction of quantum controllers employed in coherent RTFC. Development of 'hybrid' quantum control schemes incorporating both AFC and RTFC (in particular, for control and stabilization of quantum computing systems) could provide significantly enhanced flexibility in the laboratory.

8.5. Material control

In addition to the manipulation of quantum dynamics via application of optimal external fields, there is the prospect of performing material control through alteration of the internal system properties (i.e. the spatial structure or matrix elements of the system Hamiltonian), with the aim of identifying optimal materials and system designs. Analogous to the circumstance of a particular quantum system acted upon by a family of homologous external control fields, we can consider the controlled response of a family of homologous quantum systems to a particular field. In the former case, a control level set consists of all homologous control fields that produce the same expectation value of the target observable when applied to a particular quantum system. This level set can be explored, for example, by homotopy trajectory methods (e.g. D-MORPH), in order to identify control solutions with desired properties (see section 4.4). In the latter case of material control, a level set consists of all dynamically homologous quantum systems that produce the same expectation value of the target observable when controlled by a particular field. For example, each quantum system may be specified by a point in a hypercube whose edges are labeled by Hamiltonian matrix elements. A variation of the D-MORPH method can be used to explore a system level set by continuously warping the corresponding Hamiltonian [720]. At this juncture little is known about either homologous control fields or homologous quantum systems. Exploration of these topics could reveal systematic aspects of control over quantum phenomena.

Morphing through Hamiltonian structure in the laboratory can be physically realized in many different ways, with broad and yet largely unexplored possibilities. For example, the properties of light-sensitive materials could be varied using families of structurally similar chemical compounds, characteristics of doped semiconductors can be varied by changing the concentration of dopant atoms and the depth of implanting, etc. Material control is potentially applicable to a wide set of problems in various areas of science and technology. Possible applications include, for example, development of photodetectors with higher efficiency and

faster response time, molecular switches with increased sensitivity and durability, quantum computing systems with enhanced immunity to environmentally induced decoherence and improved robustness to instrumental noise, etc. Exploiting the accessible variations in Hamiltonian structure as a means for achieving optimal quantum control is a potentially important area of future research, including exploration of the associated control landscapes, development of adaptive and open-loop techniques, investigation of effective methods of combining material and electromagnetic control, and adaptation of the theoretical concepts to various practical applications.

8.6. Scientific and engineering goals of optimal quantum control

The general goal of science is to understand nature, including the structure of physical systems and characteristics of the system dynamics, while the goal of engineering is to design and implement a system that will function in a prescribed manner in the best possible way. Optimal quantum control draws together science and engineering to incorporate both goals: (i) to understand the dynamical behavior of quantum systems and the mechanisms by which these processes can be managed and (ii) to require optimal functional performance through the achievement of prescribed control objectives in the best possible way.

An important feature evident in the prior development of quantum control is the impact of progress in one aspect of the subject on advancing another. We expect that this trend will continue in the future, as a better understanding of the underlying physical processes would aid in choosing better control tools and thereby achieving a higher degree of performance. In turn, the ability to steer system evolution in an optimal fashion should facilitate the acquisition of knowledge about the underlying control mechanisms and other properties of the system. For example, in many AFC experiments, the characteristics of the resultant optimal control fields were used (often in combination with additional measurements and/or simulations) to decipher physical mechanisms responsible for the achieved control [459]–[463], [465, 467, 468, 472], [474]–[480], [501, 518, 520, 521, 533, 535, 537, 557, 558, 560], [567]–[569]. Also, a method for analysis of quantum control mechanisms through Hamiltonian encoding was recently developed [721]–[728] and experimentally tested [729]. However, much additional theoretical and experimental work is still needed to better understand the controlled dynamics of complex systems, especially those in the condensed phases.

Recent experiments [730]–[734] discovered manifestations of long-lived electronic quantum coherence in energy transfer processes in light-harvesting complexes of photosynthetic systems. Evidence of long-lived electronic and vibrational quantum coherence was also found in intrachain energy transfer in a conjugated polymer [735, 736]. These findings raise an important question about the role of coherent quantum effects in the dynamics of energy transfer and other photoinduced processes in complex chemical and biological systems. This issue already attracted significant attention [737]–[740], and a number of theoretical models [741]–[761] were developed to explain the existence of quantum transport in the presence of strong coupling to a thermal environment. Further advances in this area may lead to a better understanding and more effective control of photophysical and photochemical quantum phenomena in the condensed phase.

Hamiltonian identification is a potentially important application of quantum control aimed at revealing detailed information about physical systems. Extraction of the Hamiltonian from measured data is an inverse problem that generally suffers from being ill-posed (i.e. the

Hamiltonian information is unstable against small changes of the data), which arises because the data used for inversion are inevitably incomplete. Recent attempts to address this challenging problem include Hamiltonian identification via inversion of time-dependent data (instead of the traditional use of time-independent spectroscopic data) [762]–[767] and application of global, nonlinear, map-facilitated inversion procedures [768, 769]. In this context, it appears that suitable controls can be used to significantly increase the information content of the measured data. For example, it may be possible to control the motion of a molecular wave packet to gain more information on interatomic forces in selected regions of a potential energy surface [14]. This concept has seen some nascent development by Geremia and Rabitz [770, 771], who proposed the notion of optimal Hamiltonian identification (OHI). OHI aims to employ coherent control of quantum dynamics to minimize the uncertainty in the extracted Hamiltonian despite data limitations such as finite resolution and noise. The proposed OHI implementation operates in a manner similar to an AFC experiment, using closed-loop optimization guided by a learning algorithm to discover controls that minimize the dispersion of the distribution of Hamiltonians consistent with the measured data. Numerical simulations indicate that an optimal experiment can act as a tailored filter to prevent laboratory noise from significantly propagating into the extracted Hamiltonian [771]. Ideally, upon each cycle of the experiment more information about the Hamiltonian will be extracted, which in turn would be used to guide the next cycle, etc. A critical component of OHI is the need for real-time numerical simulations of the quantum system's dynamics on the fly. OHI will require further development [203] of inversion algorithms, computational capabilities (e.g. possibly including input–output maps discussed in section 8.1) and experimental techniques to become practical.

9. Concluding remarks

It would be impossible to cover in a paper of any reasonable length all of the advances that have been made in the last two decades in the field of quantum control. Some areas that did not receive full attention here were considered in more detail in other review articles and books (in particular, those cited in section 1), to which we refer the interested reader. For example, thematic reviews are available on control via two-pathway quantum interference [1, 8, 21, 24], pump–dump control [7, 11], control via STIRAP [10, 16], control via WPI [42], the formalism and applications of QOCT [14, 36, 38, 40], controllability of quantum systems [36], the formalism of quantum control landscape theory [39], femtosecond pulse-shaping technology [4, 5, 12, 27], femtosecond laser control of x-ray generation [35, 41], quantum control experiments with 'rational' control designs [30], quantum control applications in nonlinear spectroscopy and microscopy [34, 44] and control of quantum dynamics on the attosecond time scale [45]. While we tried to provide a comprehensive account of laboratory AFC of quantum phenomena, more detailed discussions of some important AFC experiments are available in earlier reviews [15, 18, 19, 25, 26, 31, 34, 35, 37, 41]. New papers, often containing significant theoretical and experimental results in quantum control, appear now almost on a daily basis.

In this paper, our goal was to give a perspective and prospective on the field highlighting the evolution of important trends in quantum control. A look into the past together with a review of current, cutting-edge research were used to cautiously forecast topics of future interest. We also attempted to emphasize the synergistic connection between the theoretical and experimental advances, which has been immensely beneficial for the development of the field. We believe that sustaining this productive interplay between theory and experiment will be critical for future

IOP Institute of Physics Φ DEUTSCHE PHYSIKALISCHE GESELLSCHAFT

progress. This paper aimed to provide the basis to better understand which aspects of theoretical research have a high impact on laboratory control of quantum phenomena. At the same time, a complementary goal of this work was to point out the experimental aspects of quantum control that have special significance and relation to theory. Although the scope of experimental and theoretical research in quantum control is vast, we hope that this work provides a valuable bridge for the community involved as well as for those outside who are interested in understanding the reasons for the fervor in the field.

Acknowledgments

References

[1] Brumer P and Shapiro M 1992 *Ann. Rev. Phys. Chem.* **43** 257–82
[2] Warren W S, Rabitz H and Dahleh M 1993 *Science* **259** 1581–9
[3] Kohler B, Krause J L, Raksi F, Wilson K R, Yakovlev V V, Whitnell R M and Yan Y 1995 *Acc. Chem. Res.* **28** 133–40
[4] Kawashima H, Wefers M M and Nelson K A 1995 *Ann. Rev. Phys. Chem.* **46** 627–56
[5] Weiner A M 1995 *Prog. Quantum Electron.* **19** 161–237
[6] Manz J 1996 Molecular wavepacket dynamics: theory for experiments 1926–1996 *Femtochemistry and Femtobiology: Ultrafast Reaction Dynamics at Atomic-Scale Resolution* ed V Sundström (London, UK: Imperial College Press) chapter 3, pp 80–318
[7] Gordon R J and Rice S A 1997 *Ann. Rev. Phys. Chem.* **48** 601–41
[8] Shapiro M and Brumer P 1997 *J. Chem. Soc., Faraday Trans.* **93** 1263–77
[9] Gaspard P and Burghardt I (eds) 1997 *Chemical Reactions and Their Control on the Femtosecond Time Scale* (*Adv. Chem. Phys.* vol 101) (New York: Wiley)
[10] Bergmann K, Theuer H and Shore B W 1998 *Rev. Mod. Phys.* **70** 1003–25
[11] Rice S A and Zhao M 2000 *Optical Control of Molecular Dynamics* (New York: Wiley)
[12] Weiner A M 2000 *Rev. Sci. Instrum.* **71** 1929–60
[13] Rabitz H, de Vivie-Riedle R, Motzkus M and Kompa K 2000 *Science* **288** 824–8
[14] Rabitz H and Zhu W S 2000 *Acc. Chem. Res.* **33** 572–8
[15] Brixner T, Damrauer N and Gerber G 2001 Femtosecond quantum control *Adv. At. Mol. Opt. Phys.* vol 46 ed B Bederson and H Walther (San Diego: Academic Press) pp 1–54
[16] Vitanov N V, Halfmann T, Shore B W and Bergmann K 2001 *Ann. Rev. Phys. Chem.* **52** 763–809
[17] Brown E and Rabitz H 2002 *J. Math. Chem.* **31** 17–63
[18] Levis R J and Rabitz H A 2002 *J. Phys. Chem.* A **106** 6427–44
[19] Weinacht T C and Bucksbaum P H 2002 *J. Opt. B: Quantum Semiclass. Opt.* **4** R35–52
[20] Bandrauk A D, Fujimura Y and Gordon R J (eds) 2002 *Laser Control and Manipulation of Molecules* (*Symp. Series* vol 821) (Washington, DC: ACS Publications)
[21] Brumer P and Shapiro M 2003 *Principles of the Quantum Control of Molecular Processes* (Hoboken, NJ: Wiley-Interscience)
[22] Brif C and Rabitz H 2003 Optimal control of molecular scale phenomena *Fundamentals of Chemistry (Encyclopedia of Life Support Systems* vol 6*)* ed S Carra (Oxford, UK: EOLSS Publishers)
[23] Rabitz H 2003 *Theor. Chem. Acc.* **109** 64–70
[24] Shapiro M and Brumer P 2003 *Rep. Prog. Phys.* **66** 859–942
[25] Brixner T, Damrauer N H, Krampert G, Niklaus P and Gerber G 2003 *J. Mod. Opt.* **50** 539–60
[26] Brixner T and Gerber G 2003 *ChemPhysChem* **4** 418–38

[27] Goswami D 2003 *Phys. Rep.* **374** 385–481

[28] Walmsley I and Rabitz H 2003 *Phys. Today* **56** 43–9

[29] Brixner T and Gerber G 2004 *Phys. Scr.* **T110** 101–7

[30] Dantus M and Lozovoy V V 2004 *Chem. Rev.* **104** 1813–60

[31] Brixner T, Pfeifer T, Gerber G, Wollenhaupt M and Baumert T 2005 Optimal control of atomic, molecular and electron dynamics with tailored femtosecond laser pulses *Femtosecond Laser Spectroscopy* ed P Hannaford (New York: Springer) chapter 9

[32] Carley R E, Heesel E and Fielding H H 2005 *Chem. Soc. Rev.* **34** 949–69

[33] Wollenhaupt M, Engel V and Baumert T 2005 *Ann. Rev. Phys. Chem.* **56** 25–56

[34] Wohlleben W, Buckup T, Herek J L and Motzkus M 2005 *ChemPhysChem* **6** 850–7

[35] Pfeifer T, Spielmann C and Gerber G 2006 *Rep. Prog. Phys.* **69** 443–505

[36] D'Alessandro D 2007 *Introduction to Quantum Control and Dynamics* (Boca Raton, FL: Chapman & Hall/CRC)

[37] Nuernberger P, Vogt G, Brixner T and Gerber G 2007 *Phys. Chem. Chem. Phys.* **9** 2470–97

[38] Werschnik J and Gross E K U 2007 *J. Phys. B: At. Mol. Opt. Phys.* **40** R175–211

[39] Chakrabarti R and Rabitz H 2007 *Int. Rev. Phys. Chem.* **26** 671–735

[40] Balint-Kurti G G, Zou S and Brown A 2008 Optimal control theory for manipulating molecular processes *Adv. Chem. Phys.* vol 138 ed S A Rice (New York: Wiley) pp 43–94

[41] Winterfeldt C, Spielmann C and Gerber G 2008 *Rev. Mod. Phys.* **80** 117–40

[42] Ohmori K 2009 *Ann. Rev. Phys. Chem.* **60** 487–511

[43] Rego L G C, Santos L F and Batista V S 2009 *Ann. Rev. Phys. Chem.* **60** 293–320

[44] Silberberg Y 2009 *Ann. Rev. Phys. Chem.* **60** 277–92

[45] Krausz F and Ivanov M 2009 *Rev. Mod. Phys.* **81** 163–234

[46] Letokhov V S 1977 *Phys. Today* **30** 23–32

[47] Bloembergen N and Yablonovitch E 1978 *Phys. Today* **31** 23–30

[48] Zewail A H 1980 *Phys. Today* **33** 25–33

[49] Bloembergen N and Zewail A H 1984 *J. Phys. Chem.* **88** 5459–65

[50] Elsaesser T and Kaiser W 1991 *Ann. Rev. Phys. Chem.* **42** 83–107

[51] Zewail A H 1996 *J. Phys. Chem.* **100** 12701–24

[52] Brumer P and Shapiro M 1986 *Chem. Phys. Lett.* **126** 541–6

[53] Brumer P and Shapiro M 1986 *Faraday Discuss. Chem. Soc.* **82** 177–85

[54] Shapiro M, Hepburn J W and Brumer P 1988 *Chem. Phys. Lett.* **149** 451–4

[55] Brumer P and Shapiro M 1989 *Acc. Chem. Res.* **22** 407–13

[56] Chan C K, Brumer P and Shapiro M 1991 *J. Chem. Phys.* **94** 2688–96

[57] Chen Z, Brumer P and Shapiro M 1993 *J. Chem. Phys.* **98** 6843–52

[58] Lee S 1998 *J. Chem. Phys.* **108** 3903–8

[59] Chen C, Yin Y Y and Elliott D S 1990 *Phys. Rev. Lett.* **64** 507–10

[60] Chen C and Elliott D S 1990 *Phys. Rev. Lett.* **65** 1737–40

[61] Park S M, Lu S P and Gordon R J 1991 *J. Chem. Phys.* **94** 8622–4

[62] Lu S P, Park S M, Xie Y and Gordon R J 1992 *J. Chem. Phys.* **96** 6613–20

[63] Xing G, Wang X, Huang X, Bersohn R and Katz B 1996 *J. Chem. Phys.* **104** 826–31

[64] Wang X, Bersohn R, Takahashi K, Kawasaki M and Kim H L 1996 *J. Chem. Phys.* **105** 2992–7

[65] Muller H G, Bucksbaum P H, Schumacher D W and Zavriyev A 1990 *J. Phys. B: At. Mol. Opt. Phys.* **23** 2761–9

[66] Schumacher D W, Weihe F, Muller H G and Bucksbaum P H 1994 *Phys. Rev. Lett.* **73** 1344–7

[67] Yin Y Y, Chen C, Elliott D S and Smith A V 1992 *Phys. Rev. Lett.* **69** 2353–6

[68] Yin Y Y, Elliott D S, Shehadeh R and Grant E R 1995 *Chem. Phys. Lett.* **241** 591–6

[69] Sheehy B, Walker B and DiMauro L F 1995 *Phys. Rev. Lett.* **74** 4799–802

[70] Kleiman V D, Zhu L, Li X and Gordon R J 1995 *J. Chem. Phys.* **102** 5863–6

[71] Kleiman V D, Zhu L, Allen J and Gordon R J 1995 *J. Chem. Phys.* **103** 10800–3

[72] Zhu L, Kleiman V, Li X, Lu S P, Trentelman K and Gordon R J 1995 *Science* **270** 77–80

[73] Dupont E, Corkum P B, Liu H C, Buchanan M and Wasilewski Z R 1995 *Phys. Rev. Lett.* **74** 3596–9

[74] Haché A, Kostoulas Y, Atanasov R, Hughes J L P, Sipe J E and van Driel H M 1997 *Phys. Rev. Lett.* **78** 306–9

[75] Chen C and Elliott D S 1996 *Phys. Rev.* A **53** 272–9

[76] Tannor D J and Rice S A 1985 *J. Chem. Phys.* **83** 5013–8

[77] Tannor D J, Kosloff R and Rice S A 1986 *J. Chem. Phys.* **85** 5805–20

[78] Baumert T, Grosser M, Thalweiser R and Gerber G 1991 *Phys. Rev. Lett.* **67** 3753–6

[79] Baumert T, Bühler B, Grosser M, Thalweiser R, Weiss V, Wiedenmann E and Gerber G 1991 *J. Phys. Chem.* **95** 8103–10

[80] Baumert T and Gerber G 1994 *Isr. J. Chem.* **34** 103–14

[81] Potter E D, Herek J L, Pedersen S, Liu Q and Zewail A H 1992 *Nature* **355** 66–8

[82] Herek J L, Materny A and Zewail A H 1994 *Chem. Phys. Lett.* **228** 15–25

[83] Gai F, McDonald J C and Anfinrud P A 1997 *J. Am. Chem. Soc.* **119** 6201–2

[84] Logunov S L, Volkov V V, Braun M and El-Sayed M A 2001 *Proc. Natl Acad. Sci.* **98** 8475–9

[85] Ruhman S, Hou B, Friedman N, Ottolenghi M and Sheves M 2002 *J. Am. Chem. Soc.* **124** 8854–8

[86] Larsen D S, Vengris M, van Stokkum I H, van der Horst M A, de Weerd F L, Hellingwerf K J and van Grondelle R 2004 *Biophys. J.* **86** 2538–50

[87] Larsen D S, van Stokkum I H, Vengris M, van der Horst M A, de Weerd F L, Hellingwerf K J and van Grondelle R 2004 *Biophys. J.* **87** 1858–72

[88] Larsen D S and van Grondelle R 2005 *ChemPhysChem* **6** 828–37

[89] Vengris M, Larsen D S, van der Horst M A, Larsen O F A, Hellingwerf K J and van Grondelle R 2005 *J. Phys. Chem.* B **109** 4197–208

[90] Vengris M, van Stokkum I H M, He X, Bell A F, Tonge P J, van Grondelle R and Larsen D S 2004 *J. Phys. Chem.* A **108** 4587–98

[91] Gaubatz U, Rudecki P, Becker M, Schiemann S, Külz M and Bergmann K 1988 *Chem. Phys. Lett.* **149** 463–8

[92] Kuklinski J R, Gaubatz U, Hioe F T and Bergmann K 1989 *Phys. Rev.* A **40** 6741–4

[93] Gaubatz U, Rudecki P, Schiemann S and Bergmann K 1990 *J. Chem. Phys.* **92** 5363–76

[94] Shore B W, Bergmann K, Oreg J and Rosenwaks S 1991 *Phys. Rev.* A **44** 7442–7

[95] Salour M M and Cohen-Tannoudji C 1977 *Phys. Rev. Lett.* **38** 757–60

[96] Teets R, Eckstein J and Hänsch T W 1977 *Phys. Rev. Lett.* **38** 760–4

[97] Noordam L D, Duncan D I and Gallagher T F 1992 *Phys. Rev.* A **45** 4734–7

[98] Jones R R, Raman C S, Schumacher D W and Bucksbaum P H 1993 *Phys. Rev. Lett.* **71** 2575–8

[99] Jones R R, Schumacher D W, Gallagher T F and Bucksbaum P H 1995 *J. Phys. B: At. Mol. Opt. Phys.* **28** L405–11

[100] Blanchet V, Nicole C, Bouchene M A and Girard B 1997 *Phys. Rev. Lett.* **78** 2716–9

[101] Bouchene M A, Blanchet V, Nicole C, Melikechi N, Girard B, Ruppe H, Rutz S, Schreiber E and Wöste L 1998 *Eur. Phys. J.* D **2** 131–41

[102] Scherer N F, Carlson R J, Matro A, Du M, Ruggiero A J, Romero-Rochin V, Cina J A, Fleming G R and Rice S A 1991 *J. Chem. Phys.* **95** 1487–511

[103] Scherer N F, Matro A, Ziegler L D, Du M, Carlson R J, Cina J A and Fleming G R 1992 *J. Chem. Phys.* **96** 4180–94

[104] Blanchet V, Bouchène M A and Girard B 1998 *J. Chem. Phys.* **108** 4862–76

[105] Doulé C, Hertz E, Berguiga L, Chaux R, Lavorel B and Faucher O 2001 *J. Phys. B: At. Mol. Opt. Phys.* **34** 1133–42

[106] Ohmori K, Sato Y, Nikitin E E and Rice S A 2003 *Phys. Rev. Lett.* **91** 243003

[107] Hertz E, Faucher O, Lavorel B and Chaux R 2000 *J. Chem. Phys.* **113** 6132–8

[108] Bonadeo N H, Erland J, Gammon D, Park D, Katzer D S and Steel D G 1998 *Science* **282** 1473–6

[109] Flissikowski T, Betke A, Akimov I A and Henneberger F 2004 *Phys. Rev. Lett.* **92** 227401

[110] Cina J A 2008 *Ann. Rev. Phys. Chem.* **59** 319–42

[111] Shi S, Woody A and Rabitz H 1988 *J. Chem. Phys.* **88** 6870–83

[112] Peirce A P, Dahleh M A and Rabitz H 1988 *Phys. Rev.* A **37** 4950–64

[113] Shi S and Rabitz H 1989 *Chem. Phys.* **139** 185–99

[114] Kosloff R, Rice S A, Gaspard P, Tersigni S and Tannor D J 1989 *Chem. Phys.* **139** 201–20

[115] Jakubetz W, Manz J and Schreier H J 1990 *Chem. Phys. Lett.* **165** 100–6

[116] Shi S and Rabitz H 1990 *J. Chem. Phys.* **92** 364–76

[117] Shi S and Rabitz H 1990 *J. Chem. Phys.* **92** 2927–37

[118] Dahleh M, Peirce A P and Rabitz H 1990 *Phys. Rev.* A **42** 1065–79

[119] Shi S and Rabitz H 1991 *Comput. Phys. Commun.* **63** 71–83

[120] Gross P, Neuhauser D and Rabitz H 1991 *J. Chem. Phys.* **94** 1158–66

[121] Kaluža M, Muckerman J T, Gross P and Rabitz H 1994 *J. Chem. Phys.* **100** 4211–28

[122] Sugawara M and Fujimura Y 1994 *J. Chem. Phys.* **100** 5646–55

[123] Bardeen C J, Yakovlev V V, Wilson K R, Carpenter S D, Weber P M and Warren W S 1997 *Chem. Phys. Lett.* **280** 151–8

[124] Assion A, Baumert T, Bergt M, Brixner T, Kiefer B, Seyfried V, Strehle M and Gerber G 1998 *Science* **282** 919–22

[125] Bardeen C J, Wang Q and Shank C V 1995 *Phys. Rev. Lett.* **75** 3410–3

[126] Kohler B, Yakovlev V V, Che J, Krause J L, Messina M, Wilson K R, Schwentner N, Whitnell R M and Yan Y 1995 *Phys. Rev. Lett.* **74** 3360–3

[127] Bardeen C J, Che J, Wilson K R, Yakovlev V V, Apkarian V A, Martens C C, Zadoyan R, Kohler B and Messina M 1997 *J. Chem. Phys.* **106** 8486–503

[128] Bardeen C J, Che J, Wilson K R, Yakovlev V V, Cong P, Kohler B, Krause J L and Messina M 1997 *J. Phys. Chem.* A **101** 3815–22

[129] Bardeen C J, Wang Q and Shank C V 1998 *J. Phys. Chem.* A **102** 2759–66

[130] Misawa K and Kobayashi T 2000 *J. Chem. Phys.* **113** 7546–53

[131] Malkmus S, Dürr R, Sobotta C, Pulvermacher H, Zinth W and Braun M 2005 *J. Phys. Chem.* A **109** 10488–92

[132] Melinger J S, Gandhi S R, Hariharan A, Tull J X and Warren W S 1992 *Phys. Rev. Lett.* **68** 2000–3

[133] Broers B, van Linden van den Heuvell H B and Noordam L D 1992 *Phys. Rev. Lett.* **69** 2062–5

[134] Balling P, Maas D J and Noordam L D 1994 *Phys. Rev.* A **50** 4276–85

[135] Kleiman V D, Arrivo S M, Melinger J S and Heilweil E J 1998 *Chem. Phys.* **233** 207–16

[136] Witte T, Hornung T, Windhorn L, Proch D, de Vivie-Riedle R, Motzkus M and Kompa K L 2003 *J. Chem. Phys.* **118** 2021–4

[137] Witte T, Yeston J S, Motzkus M, Heilweil E J and Kompa K L 2004 *Chem. Phys. Lett.* **392** 156–61

[138] Assion A, Baumert T, Helbing J, Seyfried V and Gerber G 1996 *Chem. Phys. Lett.* **259** 488–94

[139] Cerullo G, Bardeen C J, Wang Q and Shank C V 1996 *Chem. Phys. Lett.* **262** 362–8

[140] Bardeen C J, Yakovlev V V, Squier J A and Wilson K R 1998 *J. Am. Chem. Soc.* **120** 13023–7

[141] Brakenhoff G J, Buist A H, Müller M, Squier J A, Bardeen C J, Yakovlev V V and Wilson K R 1999 *Proc. SPIE* **3605** 40–7

[142] Vogt G, Nuernberger P, Selle R, Dimler F, Brixner T and Gerber G 2006 *Phys. Rev.* A **74** 033413

[143] Chen T, Vierheilig A, Waltner P, Heid M, Kiefer W and Materny A 2000 *Chem. Phys. Lett.* **326** 375–82

[144] Hellerer T, Enejder A M and Zumbusch A 2004 *Appl. Phys. Lett.* **85** 25–7

[145] Knutsen K P, Johnson J C, Miller A E, Petersen P B and Saykally R J 2004 *Chem. Phys. Lett.* **387** 436–41

[146] Wollenhaupt M, Präkelt A, Sarpe-Tudoran C, Liese D and Baumert T 2006 *Appl. Phys.* B **82** 183–8

[147] Krug M, Bayer T, Wollenhaupt M, Sarpe-Tudoran C, Baumert T, Ivanov S S and Vitanov N V 2009 *New J. Phys.* **11** 105051

[148] Branderhorst M P A, Londero P, Wasylczyk P, Brif C, Kosut R L, Rabitz H and Walmsley I A 2008 *Science* **320** 638–43

[149] Underwood J G, Spanner M, Ivanov M Y, Mottershead J, Sussman B J and Stolow A 2003 *Phys. Rev. Lett.* **90** 223001

[150] Sussman B J, Underwood J G, Lausten R, Ivanov M Y and Stolow A 2006 *Phys. Rev.* A **73** 053403

[151] Sussman B J, Ivanov M Y and Stolow A 2005 *Phys. Rev.* A **71** 051401

[152] Sussman B J, Townsend D, Ivanov M Y and Stolow A 2006 *Science* **314** 278–81

[153] Abragam A 1983 *Principles of Nuclear Magnetism* (Oxford, UK: Oxford University Press)

[154] Ernst R R, Bodenhausen G and Wokaun A 1990 *Principles of Nuclear Magnetic Resonance in One and Two Dimensions* (Oxford, UK: Oxford University Press)

[155] Freeman R 1998 *Spin Choreography: Basic Steps in High Resolution NMR* (Oxford, UK: Oxford University Press)

[156] Levitt M H 2008 *Spin Dynamics: Basics of Nuclear Magnetic Resonance* 2nd edn (Chichester, UK: Wiley)

[157] Slichter C P 2010 *Principles of Magnetic Resonance* (Berlin: Springer)

[158] Freeman R 1998 *Prog. Nucl. Magn. Reson. Spectrosc.* **32** 59–106

[159] Cory D G *et al* 2000 *Fortschr. Phys.* **48** 875–907

[160] Jones J A 2000 *Fortschr. Phys.* **48** 909–24

[161] Jones J A 2001 *Prog. Nucl. Magn. Reson. Spectrosc.* **38** 325–60

[162] Vandersypen L M K and Chuang I L 2005 *Rev. Mod. Phys.* **76** 1037–69

[163] Ryan C A, Negrevergne C, Laforest M, Knill E and Laflamme R 2008 *Phys. Rev.* A **78** 012328

[164] Khaneja N, Reiss T, Kehlet C, Schulte-Herbrüggen T and Glaser S J 2005 *J. Magn. Reson.* **172** 296–305

[165] Bryson A E and Ho Y C 1975 *Applied Optimal Control: Optimization, Estimation and Control* (Boca Raton, FL: Taylor and Francis)

[166] Stengel R F 1994 *Optimal Control and Estimation* (Mineola, NY: Dover)

[167] Kraus K 1983 *States, Effects and Operations: Fundamental Notions of Quantum Theory (Lecture Notes in Physics* vol 190*)* (Berlin: Springer)

[168] Breuer H P and Petruccione F 2002 *The Theory of Open Quantum Systems* (New York: Oxford University Press)

[169] Gardiner C W and Zoller P 2004 *Quantum Noise: A Handbook of Markovian and Non-Markovian Quantum Stochastic Methods with Applications to Quantum Optics* (Berlin: Springer)

[170] Lindblad G 1976 *Commun. Math. Phys.* **48** 119–30

[171] Yan Y J, Gillilan R E, Whitnell R M, Wilson K R and Mukamel S 1993 *J. Phys. Chem.* **97** 2320–33

[172] Bartana A, Kosloff R and Tannor D J 1993 *J. Chem. Phys.* **99** 196–210

[173] Bartana A, Kosloff R and Tannor D J 1997 *J. Chem. Phys.* **106** 1435–48

[174] Ohtsuki Y, Zhu W S and Rabitz H 1999 *J. Chem. Phys.* **110** 9825–32

[175] Nielsen M A and Chuang I L 2000 *Quantum Computation and Quantum Information* (Cambridge, UK: Cambridge University Press)

[176] Palao J P and Kosloff R 2002 *Phys. Rev. Lett.* **89** 188301

[177] Palao J P and Kosloff R 2003 *Phys. Rev.* A **68** 062308

[178] Horn R A and Johnson C R 1990 *Matrix Analysis* (Cambridge, UK: Cambridge University Press)

[179] Rabitz H, Hsieh M and Rosenthal C 2005 *Phys. Rev.* A **72** 052337

[180] Hsieh M and Rabitz H 2008 *Phys. Rev.* A **77** 042306

[181] Ho T S, Dominy J and Rabitz H 2009 *Phys. Rev.* A **79** 013422

[182] Gilchrist A, Langford N K and Nielsen M A 2005 *Phys. Rev.* A **71** 062310

[183] Kosut R L, Grace M, Brif C and Rabitz H 2006 On the distance between unitary propagators of quantum systems of differing dimensions arXiv:quant-ph/0606064

[184] Grace M D, Dominy J, Kosut R L, Brif C and Rabitz H 2010 *New J. Phys.* **12** 015001

[185] Demiralp M and Rabitz H 1993 *Phys. Rev.* A **47** 809–16

[186] Jozsa R 1994 *J. Mod. Opt.* **41** 2315–23

[187] Fuchs C A and van de Graaf J 1999 *Trans IEEE. Inf. Theory* **45** 1216–27

[188] Jirari H and Pötz W 2005 *Phys. Rev.* A **72** 013409

[189] Rabitz H, Hsieh M and Rosenthal C 2006 *J. Chem. Phys.* **124** 204107
[190] Shen Z, Hsieh M and Rabitz H 2006 *J. Chem. Phys.* **124** 204106
[191] Wu R B, Rabitz H and Hsieh M 2008 *J. Phys. A: Math. Theor.* **41** 015006
[192] Hsieh M, Wu R B and Rabitz H 2009 *J. Chem. Phys.* **130** 104109
[193] Rabitz H, Hsieh M and Rosenthal C 2004 *Science* **303** 1998–2001
[194] Rabitz H, Ho T S, Hsieh M, Kosut R and Demiralp M 2006 *Phys. Rev.* A **74** 012721
[195] Bertrand J and Bertrand P 1987 *Found. Phys.* **17** 397–405
[196] Vogel K and Risken H 1989 *Phys. Rev.* A **40** 2847–9
[197] Leonhardt U 1997 *Measuring the Quantum State of Light* (Cambridge, UK: Cambridge University Press)
[198] Bužek V, Derka R, Adam G and Knight P L 1998 *Ann. Phys., NY* **266** 454–96
[199] Brif C and Mann A 1999 *Phys. Rev.* A **59** 971–87
[200] Brif C and Mann A 2000 *J. Opt. B: Quantum Semiclass. Opt.* **2** 245–51
[201] Řeháček J, Mogilevtsev D and Hradil Z 2008 *New J. Phys.* **10** 043022
[202] D'Ariano G M and Lo Presti P 2001 *Phys. Rev. Lett.* **86** 4195–8
[203] Kosut R, Walmsley I A and Rabitz H 2004 Optimal experiment design for quantum state and process tomography and Hamiltonian parameter estimation arXiv:quant-ph/0411093
[204] Branderhorst M P A, Walmsley I A, Kosut R L and Rabitz H 2008 *J. Phys. B: At. Mol. Opt. Phys.* **41** 074004
[205] Mohseni M, Rezakhani A T and Lidar D A 2008 *Phys. Rev.* A **77** 032322
[206] Young K C, Sarovar M, Kosut R and Whaley K B 2009 *Phys. Rev.* A **79** 062301
[207] Emerson J, Silva M, Moussa O, Ryan C, Laforest M, Baugh J, Cory D G and Laflamme R 2007 *Science* **317** 1893–6
[208] Kosut R L 2009 Quantum process tomography via ℓ_1-norm minimization arXiv:0812.4323
[209] Branderhorst M P A, Nunn J, Walmsley I A and Kosut R L 2009 *New J. Phys.* **11** 115010
[210] Shabani A, Kosut R L and Rabitz H 2009 Compressed quantum process tomography arXiv:0910.5498
[211] Bendersky A, Pastawski F and Paz J P 2008 *Phys. Rev. Lett.* **100** 190403
[212] Schmiegelow C T, Larotonda M A and Paz J P 2010 Selective and efficient quantum process tomography with single photons arXiv:1002.4436
[213] Cramer M and Plenio M B 2010 Reconstructing quantum states efficiently arXiv:1002.3780
[214] Flammia S T, Gross D, Bartlett S D and Somma R 2010 Heralded polynomial-time quantum state tomography arXiv:1002.3839
[215] Ohtsuki Y, Nakagami K, Fujimura Y, Zhu W S and Rabitz H 2001 *J. Chem. Phys.* **114** 8867–76
[216] Shir O M, Emmerich M, Bäck T and Vrakking M J J 2007 The application of evolutionary multi-criteria optimization to dynamic molecular alignment *Proc. IEEE Congress on Evolutionary Computation (CEC 2007)* pp 4108–15
[217] Chakrabarti R, Wu R B and Rabitz H 2008 *Phys. Rev.* A **77** 063425
[218] Chakrabarti R, Wu R B and Rabitz H 2008 *Phys. Rev.* A **78** 033414
[219] Beltrani V, Ghosh P and Rabitz H 2009 *J. Chem. Phys.* **130** 164112
[220] Chankong V and Haimes Y Y 1983 *Multiobjective Decision Making Theory and Methodology* (New York: North-Holland)
[221] Steuer R E 1986 *Multiple Criteria Optimization: Theory, Computation and Application* (New York: Wiley)
[222] Miettinen K M 1998 *Nonlinear Multiobjective Optimization* (Norwell, MA: Kluwer)
[223] Jurdjevic V 1997 *Geometric Control Theory* (Cambridge, UK: Cambridge University Press)
[224] D'Alessandro D and Dahleh M 2001 *Trans. IEEE. Autom. Control* **46** 866–76
[225] Huang G M, Tarn T J and Clark J W 1983 *J. Math. Phys.* **24** 2608–18
[226] Ramakrishna V, Salapaka M V, Dahleh M, Rabitz H and Peirce A 1995 *Phys. Rev.* A **51** 960–6
[227] Turinici G and Rabitz H 2001 *Chem. Phys.* **267** 1–9
[228] Turinici G and Rabitz H 2003 *J. Phys. A: Math. Gen.* **36** 2565–76
[229] Albertini F and D'Alessandro D 2001 Notions of controllability for quantum mechanical systems *Proc. 40th IEEE Conf. on Decision and Control* vol 2 pp 1589–94

[230] Fu H, Schirmer S G and Solomon A I 2001 *J. Phys. A: Math. Gen.* **34** 1679–90
[231] Schirmer S G, Fu H and Solomon A I 2001 *Phys. Rev.* A **63** 063410
[232] Altafini C 2002 *J. Math. Phys.* **43** 2051–62
[233] Girardeau M D, Schirmer S G, Leahy J V and Koch R M 1998 *Phys. Rev.* A **58** 2684–9
[234] Schirmer S G and Leahy J V 2001 *Phys. Rev.* A **63** 025403
[235] Schirmer S G, Solomon A I and Leahy J V 2002 *J. Phys. A: Math. Gen.* **35** 4125–41
[236] Schirmer S G, Solomon A I and Leahy J V 2002 *J. Phys. A: Math. Gen.* **35** 8551–62
[237] Albertini A and D'Alessandro D 2003 *IEEE Trans. Autom. Control* **48** 1399–403
[238] Shah S P, Tannor D J and Rice S A 2002 *Phys. Rev.* A **66** 033405
[239] Gong J and Rice S A 2004 *Phys. Rev.* A **69** 063410
[240] Schirmer S G, Pullen I C H and Solomon A I 2005 *J. Opt. B: Quantum Semiclass. Opt.* **7** S293–9
[241] Turinici G and Rabitz H 2010 *J. Phys. A: Math. Theor.* **43** 105303
[242] Clark J W, Lucarelli D G and Tarn T J 2003 *Int. J. Mod. Phys.* B **17** 5397–411
[243] Wu R B, Tarn T J and Li C W 2006 *Phys. Rev.* A **73** 012719
[244] Vilela Mendes R and Man'ko V I 2010 On the problem of quantum control in infinite dimensions arXiv:1004.3447
[245] Lloyd S and Viola L 2001 *Phys. Rev.* A **65** 010101
[246] Solomon A I and Schirmer S G 2004 Dissipative quantum control arXiv:quant-ph/0401094
[247] Altafini C 2003 *J. Math. Phys.* **44** 2357–72
[248] Altafini C 2004 *Phys. Rev.* A **70** 062321
[249] Romano R 2005 *J. Phys. A: Math. Gen.* **38** 9105–14
[250] Wu R, Pechen A, Brif C and Rabitz H 2007 *J. Phys. A: Math. Theor.* **40** 5681–93
[251] Vilela Mendes R 2009 *Phys. Lett.* A **373** 2529–32
[252] Dirr G, Helmke U, Kurniawan I and Schulte-Herbrüggen T 2009 *Rep. Math. Phys.* **64** 93–121
[253] Wu R B, Chakrabarti R and Rabitz H 2008 *Phys. Rev.* A **77** 052303
[254] Ohtsuki Y, Nakagami K, Zhu W S and Rabitz H 2003 *Chem. Phys.* **287** 197–216
[255] Xu R, Yan Y J, Ohtsuki Y, Fujimura Y and Rabitz H 2004 *J. Chem. Phys.* **120** 6600–8
[256] Beyvers S and Saalfrank P 2008 *J. Chem. Phys.* **128** 074104
[257] Cui W, Xi Z R and Pan Y 2008 *Phys. Rev.* A **77** 032117
[258] Mohseni M and Rezakhani A T 2009 *Phys. Rev.* A **80** 010101
[259] Werschnik J and Gross E K U 2005 *J. Opt. B: Quantum Semiclass. Opt.* **7** S300–12
[260] Lapert M, Tehini R, Turinici G and Sugny D 2009 *Phys. Rev.* A **79** 063411
[261] Lapert M, Tehini R, Turinici G and Sugny D 2008 *Phys. Rev.* A **78** 023408
[262] Ohtsuki Y and Nakagami K 2008 *Phys. Rev.* A **77** 033414
[263] Serban I, Werschnik J and Gross E K U 2005 *Phys. Rev.* A **71** 053810
[264] Kaiser A and May V 2004 *J. Chem. Phys.* **121** 2528–35
[265] Grigorenko I, Garcia M E and Bennemann K H 2002 *Phys. Rev. Lett.* **89** 233003
[266] Mishima K and Yamashita K 2009 *J. Chem. Phys.* **130** 034108
[267] Mishima K and Yamashita K 2009 *J. Chem. Phys.* **131** 014109
[268] Khaneja N, Brockett R and Glaser S J 2001 *Phys. Rev.* A **63** 032308
[269] Khaneja N, Glaser S J and Brockett R 2002 *Phys. Rev.* A **65** 032301
[270] Reiss T O, Khaneja N and Glaser S J 2002 *J. Magn. Reson.* **154** 192–5
[271] Yuan H and Khaneja N 2005 *Phys. Rev.* A **72** 040301
[272] Zhao M and Rice S A 1991 *J. Chem. Phys.* **95** 2465–72
[273] Wu R B, Pechen A, Rabitz H, Hsieh M and Tsou B 2008 *J. Math. Phys.* **49** 022108
[274] Tannor D J, Kazakov V and Orlov V 1992 Control of photochemical branching: novel procedures for finding optimal pulses and global upper bounds *Time Dependent Quantum Molecular Dynamics* ed J Broeckhove and L Lathouwers (New York: Plenum) pp 347–60
[275] Somlói J, Kazakov V A and Tannor D J 1993 *Chem. Phys.* **172** 85–98

[276] Zhu W S, Botina J and Rabitz H 1998 *J. Chem. Phys.* **108** 1953–63
[277] Zhu W S and Rabitz H 1998 *J. Chem. Phys.* **109** 385–91
[278] Maday G and Turinici G 2003 *J. Chem. Phys.* **118** 8191–6
[279] Ohtsuki Y, Turinici G and Rabitz H 2004 *J. Chem. Phys.* **120** 5509–17
[280] Ohtsuki Y, Teranishi Y, Saalfrank P, Turinici G and Rabitz H 2007 *Phys. Rev.* A **75** 033407
[281] Borzì A, Salomon J and Volkwein S 2008 *J. Comput. Appl. Math.* **216** 170–97
[282] Ditz P and Borzì A 2008 *Comput. Phys. Commun.* **178** 393–9
[283] Zhu W S and Rabitz H 1999 *J. Chem. Phys.* **110** 7142–52
[284] Hillermeier C 2001 *Nonlinear Multiobjective Optimization: A Generalized Homotopy Approach* (Basel: Birkhäuser)
[285] Rothman A, Ho T S and Rabitz H 2005 *J. Chem. Phys.* **123** 134104
[286] Rothman A, Ho T S and Rabitz H 2006 *Phys. Rev.* A **73** 053401
[287] Castro A and Gross E K U 2009 *Phys. Rev.* E **79** 056704
[288] Yip F, Mazziotti D and Rabitz H 2003 *J. Chem. Phys.* **118** 8168–72
[289] Balint-Kurti G G, Manby F R, Ren Q, Artamonov M, Ho T S and Rabitz H 2005 *J. Chem. Phys.* **122** 084110
[290] Hsieh M and Rabitz H 2008 *Phys. Rev.* E **77** 037701
[291] Strohecker T and Rabitz H 2010 *J. Comp. Chem.* **31** 151–3
[292] Artamonov M, Ho T S and Rabitz H 2004 *Chem. Phys.* **305** 213–22
[293] Artamonov M, Ho T S and Rabitz H 2006 *Chem. Phys.* **328** 147–55
[294] Artamonov M, Ho T S and Rabitz H 2006 *J. Chem. Phys.* **124** 064306
[295] Kurosaki Y, Artamonov M, Ho T S and Rabitz H 2009 *J. Chem. Phys.* **131** 044306
[296] Kanno M, Hoki K, Kono H and Fujimura Y 2007 *J. Chem. Phys.* **127** 204314
[297] Li G Q, Welack S, Schreiber M and Kleinekathöfer U 2008 *Phys. Rev.* B **77** 075321
[298] Wang L and May V 2009 *Chem. Phys.* **361** 1–8
[299] Kosionis S G, Terzis A F and Paspalakis E 2007 *Phys. Rev.* B **75** 193305
[300] Räsänen E, Castro A, Werschnik J, Rubio A and Gross E K U 2007 *Phys. Rev. Lett.* **98** 157404
[301] Räsänen E, Castro A, Werschnik J, Rubio A and Gross E K U 2008 *Phys. Rev.* B **77** 085324
[302] Chiara G D, Calarco T, Anderlini M, Montangero S, Lee P J, Brown B L, Phillips W D and Porto J V 2008 *Phys. Rev.* A **77** 052333
[303] Hohenester U, Rekdal P K, Borzì A and Schmiedmayer J 2007 *Phys. Rev.* A **75** 023602
[304] Doria P, Calarco T and Montangero S 2010 Antiadiabatic control of many body quantum systems arXiv:1003.3750
[305] Jirari H, Hekking F W J and Buisson O 2009 *Europhys. Lett.* **87** 28004
[306] Grigorenko I and Rabitz H 2009 *Appl. Phys. Lett.* **94** 253107
[307] Hohenester U and Stadler G 2004 *Phys. Rev. Lett.* **92** 196801
[308] Sklarz S E, Tannor D J and Khaneja N 2004 *Phys. Rev.* A **69** 053408
[309] Grigorenko I A and Khveshchenko D V 2005 *Phys. Rev. Lett.* **94** 040506
[310] Jirari H and Pötz W 2006 *Phys. Rev.* A **74** 022306
[311] Wenin M and Pötz W 2006 *Phys. Rev.* A **74** 022319
[312] Pötz W 2007 *J. Comp. Electron.* **6** 171–4
[313] Pelzer A, Ramakrishna S and Seideman T 2007 *J. Chem. Phys.* **126** 034503
[314] Pelzer A, Ramakrishna S and Seideman T 2008 *J. Chem. Phys.* **129** 134301
[315] Palao J P, Kosloff R and Koch C P 2008 *Phys. Rev.* A **77** 063412
[316] Jirari H 2009 *Europhys. Lett.* **87** 40003
[317] Gordon G 2009 *J. Phys. B: At. Mol. Opt. Phys.* **42** 223001
[318] Sanders G D, Kim K W and Holton W C 1999 *Phys. Rev.* A **59** 1098–101
[319] Sklarz S E and Tannor D J 2004 Local control theory for unitary transformations: application to quantum computing without leakage arXiv:quant-ph/0404081
[320] Sklarz S E and Tannor D J 2006 *Chem. Phys.* **322** 87–97

[321] Schulte-Herbrüggen T, Spörl A, Khaneja N and Glaser S J 2005 *Phys. Rev.* A **72** 042331

[322] Spörl A, Schulte-Herbrüggen T, Glaser S J, Bergholm V, Storcz M J, Ferber J and Wilhelm F K 2007 *Phys. Rev.* A **75** 012302

[323] de Vivie-Riedle R and Troppmann U 2007 *Chem. Rev.* **107** 5082–100

[324] Dominy J and Rabitz H 2008 *J. Phys. A: Math. Theor.* **41** 205305

[325] Schröder M and Brown A 2009 *J. Chem. Phys.* **131** 034101

[326] Nebendahl V, Häffner H and Roos C F 2009 *Phys. Rev.* A **79** 012312

[327] Schirmer S 2009 *J. Mod. Opt.* **56** 831–9

[328] Nigmatullin R and Schirmer S G 2009 *New J. Phys.* **11** 105032

[329] Fisher R, Helmer F, Glaser S J, Marquardt F and Schulte-Herbrüggen T 2010 *Phys. Rev.* B **81** 085328

[330] Gollub C, Kowalewski M and de Vivie-Riedle R 2008 *Phys. Rev. Lett.* **101** 073002

[331] Schröder M and Brown A 2009 *New J. Phys.* **11** 105031

[332] Li R and Gaitan F 2010 High-fidelity universal quantum gates through group-symmetrized rapid passage arXiv:1004.0710

[333] Grigorenko I A and Khveshchenko D V 2005 *Phys. Rev. Lett.* **95** 110501

[334] Schulte-Herbrüggen T, Spörl A, Khaneja N and Glaser S J 2009 Optimal control for generating quantum gates in open dissipative systems arXiv:quant-ph/0609037

[335] Hohenester U 2006 *Phys. Rev.* B **74** 161307

[336] Montangero S, Calarco T and Fazio R 2007 *Phys. Rev. Lett.* **99** 170501

[337] Grace M, Brif C, Rabitz H, Walmsley I A, Kosut R L and Lidar D A 2007 *J. Phys. B: At. Mol. Opt. Phys.* **40** S103–25

[338] Grace M D, Brif C, Rabitz H, Lidar D A, Walmsley I A and Kosut R L 2007 *J. Mod. Opt.* **54** 2339–49

[339] Wenin M and Pötz W 2008 *Phys. Rev.* A **78** 012358

[340] Wenin M and Pötz W 2008 *Phys. Rev.* B **78** 165118

[341] Rebentrost P, Serban I, Schulte-Herbrüggen T and Wilhelm F K 2009 *Phys. Rev. Lett.* **102** 090401

[342] Rebentrost P and Wilhelm F K 2009 *Phys. Rev.* B **79** 060507

[343] Motzoi F, Gambetta J M, Rebentrost P and Wilhelm F K 2009 *Phys. Rev. Lett.* **103** 110501

[344] Safaei S, Montangero S, Taddei F and Fazio R 2009 *Phys. Rev.* B **79** 064524

[345] Roloff R and Pötz W 2009 *Phys. Rev.* B **79** 224516

[346] Wenin M, Roloff R and Pötz W 2009 *J. Appl. Phys.* **105** 084504

[347] Roloff R, Wenin M and Pötz W 2009 *J. Comp. Electron.* **8** 29–34

[348] Roloff R, Wenin M and Pötz W 2009 *J. Comput. Theor. Nanosci.* **6** 1837–63

[349] Galve F and Lutz E 2009 *Phys. Rev.* A **79** 032327

[350] Fisher R, Yuan H, Spörl A and Glaser S 2009 *Phys. Rev.* A **79** 042304

[351] Wang X and Schirmer S G 2009 *Phys. Rev.* A **80** 042305

[352] Murphy M, Montangero S, Giovannetti V and Calarco T 2010 Communication at the quantum speed limit along a spin chain arXiv:1004.3445

[353] Timoney N, Elman V, Glaser S, Weiss C, Johanning M, Neuhauser W and Wunderlich C 2008 *Phys. Rev.* A **77** 052334

[354] Nunn J, Walmsley I A, Raymer M G, Surmacz K, Waldermann F C, Wang Z and Jaksch D 2007 *Phys. Rev.* A **75** 011401

[355] Gorshkov A V, André A, Fleischhauer M, Sørensen A S and Lukin M D 2007 *Phys. Rev. Lett.* **98** 123601

[356] Gorshkov A V, Calarco T, Lukin M D and Sørensen A S 2008 *Phys. Rev.* A **77** 043806

[357] Novikova I, Gorshkov A V, Phillips D F, Sørensen A S, Lukin M D and Walsworth R L 2007 *Phys. Rev. Lett.* **98** 243602

[358] Novikova I, Phillips N B and Gorshkov A V 2008 *Phys. Rev.* A **78** 021802

[359] Phillips N B, Gorshkov A V and Novikova I 2008 *Phys. Rev.* A **78** 023801

[360] Chakrabarti R and Ghosh A 2009 Asymptotic efficiency and finite sample performance of frequentist quantum state estimation arXiv:0904.1628

[361] Ho T S and Rabitz H 2006 *J. Photochem. Photobiol.* A **180** 226–40
[362] Glaser S J, Schulte-Herbrüggen T, Sieveking M, Schedletzky O, Nielsen N C, Sørensen O W and Griesinger C 1998 *Science* **280** 421–4
[363] Bonnard B and Chyba M 2003 *Singular Trajectories and Their Role in Control Theory* (Berlin: Springer)
[364] Wu R B, Dominy J, Ho T S and Rabitz H 2009 Singularities of quantum control landscapes arXiv:0907.2354
[365] Lapert M, Zhang Y, Braun M, Glaser S J and Sugny D 2010 *Phys. Rev. Lett.* **104** 083001
[366] Brockett R W 1991 *Linear Alg. Appl.* **146** 79–91
[367] von Neumann J 1937 *Tomsk Univ. Rev.* **1** 286–300
[368] Chakrabarti R, Wu R B and Rabitz H 2008 Computational complexity of quantum optimal control landscapes arXiv:0708.3513
[369] Moore K, Hsieh M and Rabitz H 2008 *J. Chem. Phys.* **128** 154117
[370] Oza A, Pechen A, Dominy J, Beltrani V, Moore K and Rabitz H 2009 *J. Phys. A: Math. Theor.* **42** 205305
[371] Roslund J and Rabitz H 2009 *Phys. Rev.* A **79** 053417
[372] Roslund J, Roth M and Rabitz H 2006 *Phys. Rev.* A **74** 043414
[373] Wollenhaupt M, Präkelt A, Sarpe-Tudoran C, Liese D and Baumert T 2005 *J. Mod. Opt.* **52** 2187–95
[374] Bayer T, Wollenhaupt M and Baumert T 2008 *J. Phys. B: At. Mol. Opt. Phys.* **41** 074007
[375] Marquetand P, Nuernberger P, Vogt G, Brixner T and Engel V 2007 *Europhys. Lett.* **80** 53001
[376] Roslund J and Rabitz H 2009 *Phys. Rev.* A **80** 013408
[377] Judson R S and Rabitz H 1992 *Phys. Rev. Lett.* **68** 1500–3
[378] Geremia J M, Zhu W S and Rabitz H 2000 *J. Chem. Phys.* **113** 10841–8
[379] Omenetto F G, Luce B P and Taylor A J 1999 *J. Opt. Soc. Am.* B **16** 2005–9
[380] Brixner T, García de Abajo F J, Schneider J and Pfeiffer W 2005 *Phys. Rev. Lett.* **95** 093901
[381] Brixner T, de Abajo F J G, Schneider J, Spindler C and Pfeiffer W 2006 *Phys. Rev.* B **73** 125437
[382] Brixner T, García de Abajo F, Spindler C and Pfeiffer W 2006 *Appl. Phys.* B **84** 89–95
[383] Hertz E, Rouzée A, Guérin S, Lavorel B and Faucher O 2007 *Phys. Rev.* A **75** 031403
[384] Voronine D, Abramavicius D and Mukamel S 2006 *J. Chem. Phys.* **124** 034104
[385] Voronine D V, Abramavicius D and Mukamel S 2007 *J. Chem. Phys.* **126** 044508
[386] Tuchscherer P, Rewitz C, Voronine D V, García de Abajo F J, Pfeiffer W and Brixner T 2009 *Opt. Expr.* **17** 14235–59
[387] Zhu W S and Rabitz H 2003 *J. Chem. Phys.* **118** 6751–7
[388] Grace M, Brif C, Rabitz H, Walmsley I, Kosut R and Lidar D 2006 *New J. Phys.* **8** 35
[389] Gollub C and de Vivie-Riedle R 2008 *Phys. Rev.* A **78** 033424
[390] Gollub C and de Vivie-Riedle R 2009 *Phys. Rev.* A **79** 021401
[391] Belavkin V P 1983 *Autom. Remote Control* **44** 178–88 arXiv:quant-ph/0408003
[392] Wiseman H M and Milburn G J 1993 *Phys. Rev. Lett.* **70** 548–51
[393] Wiseman H M 1994 *Phys. Rev.* A **49** 2133–50
[394] Doherty A C, Habib S, Jacobs K, Mabuchi H and Tan S M 2000 *Phys. Rev.* A **62** 012105
[395] Doherty A, Doyle J, Mabuchi H, Jacobs K and Habib S 2000 Robust control in the quantum domain *Proc. 39th IEEE Conf. on Decision and Control* vol 1 pp 949–54 arXiv:quant-ph/0105018
[396] Wiseman H M and Milburn G J 2010 *Quantum Measurement and Control* (Cambridge, UK: Cambridge University Press)
[397] Weiner A M, Leaird D E, Patel J S and Wullert J R 1990 *Opt. Lett.* **15** 326
[398] Wefers M M and Nelson K A 1993 *Opt. Lett.* **18** 2032–4
[399] Wefers M M and Nelson K A 1995 *Opt. Lett.* **20** 1047
[400] Hillegas C W, Tull J X, Goswami D, Strickland D and Warren W S 1994 *Opt. Lett.* **19** 737–9
[401] Verluise F, Laude V, Cheng Z, Spielmann C and Tournois P 2000 *Opt. Lett.* **25** 575–7
[402] Stobrawa G, Hacker M, Feurer T, Zeidler D, Motzkus M and Reichel F 2001 *Appl. Phys.* B **72** 627–30
[403] Monmayrant A and Chatel B 2004 *Rev. Sci. Instrum.* **75** 2668–71
[404] Präkelt A, Wollenhaupt M, Assion A, Horn C, Sarpe-Tudoran C, Winter M and Baumert T 2003 *Rev. Sci. Instrum.* **74** 4950–3

[405] Frumker E, Tal E, Silberberg Y and Majer D 2005 *Opt. Lett.* **30** 2796–8
[406] Jiang Z, Huang C B, Leaird D E and Weiner A M 2007 *Nat. Photon.* **1** 463–7
[407] Jiang Z, Huang C B, Leaird D E and Weiner A M 2007 *J. Opt. Soc. Am.* B **24** 2124–8
[408] Brixner T and Gerber G 2001 *Opt. Lett.* **26** 557–9
[409] Brixner T, Krampert G, Niklaus P and Gerber G 2002 *Appl. Phys.* B **74** S133–44
[410] Polachek L, Oron D and Silberberg Y 2006 *Opt. Lett.* **31** 631–3
[411] Plewicki M, Weise F, Weber S M and Lindinger A 2006 *Appl. Opt.* **45** 8354–9
[412] Ninck M, Galler A, Feurer T and Brixner T 2007 *Opt. Lett.* **32** 3379–81
[413] Masihzadeh O, Schlup P and Bartels R A 2007 *Opt. Expr.* **15** 18025–32
[414] Plewicki M, Weber S M, Weise F and Lindinger A 2007 *Appl. Phys.* B **86** 259–63
[415] Weise F and Lindinger A 2009 *Opt. Lett.* **34** 1258–60
[416] Kupka D, Schlup P and Bartels R A 2009 *Rev. Sci. Instrum.* **80** 053110
[417] Nuernberger P, Vogt G, Selle R, Fechner S, Brixner T and Gerber G 2007 *Appl. Phys.* B **88** 519–26
[418] Parker D S N, Nunn A D G, Minns R S and Fielding H H 2009 *Appl. Phys.* B **94** 181–6
[419] Selle R, Nuernberger P, Langhojer F, Dimler F, Fechner S, Gerber G and Brixner T 2008 *Opt. Lett.* **33** 803–5
[420] Nuernberger P, Selle R, Langhojer F, Dimler F, Fechner S, Gerber G and Brixner T 2009 *J. Opt. A: Pure Appl. Opt.* **11** 085202
[421] Baumert T, Brixner T, Seyfried V, Strehle M and Gerber G 1997 *Appl. Phys.* B **65** 779–82
[422] Yelin D, Meshulach D and Silberberg Y 1997 *Opt. Lett.* **22** 1793–5
[423] Brixner T, Strehle M and Gerber G 1999 *Appl. Phys.* B **68** 281–4
[424] Zeek E, Maginnis K, Backus S, Russek U, Murnane M, Mourou G, Kapteyn H and Vdovin G 1999 *Opt. Lett.* **24** 493–5
[425] Zeek E, Bartels R, Murnane M M, Kapteyn H C, Backus S and Vdovin G 2000 *Opt. Lett.* **25** 587–9
[426] Zeidler D, Hornung T, Proch D and Motzkus M 2000 *Appl. Phys.* B **70** S125–31
[427] Siegner U, Haiml M, Kunde J and Keller U 2002 *Opt. Lett.* **27** 315–7
[428] Efimov A, Moores M D, Beach N M, Krause J L and Reitze D H 1998 *Opt. Lett.* **23** 1915–7
[429] Efimov A, Moores M D, Mei B, Krause J L, Siders C W and Reitze D H 2000 *Appl. Phys.* B **70** S133–41
[430] Meshulach D, Yelin D and Silberberg Y 1998 *J. Opt. Soc. Am.* B **15** 1615–9
[431] Brixner T, Oehrlein A, Strehle M and Gerber G 2000 *Appl. Phys.* B **70** S119–24
[432] Brixner T, Damrauer N H, Krampert G, Niklaus P and Gerber G 2003 *J. Opt. Soc. Am.* B **20** 878–81
[433] Suzuki T, Minemoto S and Sakai H 2004 *Appl. Opt.* **43** 6047–50
[434] Aeschlimann M, Bauer M, Bayer D, Brixner T, García de Abajo F J, Pfeiffer W, Rohmer M, Spindler C and Steeb F 2007 *Nature* **446** 301–4
[435] Bartels R, Backus S, Zeek E, Misoguti L, Vdovin G, Christov I P, Murnane M M and Kapteyn H C 2000 *Nature* **406** 164–6
[436] Bartels R, Backus S, Christov I, Kapteyn H and Murnane M 2001 *Chem. Phys.* **267** 277–89
[437] Bartels R A, Murnane M M, Kapteyn H C, Christov I and Rabitz H 2004 *Phys. Rev.* A **70** 043404
[438] Reitze D H *et al* 2004 *Opt. Lett.* **29** 86–8
[439] Pfeifer T, Kemmer R, Spitzenpfeil R, Walter D, Winterfeldt C, Gerber G and Spielmann C 2005 *Opt. Lett.* **30** 1497–9
[440] Walter D, Pfeifer T, Winterfeldt C, Kemmer R, Spitzenpfeil R, Gerber G and Spielmann C 2006 *Opt. Expr.* **14** 3433–42
[441] Spitzenpfeil R *et al* 2009 *Appl. Phys.* A **96** 69–81
[442] Pfeifer T, Walter D, Winterfeldt C, Spielmann C and Gerber G 2005 *Appl. Phys.* B **80** 277–80
[443] Pfeifer T, Spitzenpfeil R, Walter D, Winterfeldt C, Dimler F, Gerber G and Spielmann C 2007 *Opt. Expr.* **15** 3409–16
[444] Meshulach D and Silberberg Y 1998 *Nature* **396** 239–42
[445] Meshulach D and Silberberg Y 1999 *Phys. Rev.* A **60** 1287–92
[446] Hornung T, Meier R, Zeidler D, Kompa K L, Proch D and Motzkus M 2000 *Appl. Phys.* B **71** 277–84

[447] Dudovich N, Dayan B, Gallagher Faeder S M and Silberberg Y 2001 *Phys. Rev. Lett.* **86** 47–50
[448] Trallero-Herrero C, Cohen J L and Weinacht T 2006 *Phys. Rev. Lett.* **96** 063603
[449] Papastathopoulos E, Strehle M and Gerber G 2005 *Chem. Phys. Lett.* **408** 65–70
[450] Wollenhaupt M, Präkelt A, Sarpe-Tudoran C, Liese D and Baumert T 2005 *J. Opt. B: Quantum Semiclass. Opt.* **7** S270–6
[451] Weinacht T C, Ahn J and Bucksbaum P H 1999 *Nature* **397** 233–5
[452] Leichtle C, Schleich W P, Averbukh I S and Shapiro M 1998 *Phys. Rev. Lett.* **80** 1418–21
[453] Nahmias O, Bismuth O, Shoshana O and Ruhman S 2005 *J. Phys. Chem.* A **109** 8246–53
[454] Lee S H, Jung K H, Sung J H, Hong K H and Nam C H 2002 *J. Chem. Phys.* **117** 9858–61
[455] Prokhorenko V I, Nagy A M and Miller R J D 2005 *J. Chem. Phys.* **122** 184502
[456] Zhang S, Sun Z, Zhang X, Xu Y, Wang Z, Xu Z and Li R 2005 *Chem. Phys. Lett.* **415** 346–50
[457] van der Walle P, Milder M T W, Kuipers L and Herek J L 2009 *Proc. Natl Acad. Sci.* **106** 7714–7
[458] Brixner T, Damrauer N H, Kiefer B and Gerber G 2003 *J. Chem. Phys.* **118** 3692–701
[459] Montgomery M A, Meglen R R and Damrauer N H 2006 *J. Phys. Chem.* A **110** 6391–4
[460] Montgomery M A, Meglen R R and Damrauer N H 2007 *J. Phys. Chem.* A **111** 5126–9
[461] Montgomery M A and Damrauer N H 2007 *J. Phys. Chem.* A **111** 1426–33
[462] Kuroda D G, Singh C P, Peng Z and Kleiman V D 2009 *Science* **326** 263–7
[463] Otake I, Kano S S and Wada A 2006 *J. Chem. Phys.* **124** 014501
[464] Bonacina L, Extermann J, Rondi A, Boutou V and Wolf J P 2007 *Phys. Rev.* A **76** 023408
[465] Okada T, Otake I, Mizoguchi R, Onda K, Kano S S and Wada A 2004 *J. Chem. Phys.* **121** 6386–91
[466] Roth M, Guyon L, Roslund J, Boutou V, Courvoisier F, Wolf J P and Rabitz H 2009 *Phys. Rev. Lett.* **102** 253001
[467] Bergt M, Brixner T, Kiefer B, Strehle M and Gerber G 1999 *J. Phys. Chem.* A **103** 10381–7
[468] Brixner T, Kiefer B and Gerber G 2001 *Chem. Phys.* **267** 241–6
[469] Damrauer N H, Dietl C, Krampert G, Lee S H, Jung K H and Gerber G 2002 *Eur. Phys. J.* D **20** 71–6
[470] Bergt M, Brixner T, Dietl C, Kiefer B and Gerber G 2002 *J. Organomet. Chem.* **661** 199–209
[471] Levis R J, Menkir G M and Rabitz H 2001 *Science* **292** 709–13
[472] Daniel C *et al* 2001 *Chem. Phys.* **267** 247–60
[473] Vajda Š, Rosendo-Francisco P, Kaposta C, Krenz M, Lupulescu C and Wöste L 2001 *Eur. Phys. J.* D **16** 161–4
[474] Daniel C, Full J, González L, Lupulescu C, Manz J, Merli A, Vajda Š and Wöste L 2003 *Science* **299** 536–9
[475] Cardoza D, Baertschy M and Weinacht T 2005 *J. Chem. Phys.* **123** 074315
[476] Cardoza D, Baertschy M and Weinacht T 2005 *Chem. Phys. Lett.* **411** 311–5
[477] Cardoza D, Langhojer F, Trallero-Herrero C, Monti O L A and Weinacht T 2004 *Phys. Rev.* A **70** 053406
[478] Langhojer F, Cardoza D, Baertschy M and Weinacht T 2005 *J. Chem. Phys.* **122** 014102
[479] Cardoza D, Trallero-Herrero C, Langhojer F, Rabitz H and Weinacht T 2005 *J. Chem. Phys.* **122** 124306
[480] Cardoza D, Pearson B J, Baertschy M and Weinacht T 2006 *J. Photochem. Photobiol.* A **180** 277–81
[481] Vajda Š, Bartelt A, Kaposta E C, Leisner T, Lupulescu C, Minemoto S, Rosendo-Francisco P and Wöste L 2001 *Chem. Phys.* **267** 231–9
[482] Bartelt A, Minemoto S, Lupulescu C, Vajda Š and Wöste L 2001 *Eur. Phys. J.* D **16** 127–31
[483] Lindinger A, Lupulescu C, Bartelt A, Vajda Š and Wöste L 2003 *Spectrochim. Acta B: At. Spectrosc.* **58** 1109–24
[484] Bartelt A, Lindinger A, Lupulescu C, Vajda Š and Wöste L 2004 *Phys. Chem. Chem. Phys.* **6** 1679–86
[485] Wells E, Betsch K J, Conover C W S, DeWitt M J, Pinkham D and Jones R R 2005 *Phys. Rev.* A **72** 063406
[486] Wells E, McKenna J, Sayler A M, Jochim B, Gregerson N, Averin R, Zohrabi M, Carnes K D and Ben-Itzhak I 2010 *J. Phys. B: At. Mol. Opt. Phys.* **43** 015101
[487] Chen G Y, Wang Z W and Hill W T 2009 *Phys. Rev.* A **79** 011401
[488] Laarmann T, Shchatsinin I, Singh P, Zhavoronkov N, Gerhards M, Schulz C P and Hertel I V 2007 *J. Chem. Phys.* **127** 201101

[489] Laarmann T, Shchatsinin I, Singh P, Zhavoronkov N, Schulz C P and Hertel I V 2008 *J. Phys. B: At. Mol. Opt. Phys.* **41** 074005

[490] Palliyaguru L, Sloss J, Rabitz H and Levis R J 2008 *J. Mod. Opt.* **55** 177–85

[491] Lozovoy V V, Zhu X, Gunaratne T C, Harris D A, Shane J C and Dantus M 2008 *J. Phys. Chem.* A **112** 3789–12

[492] Zhu X, Gunaratne T C, Lozovoy V V and Dantus M 2009 *J. Phys. Chem.* A **113** 5264–6

[493] Levis R J 2009 *J. Phys. Chem.* A **113** 5267–8

[494] Brixner T, Krampert G, Pfeifer T, Selle R, Gerber G, Wollenhaupt M, Graefe O, Horn C, Liese D and Baumert T 2004 *Phys. Rev. Lett.* **92** 208301

[495] Suzuki T, Minemoto S, Kanai T and Sakai H 2004 *Phys. Rev. Lett.* **92** 133005

[496] Weber S M, Plewicki M, Weise F and Lindinger A 2008 *J. Chem. Phys.* **128** 174306

[497] Lupulescu C, Lindinger A, Plewicki M, Merli A, Weber S M and Wöste L 2004 *Chem. Phys.* **296** 63–9

[498] Weber S M, Lindinger A, Plewicki M, Lupulescu C, Vetter F and Wöste L 2004 *Chem. Phys.* **306** 287–93

[499] Schäfer-Bung B, Mitrić R, Bonačić-Koutecký V, Bartelt A, Lupulescu C, Lindinger A, Vajda Š, Weber S M and Wöste L 2004 *J. Phys. Chem.* A **108** 4175–9

[500] Lindinger A, Weber S M, Lupulescu C, Vetter F, Plewicki M, Merli A, Wöste L, Bartelt A F and Rabitz H 2005 *Phys. Rev.* A **71** 013419

[501] Bartelt A F, Feurer T and Wöste L 2005 *Chem. Phys.* **318** 207–16

[502] Lindinger A, Weber S M, Merli A, Sauer F, Plewicki M and Wöste L 2006 *J. Photochem. Photobiol.* A **180** 256–61

[503] Ballard J B, Stauffer H U, Amitay Z and Leone S R 2002 *J. Chem. Phys.* **116** 1350–60

[504] Lindinger A, Vetter F, Lupulescu C, Plewicki M, Weber S M, Merli A and Wöste L 2004 *Chem. Phys. Lett.* **397** 123–7

[505] Lindinger A, Lupulescu C, Plewicki M, Vetter F, Merli A, Weber S M and Wöste L 2004 *Phys. Rev. Lett.* **93** 033001

[506] Lindinger A, Lupulescu C, Vetter F, Plewicki M, Weber S M, Merli A and Wöste L 2005 *J. Chem. Phys.* **122** 024312

[507] Siedschlag C, Shir O M, Bäck T and Vrakking M J J 2006 *Opt. Commun.* **264** 511–8

[508] Shir O M, Beltrani V, Bäck T, Rabitz H and Vrakking M J J 2008 *J. Phys. B: At. Mol. Opt. Phys.* **41** 074021

[509] Rouzée A, Gijsbertsen A, Ghafur O, Shir O M, Bäck T, Stolte S and Vrakking M J J 2009 *New J. Phys.* **11** 105040

[510] Leibscher M, Averbukh I S and Rabitz H 2003 *Phys. Rev. Lett.* **90** 213001

[511] Leibscher M, Averbukh I S and Rabitz H 2004 *Phys. Rev.* A **69** 013402

[512] Stapelfeldt H and Seideman T 2003 *Rev. Mod. Phys.* **75** 543–57

[513] Bisgaard C Z, Poulsen M D, Péronne E, Viftrup S S and Stapelfeldt H 2004 *Phys. Rev. Lett.* **92** 173004

[514] Renard M, Hertz E, Lavorel B and Faucher O 2004 *Phys. Rev.* A **69** 043401

[515] Renard M, Hertz E, Guérin S, Jauslin H R, Lavorel B and Faucher O 2005 *Phys. Rev.* A **72** 025401

[516] Lee K F, Villeneuve D M, Corkum P B, Stolow A and Underwood J G 2006 *Phys. Rev. Lett.* **97** 173001

[517] Horn C, Wollenhaupt M, Krug M, Baumert T, de Nalda R and Bañares L 2006 *Phys. Rev.* A **73** 031401

[518] de Nalda R, Horn C, Wollenhaupt M, Krug M, Bañares L and Baumert T 2007 *J. Raman Spectrosc.* **38** 543–50

[519] Pinkham D, Mooney K E and Jones R R 2007 *Phys. Rev.* A **75** 013422

[520] Hornung T, Meier R and Motzkus M 2000 *Chem. Phys. Lett.* **326** 445–53

[521] Weinacht T C, Bartels R, Backus S, Bucksbaum P H, Pearson B, Geremia J M, Rabitz H, Kapteyn H C and Murnane M M 2001 *Chem. Phys. Lett.* **344** 333–8

[522] Bartels R A, Weinacht T C, Leone S R, Kapteyn H C and Murnane M M 2002 *Phys. Rev. Lett.* **88** 033001

[523] Weinacht T C, White J L and Bucksbaum P H 1999 *J. Phys. Chem.* A **103** 10166–8

[524] Pearson B J, White J L, Weinacht T C and Bucksbaum P H 2001 *Phys. Rev.* A **63** 063412

[525] White J L, Pearson B J and Bucksbaum P H 2004 *J. Phys. B: At. Mol. Opt. Phys.* **37** L399–405

[526] Pearson B J and Bucksbaum P H 2004 *Phys. Rev. Lett.* **92** 243003

[527] Spanner M and Brumer P 2006 *Phys. Rev.* A **73** 023809

[528] Spanner M and Brumer P 2006 *Phys. Rev.* A **73** 023810

[529] Zeidler D, Frey S, Wohlleben W, Motzkus M, Busch F, Chen T, Kiefer W and Materny A 2002 *J. Chem. Phys.* **116** 5231–5

[530] Konradi J, Singh A K and Materny A 2005 *Phys. Chem. Chem. Phys.* **7** 3574–9

[531] Konradi J, Scaria A, Namboodiri V and Materny A 2007 *J. Raman Spectrosc.* **38** 1006–21

[532] Konradi J, Singh A K, Scaria A V and Materny A 2006 *J. Raman Spectrosc.* **37** 697–704

[533] Konradi J, Singh A K and Materny A 2006 *J. Photochem. Photobiol.* A **180** 289–99

[534] Scaria A, Konradi J, Namboodiri V and Materny A 2008 *J. Raman Spectrosc.* **39** 739–49

[535] Zhang S, Zhang L, Zhang X, Ding L, Chen G, Sun Z and Wang Z 2007 *Chem. Phys. Lett.* **433** 416–21

[536] von Vacano B, Wohlleben W and Motzkus M 2006 *Opt. Lett.* **31** 413–5

[537] Strasfeld D B, Shim S H and Zanni M T 2007 *Phys. Rev. Lett.* **99** 038102

[538] Strasfeld D B, Middleton C T and Zanni M T 2009 *New J. Phys.* **11** 105046

[539] Kawano H, Nabekawa Y, Suda A, Oishi Y, Mizuno H, Miyawaki A and Midorikawa K 2003 *Biochem. Biophys. Res. Commun.* **311** 592–6

[540] Chen J, Kawano H, Nabekawa Y, Mizuno H, Miyawaki A, Tanabe T, Kannari F and Midorikawa K 2004 *Opt. Exp.* **12** 3408–14

[541] Tada J, Kono T, Suda A, Mizuno H, Miyawaki A, Midorikawa K and Kannari F 2007 *Appl. Opt.* **46** 3023–30

[542] Isobe K, Suda A, Tanaka M, Kannari F, Kawano H, Mizuno H, Miyawaki A and Midorikawa K 2009 *Opt. Exp.* **17** 13737–46

[543] Li B Q, Turinici G, Ramakrishna V and Rabitz H 2002 *J. Phys. Chem.* B **106** 8125–31

[544] Turinici G, Ramakrishna V, Li B Q and Rabitz H 2004 *J. Phys. A: Math. Gen.* **37** 273–82

[545] Li B, Rabitz H and Wolf J P 2005 *J. Chem. Phys.* **122** 154103

[546] Li B Q, Zhu W S and Rabitz H 2006 *J. Chem. Phys.* **124** 024101

[547] Brixner T, Damrauer N H, Niklaus P and Gerber G 2001 *Nature* **414** 57–60

[548] Tkaczyk E R, Tkaczyk A H, Mauring K, Ye J Y, Baker J R and Norris T B 2010 *J. Lumin.* **130** 29–34

[549] Herek J L, Wohlleben W, Cogdell R J, Zeidler D and Motzkus M 2002 *Nature* **417** 533–5

[550] Wohlleben W, Buckup T, Herek J L, Cogdell R J and Motzkus M 2003 *Biophys. J.* **85** 442–50

[551] Buckup T, Lebold T, Weigel A, Wohlleben W and Motzkus M 2006 *J. Photochem. Photobiol.* A **180** 314–21

[552] Brüggemann B, Organero J A, Pascher T, Pullerits T and Yartsev A 2006 *Phys. Rev. Lett.* **97** 208301

[553] Vogt G, Krampert G, Niklaus P, Nuernberger P and Gerber G 2005 *Phys. Rev. Lett.* **94** 068305

[554] Hoki K and Brumer P 2005 *Phys. Rev. Lett.* **95** 168305

[555] Hunt P A and Robb M A 2005 *J. Am. Chem. Soc.* **127** 5720–6

[556] Improta R and Santoro F 2005 *J. Chem. Theory Comput.* **1** 215–29

[557] Dietzek B, Brüggemann B, Pascher T and Yartsev A 2006 *Phys. Rev. Lett.* **97** 258301

[558] Dietzek B, Brüggemann B, Pascher T and Yartsev A 2007 *J. Am. Chem. Soc.* **129** 13014–21

[559] Prokhorenko V I, Nagy A M, Waschuk S A, Brown L S, Birge R R and Miller R J D 2006 *Science* **313** 1257–61

[560] Prokhorenko V I, Nagy A M, Brown L S and Miller R J D 2007 *Chem. Phys.* **341** 296–309

[561] Vogt G, Nuernberger P, Brixner T and Gerber G 2006 *Chem. Phys. Lett.* **433** 211–5

[562] Florean A C, Cardoza D, White J L, Lanyi J K, Sension R J and Bucksbaum P H 2009 *Proc. Natl Acad. Sci.* **106** 10896–900

[563] Hoki K and Brumer P 2009 *Chem. Phys. Lett.* **468** 23–7

[564] Katz G, Ratner M A and Kosloff R 2010 *New J. Phys.* **12** 015003

[565] Shuang F and Rabitz H 2006 *J. Chem. Phys.* **124** 154105

[566] Carroll E C, Pearson B J, Florean A C, Bucksbaum P H and Sension R J 2006 *J. Chem. Phys.* **124** 114506

[567] Carroll E C, White J L, Florean A C, Bucksbaum P H and Sension R J 2008 *J. Phys. Chem.* A **112** 6811–22

[568] Kotur M, Weinacht T, Pearson B J and Matsika S 2009 *J. Chem. Phys.* **130** 134311

[569] Greenfield M, McGrane S D and Moore D S 2009 *J. Phys. Chem.* A **113** 2333–9

[570] Laarmann T, Shchatsinin I, Stalmashonak A, Boyle M, Zhavoronkov N, Handt J, Schmidt R, Schulz C P and Hertel I V 2007 *Phys. Rev. Lett.* **98** 058302

[571] Kunde J, Baumann B, Arlt S, Morier-Genoud F, Siegner U and Keller U 2000 *Appl. Phys. Lett.* **77** 924–6

[572] Kunde J, Baumann B, Arlt S, Morier-Genoud F, Siegner U and Keller U 2001 *J. Opt. Soc. Am.* B **18** 872–81

[573] Chung J H and Weiner A 2006 *IEEE J. Sel. Top. Quantum Electron.* **12** 297–306

[574] Brif C, Rabitz H, Wallentowitz S and Walmsley I A 2001 *Phys. Rev.* A **63** 063404

[575] Haeberlen U 1976 *High Resolution NMR in Solids* (New York: Academic)

[576] Viola L and Lloyd S 1998 *Phys. Rev.* A **58** 2733–44

[577] Viola L, Knill E and Lloyd S 1999 *Phys. Rev. Lett.* **82** 2417–21

[578] Zanardi P 1999 *Phys. Lett.* A **258** 77–82

[579] Vitali D and Tombesi P 1999 *Phys. Rev.* A **59** 4178–86

[580] Vitali D and Tombesi P 2001 *Phys. Rev.* A **65** 012305

[581] Byrd M S and Lidar D A 2003 *Phys. Rev.* A **67** 012324

[582] Khodjasteh K and Lidar D A 2005 *Phys. Rev. Lett.* **95** 180501

[583] Facchi P, Tasaki S, Pascazio S, Nakazato H, Tokuse A and Lidar D A 2005 *Phys. Rev.* A **71** 022302

[584] Viola L and Knill E 2005 *Phys. Rev. Lett.* **94** 060502

[585] Uhrig G S 2007 *Phys. Rev. Lett.* **98** 100504

[586] Pasini S and Uhrig G S 2010 *Phys. Rev.* A **81** 012309

[587] Uhrig G S and Pasini S 2010 *New J. Phys.* **12** 045001

[588] Fraval E, Sellars M J and Longdell J J 2005 *Phys. Rev. Lett.* **95** 030506

[589] Morton J J L, Tyryshkin A M, Ardavan A, Benjamin S C, Porfyrakis K, Lyon S A and Briggs G A D 2006 *Nat. Phys.* **2** 40–3

[590] Morton J J L, Tyryshkin A M, Brown R M, Shankar S, Lovett B W, Ardavan A, Schenkel T, Haller E E, Ager J W and Lyon S A 2008 *Nature* **455** 1085–8

[591] Damodarakurup S, Lucamarini M, Di Giuseppe G, Vitali D and Tombesi P 2009 *Phys. Rev. Lett.* **103** 040502

[592] Sagi Y, Almog I and Davidson N 2009 Suppression of collisional decoherence arXiv:0905.0286

[593] Sagi Y, Almog I and Davidson N 2010 Process tomography of dynamical decoupling in a dense optically trapped atomic ensemble arXiv:1004.1011

[594] Biercuk M J, Uys H, VanDevender A P, Shiga N, Itano W M and Bollinger J J 2009 *Nature* **458** 996–1000

[595] Schwefel H P 1995 *Evolution and Optimum Seeking* (New York: Wiley)

[596] Goldberg D E 2007 *Genetic Algorithms in Search, Optimization and Machine Learning* (Reading, MA: Addison-Wesley)

[597] Bartelt A F, Roth M, Mehendale M and Rabitz H 2005 *Phys. Rev.* A **71** 063806

[598] Zeidler D, Frey S, Kompa K L and Motzkus M 2001 *Phys. Rev.* A **64** 023420

[599] Shir O M, Siedschlag C, Bäck T and Vrakking M J J 2006 Niching in evolution strategies and its application to laser pulse shaping *Artificial Evolution (Lecture Notes in Computer Science* vol 3871*)* (Berlin: Springer) pp 85–96

[600] Fonseca C M and Fleming P J 1995 *Evol. Comput.* **3** 1–16

[601] Deb K 1999 *Evol. Comput.* **7** 205–30

[602] Gollub C and de Vivie-Riedle R 2009 *New J. Phys.* **11** 013019

[603] Kirkpatrick S, Gelatt C D and Vecchi M P 1983 *Science* **220** 671–80

[604] Dorigo M, Maniezzo V and Colorni A 1996 *IEEE Trans. Syst. Man Cybern.* B **26** 29–41

[605] Bonabeau E, Dorigo M and Theraulaz G 2000 *Nature* **406** 39–42

[606] Feurer T 1999 *Appl. Phys.* B **68** 55–60

[607] Glaß A, Rozgonyi T, Feurer T, Sauerbrey R and Szabó G 2000 *Appl. Phys.* B **71** 267–76

[608] Roslund J, Shir O M, Bäck T and Rabitz H 2009 *Phys. Rev.* A **80** 043415

[609] Dudovich N, Oron D and Silberberg Y 2002 *Nature* **418** 512–4

[610] Oron D, Dudovich N, Yelin D and Silberberg Y 2002 *Phys. Rev. Lett.* **88** 063004

[611] Oron D, Dudovich N and Silberberg Y 2002 *Phys. Rev. Lett.* **89** 273001
[612] Oron D, Dudovich N, Yelin D and Silberberg Y 2002 *Phys. Rev.* A **65** 043408
[613] Dudovich N, Oron D and Silberberg Y 2003 *J. Chem. Phys.* **118** 9208–15
[614] Oron D, Dudovich N and Silberberg Y 2003 *Phys. Rev. Lett.* **90** 213902
[615] Gershgoren E, Bartels R A, Fourkas J T, Tobey R, Murnane M M and Kapteyn H C 2003 *Opt. Lett.* **28** 361–3
[616] Pastirk I, Cruz J D, Walowicz K, Lozovoy V and Dantus M 2003 *Opt. Exp.* **11** 1695–701
[617] Lim S H, Caster A G and Leone S R 2005 *Phys. Rev.* A **72** 041803
[618] Ogilvie J P, Débarre D, Solinas X, Martin J L, Beaurepaire E and Joffre M 2006 *Opt. Exp.* **14** 759–66
[619] von Vacano B and Motzkus M 2007 *J. Chem. Phys.* **127** 144514
[620] Pestov D, Wang X, Murawski R K, Ariunbold G O, Sautenkov V A and Sokolov A V 2008 *J. Opt. Soc. Am.* B **25** 768–72
[621] Postma S, van Rhijn A C W, Korterik J P, Gross P, Herek J L and Offerhaus H L 2008 *Opt. Exp.* **16** 7985–96
[622] Isobe K, Suda A, Tanaka M, Hashimoto H, Kannari F, Kawano H, Mizuno H, Miyawaki A and Midorikawa K 2009 *Opt. Exp.* **17** 11259–66
[623] Dudovich N, Oron D and Silberberg Y 2004 *Phys. Rev. Lett.* **92** 103003
[624] Wollenhaupt M, Krug M, Köhler J, Bayer T, Sarpe-Tudoran C and Baumert T 2009 *Appl. Phys.* B **95** 245–59
[625] Präkelt A, Wollenhaupt M, Sarpe-Tudoran C and Baumert T 2004 *Phys. Rev.* A **70** 063407
[626] Barros H G, B W L, Vianna S S and Acioli L H 2005 *Opt. Lett.* **30** 3081–3
[627] Barros H G, Ferraz J, B W L, Acioli L H and Vianna S S 2006 *Phys. Rev.* A **74** 055402
[628] Wollenhaupt M, Präkelt A, Sarpe-Tudoran C, Liese D, Bayer T and Baumert T 2006 *Phys. Rev.* A **73** 063409
[629] Dudovich N, Polack T, Pe'er A and Silberberg Y 2005 *Phys. Rev. Lett.* **94** 083002
[630] Amitay Z, Gandman A, Chuntonov L and Rybak L 2008 *Phys. Rev. Lett.* **100** 193002
[631] Zhdanovich S, Shapiro E A, Hepburn J W, Shapiro M and Milner V 2009 *Phys. Rev.* A **80** 063405
[632] Viftrup S S, Kumarappan V, Holmegaard L, Bisgaard C Z, Stapelfeldt H, Artamonov M, Hamilton E and Seideman T 2009 *Phys. Rev.* A **79** 023404
[633] Ibrahim H, Héjjas M, Fushitani M and Schwentner N 2009 *J. Phys. Chem.* A **113** 7439–50
[634] Nakamura Y, Pashkin Y A and Tsai J S 1999 *Nature* **398** 786–8
[635] Feurer T, Vaughan J C and Nelson K A 2003 *Science* **299** 374–7
[636] Fanciulli R, Weiner A M, Dignam M M, Meinhold D and Leo K 2005 *Phys. Rev.* B **71** 153304
[637] Golan B, Fradkin Z, Kopnov G, Oron D and Naaman R 2009 *J. Chem. Phys.* **130** 064705
[638] Lloyd S 2000 *Phys. Rev.* A **62** 022108
[639] Belavkin V P 1999 *Rep. Math. Phys.* **43** A405–25
[640] Bouten L, van Handel R and James M R 2007 *SIAM J. Control Optim.* **46** 2199–241
[641] Bouten L, van Handel R and James M R 2009 *SIAM Rev.* **51** 239–316
[642] Nelson R J, Weinstein Y, Cory D and Lloyd S 2000 *Phys. Rev. Lett.* **85** 3045–8
[643] Yanagisawa M and Kimura H 2003 *IEEE Trans. Autom. Control* **48** 2107–20
[644] Yanagisawa M and Kimura H 2003 *IEEE Trans. Autom. Control* **48** 2121–32
[645] Wiseman H M and Milburn G J 1994 *Phys. Rev.* A **49** 4110–25
[646] D'Helon C and James M R 2006 *Phys. Rev.* A **73** 053803
[647] James M R, Nurdin H I and Petersen I R 2008 *IEEE Trans. Autom. Control* **53** 1787–803
[648] Mabuchi H 2008 *Phys. Rev.* A **78** 032323
[649] Kallush S and Kosloff R 2006 *Phys. Rev.* A **73** 032324
[650] Pechen A, Brif C, Wu R B, Chakrabarti R and Rabitz H 2010 General unifying features of controlled quantum phenomena arXiv:1003.3506
[651] Bushev P, Rotter D, Wilson A, Dubin F, Becher C, Eschner J, Blatt R, Steixner V, Rabl P and Zoller P 2006 *Phys. Rev. Lett.* **96** 043003
[652] Berglund A J, McHale K and Mabuchi H 2007 *Opt. Lett.* **32** 145–7
[653] Gillett G G, Dalton R B, Lanyon B P, Almeida M P, Barbieri M, Pryde G J, O'Brien J L, Resch K J, Bartlett S D and White A G 2010 *Phys. Rev. Lett.* **104** 080503

[654] Doherty A C, Jacobs K and Jungman G 2001 *Phys. Rev.* A **63** 062306
[655] Thomsen L K, Mancini S and Wiseman H M 2002 *Phys. Rev.* A **65** 061801
[656] Thomsen L K, Mancini S and Wiseman H M 2002 *J. Phys. B: At. Mol. Opt. Phys.* **35** 4937–52
[657] Stockton J K, Geremia J M, Doherty A C and Mabuchi H 2004 *Phys. Rev.* A **69** 032109
[658] Berglund A J and Mabuchi H 2004 *Appl. Phys.* B **78** 653–9
[659] Mabuchi H and Khaneja N 2005 *Int. J. Robust Nonlinear Control* **15** 647–67
[660] Wiseman H M and Doherty A C 2005 *Phys. Rev. Lett.* **94** 070405
[661] Gough J, Belavkin V P and Smolyanov O G 2005 *J. Opt. B: Quantum Semiclass. Opt.* **7** S237–44
[662] Belavkin V P, Negretti A and Mølmer K 2009 *Phys. Rev.* A **79** 022123
[663] Jacobs K and Shabani A 2008 *Contemp. Phys.* **49** 435–48
[664] Nielsen A E B, Hopkins A S and Mabuchi H 2009 *New J. Phys.* **11** 105043
[665] Jacobs K 2010 *New J. Phys.* **12** 043005
[666] Mirrahimi M and van Handel R 2007 *SIAM J. Control Optim.* **46** 445–67
[667] Jacobs K and Lund A P 2007 *Phys. Rev. Lett.* **99** 020501
[668] Yamamoto N, Tsumura K and Hara S 2007 *Automatica* **43** 981–92
[669] Dotsenko I, Mirrahimi M, Brune M, Haroche S, Raimond J M and Rouchon P 2009 *Phys. Rev.* A **80** 013805
[670] Dong D and Petersen I R 2009 *New J. Phys.* **11** 105033
[671] Ahn C, Doherty A C and Landahl A J 2002 *Phys. Rev.* A **65** 042301
[672] Ahn C, Wiseman H M and Milburn G J 2003 *Phys. Rev.* A **67** 052310
[673] Ahn C, Wiseman H and Jacobs K 2004 *Phys. Rev.* A **70** 024302
[674] Sarovar M, Ahn C, Jacobs K and Milburn G J 2004 *Phys. Rev.* A **69** 052324
[675] Chase B A, Landahl A J and Geremia J M 2008 *Phys. Rev.* A **77** 032304
[676] Kerckhoff J, Nurdin H I, Pavlichin D S and Mabuchi H 2010 Designing quantum memories with embedded control: photonic circuits for autonomous quantum error correction arXiv:0907.0236
[677] Stockton J K, van Handel R and Mabuchi H 2004 *Phys. Rev.* A **70** 022106
[678] van Handel R, Stockton J K and Mabuchi H 2005 *J. Opt. B: Quantum Semiclass. Opt.* **7** S179–97
[679] Mancini S 2006 *Phys. Rev.* A **73** 010304
[680] Mancini S and Wiseman H M 2007 *Phys. Rev.* A **75** 012330
[681] Yamamoto N, Nurdin H I, James M R and Petersen I R 2008 *Phys. Rev.* A **78** 042339
[682] Nielsen A E B 2010 *Phys. Rev.* A **81** 012307
[683] Hopkins A, Jacobs K, Habib S and Schwab K 2003 *Phys. Rev.* B **68** 235328
[684] Steck D A, Jacobs K, Mabuchi H, Bhattacharya T and Habib S 2004 *Phys. Rev. Lett.* **92** 223004
[685] Steck D A, Jacobs K, Mabuchi H, Habib S and Bhattacharya T 2006 *Phys. Rev.* A **74** 012322
[686] Wilson S D, Carvalho A R R, Hope J J and James M R 2007 *Phys. Rev.* A **76** 013610
[687] Jacobs K 2003 *Phys. Rev.* A **67** 030301
[688] Combes J and Jacobs K 2006 *Phys. Rev. Lett.* **96** 010504
[689] van Handel R, Stockton J K and Mabuchi H 2005 *IEEE Trans. Autom. Control* **50** 768–80
[690] Wiseman H M and Ralph J F 2006 *New J. Phys.* **8** 90
[691] Wiseman H M and Bouten L 2008 *Quant. Inf. Process.* **7** 71–83
[692] Chiruvelli A and Jacobs K 2008 *Phys. Rev.* A **77** 012102
[693] Shabani A and Jacobs K 2008 *Phys. Rev. Lett.* **101** 230403
[694] Armen M A, Au J K, Stockton J K, Doherty A C and Mabuchi H 2002 *Phys. Rev. Lett.* **89** 133602
[695] Cook R L, Martin P J and Geremia J M 2007 *Nature* **446** 774–7
[696] Shorter J A, Ip P C and Rabitz H A 1999 *J. Phys. Chem.* A **103** 7192–8
[697] Rabitz H and Alış Ö F 1999 *J. Math. Chem.* **25** 197–233
[698] Rabitz H, Alış Ö F, Shorter J and Shim K 1999 *Comput. Phys. Commun.* **117** 11–20
[699] Alış Ö F and Rabitz H 2001 *J. Math. Chem.* **29** 127–42
[700] Li G, Rosenthal C and Rabitz H 2001 *J. Phys. Chem.* A **105** 7765–77
[701] Geremia J M, Weiss E and Rabitz H 2001 *Chem. Phys.* **267** 209–22

[702] Hertz J, Krogh A and Palmer R G 1991 *Introduction to the Theory of Neural Computation* (New York: Westview Press)

[703] Freeman J A and Skapura D M 1991 *Neural Networks: Algorithms, Applications and Programming Techniques* (Redwood City, CA: Addison-Wesley)

[704] Selle R, Vogt G, Brixner T, Gerber G, Metzler R and Kinzel W 2007 *Phys. Rev.* A **76** 023810

[705] Selle R, Brixner T, Bayer T, Wollenhaupt M and Baumert T 2008 *J. Phys. B: At. Mol. Opt. Phys.* **41** 074019

[706] McGrane S D, Scharff R J, Greenfield M and Moore D S 2009 *New J. Phys.* **11** 105047

[707] Rossi F and Kuhn T 2002 *Rev. Mod. Phys.* **74** 895–50

[708] Hanson R, Kouwenhoven L P, Petta J R, Tarucha S and Vandersypen L M K 2007 *Rev. Mod. Phys.* **79** 1217

[709] Appel J, Figueroa E, Korystov D, Lobino M and Lvovsky A I 2008 *Phys. Rev. Lett.* **100** 093602

[710] Choi K S, Deng H, Laurat J and Kimble H J 2008 *Nature* **452** 67–71

[711] Staudt M U, Hastings-Simon S R, Nilsson M, Afzelius M, Scarani V, Ricken R, Suche H, Sohler W, Tittel W and Gisin N 2007 *Phys. Rev. Lett.* **98** 113601

[712] Reim K F, Nunn J, Lorenz V O, Sussman B J, Lee K, Langford N K, Jaksch D and Walmsley I A 2009 Towards high-speed optical quantum memories arXiv:0912.2970

[713] Lvovsky A I, Sanders B C and Tittel W 2009 *Nature Photon.* **3** 706–14

[714] Simon C *et al* 2010 Quantum memories. A review based on the European integrated project 'Qubit applications (QAP)' arXiv:1003.1107

[715] Solas F, Ashton J M, Markmann A and Rabitz H A 2009 *J. Chem. Phys.* **130** 214702

[716] Makhlin Y, Schön G and Shnirman A 2001 *Rev. Mod. Phys.* **73** 357–400

[717] Clarke J and Wilhelm F K 2008 *Nature* **453** 1031–42

[718] Walmsley I A 2009 private communication

[719] Liu C, Kohler M C, Hatsagortsyan K Z, Muller C and Keitel C H 2009 *New J. Phys.* **11** 105045

[720] Beltrani V, Dominy J, Ho T S and Rabitz H 2007 *J. Chem. Phys.* **126** 094105

[721] Mitra A and Rabitz H 2003 *Phys. Rev.* A **67** 033407

[722] Mitra A, Solá I R and Rabitz H 2003 *Phys. Rev.* A **67** 043409

[723] Mitra A and Rabitz H 2004 *J. Phys. Chem.* A **108** 4778–85

[724] Sharp R W and Rabitz H 2004 *J. Chem. Phys.* **121** 4516–27

[725] Mitra A and Rabitz H 2006 *J. Chem. Phys.* **125** 194107

[726] Mitra A and Rabitz H 2008 *J. Chem. Phys.* **128** 044112

[727] Mitra A, Sola I R and Rabitz H 2008 *Phys. Rev.* A **77** 043415

[728] Sharp R, Mitra A and Rabitz H 2008 *J. Math. Chem.* **44** 142–71

[729] Rey-de-Castro R and Rabitz H 2010 Laboratory implementation of quantum control mechanism identification through Hamiltonian-encoding and observable-decoding *Phys. Rev.* A to be published

[730] Engel G S, Calhoun T R, Read E L, Ahn T K, Mančal T, Cheng Y C, Blankenship R E and Fleming G R 2007 *Nature* **446** 782–6

[731] Lee H, Cheng Y C and Fleming G R 2007 *Science* **316** 1462–5

[732] Mercer I P, El-Taha Y C, Kajumba N, Marangos J P, Tisch J W G, Gabrielsen M, Cogdell R J, Springate E and Turcu E 2009 *Phys. Rev. Lett.* **102** 057402

[733] Collini E, Wong C Y, Wilk K E, Curmi P M G, Brumer P and Scholes G D 2010 *Nature* **463** 644–7

[734] Panitchayangkoon G, Hayes D, Fransted K A, Caram J R, Harel E, Wen J, Blankenship R E and Engel G S 2010 Long-lived quantum coherence in photosynthetic complexes at physiological temperature arXiv:1001.5108

[735] Collini E and Scholes G D 2009 *Science* **323** 369–73

[736] Collini E and Scholes G D 2009 *J. Phys. Chem.* A **113** 4223–41

[737] Cheng Y C and Fleming G R 2009 *Ann. Rev. Phys. Chem.* **60** 241–62

[738] Beljonne D, Curutchet C, Scholes G D and Silbey R J 2009 *J. Phys. Chem.* B **113** 6583–99

[739] Abramavicius D, Palmieri B, Voronine D V, Šanda F and Mukamel S 2009 *Chem. Rev.* **109** 2350–408

[740] Arndt M, Juffmann T and Vedral V 2009 *HFSP J.* **3** 386–400

[741] Cheng Y C and Fleming G R 2008 *J. Phys. Chem.* A **112** 4254–60
[742] Ishizaki A and Fleming G R 2009 *Proc. Natl Acad. Sci.* **106** 17255–60
[743] Ishizaki A and Fleming G R 2009 *J. Chem. Phys.* **130** 234110
[744] Ishizaki A and Fleming G R 2009 *J. Chem. Phys.* **130** 234111
[745] Olaya-Castro A, Lee C F, Olsen F F and Johnson N F 2008 *Phys. Rev.* B **78** 085115
[746] Yu Z G, Berding M A and Wang H 2008 *Phys. Rev.* E **78** 050902
[747] Jang S, Cheng Y C, Reichman D R and Eaves J D 2008 *J. Chem. Phys.* **129** 101104
[748] Jang S 2009 *J. Chem. Phys.* **131** 164101
[749] Mohseni M, Rebentrost P, Lloyd S and Aspuru-Guzik A 2008 *J. Chem. Phys.* **129** 174106
[750] Rebentrost P, Mohseni M, Kassal I, Lloyd S and Aspuru-Guzik A 2009 *New J. Phys.* **11** 033003
[751] Rebentrost P, Mohseni M and Aspuru-Guzik A 2009 *J. Phys. Chem.* B **113** 9942–7
[752] Rebentrost P, Chakraborty R and Aspuru-Guzik A 2009 *J. Chem. Phys.* **131** 184102
[753] Plenio M B and Huelga S F 2008 *New J. Phys.* **10** 113019
[754] Caruso F, Chin A W, Datta A, Huelga S F and Plenio M B 2009 *J. Chem. Phys.* **131** 105106
[755] Palmieri B, Abramavicius D and Mukamel S 2009 *J. Chem. Phys.* **130** 204512
[756] Thorwart M, Eckel J, Reina J, Nalbach P and Weiss S 2009 *Chem. Phys. Lett.* **478** 234–7
[757] Nazir A 2009 *Phys. Rev. Lett.* **103** 146404
[758] Caruso F, Chin A W, Datta A, Huelga S F and Plenio M B 2009 Entanglement and entangling power of the dynamics in light-harvesting complexes arXiv:0912.0122
[759] Brádler K, Wilde M M, Vinjanampathy S and Uskov D B 2009 Identifying the quantum correlations in light-harvesting complexes arXiv:0912.5112
[760] Perdomo A, Vogt L, Najmaie A and Aspuru-Guzik A 2010 Engineering directed excitonic energy transfer arXiv:1001.2602
[761] Fassioli F and Olaya-Castro A 2010 Distribution of entanglement in light-harvesting complexes and their quantum efficiency arXiv:1003.3610
[762] Lu Z M and Rabitz H 1995 *Phys. Rev.* A **52** 1961–7
[763] Lu Z M and Rabitz H 1995 *J. Phys. Chem.* **99** 13731–5
[764] Zhu W S and Rabitz H 1999 *J. Chem. Phys.* **111** 472–80
[765] Zhu W S and Rabitz H 1999 *J. Phys. Chem.* A **103** 10187–93
[766] Brif C and Rabitz H 2000 *J. Phys. B: At. Mol. Opt. Phys.* **33** L519–25
[767] Kurtz L, Rabitz H and de Vivie-Riedle R 2002 *Phys. Rev.* A **65** 032514
[768] Geremia J M and Rabitz H 2001 *J. Chem. Phys.* **115** 8899–912
[769] Geremia J M and Rabitz H A 2004 *Phys. Rev.* A **70** 023804
[770] Geremia J M and Rabitz H 2002 *Phys. Rev. Lett.* **89** 263902
[771] Geremia J M and Rabitz H 2003 *J. Chem. Phys.* **118** 5369–82